

Dissertation zur Erlangung des Doktorgrades
der Fakultät für Chemie und Pharmazie
der Ludwig-Maximilians-Universität München

Investigations on Protein Adsorption to Coated Glass Vials

Kerstin Höger

aus

Regensburg, Deutschland

2014

Erklärung

Diese Dissertation wurde im Sinne von § 7 der Promotionsordnung vom 28. November 2011 von Herrn Prof. Dr. Wolfgang Frieß betreut.

Eidesstattliche Versicherung

Diese Dissertation wurde eigenständig und ohne unerlaubte Hilfe erarbeitet.

München, 31. Januar 2014

(Kerstin Höger)

Dissertation eingereicht am 31. Januar 2014

1. Gutachter: Prof. Dr. Wolfgang Frieß

2. Gutachter: Prof. Dr. Gerhard Winter

Mündliche Prüfung am 19. März 2014

Für meine Eltern

Acknowledgments

This thesis was prepared at the Department of Pharmacy, Pharmaceutical Technology and Biopharmaceutics at the Ludwig-Maximilians-Universität in Munich under the supervision of Prof. Dr. Wolfgang Frieß.

First of all I would like to express my deepest gratitude to my supervisor Prof. Dr. Wolfgang Frieß for giving me the opportunity to join his research group. I am very thankful for your scientific support and advice and the possibility to present my work on various conferences. Your encouragements, patience and enthusiastic way were invaluable during my time in your lab. I really enjoyed the pleasant and motivating atmosphere in your group.

I also would like to thank Prof. Dr. Gerhard Winter, the leader of the chair, for creating excellent working conditions and for initiating and organizing numerous social activities. Thank you a lot for being the co-referee of this thesis.

My thanks are also going to Dr. Sarah Küchler, who made way for the collaboration with the group of Prof. Dr. Rainer Haag at the FU Berlin. I received great support from her, especially on the experiments on protein adsorption to polyglycerol coated vials and on paper writing.

I would like to acknowledge SCHOTT AG Mainz for providing the siliconized vials for my experiments. Thanks to Wolfgang Streu and Dr. Robert Hormes for their information on the siliconized containers. Furthermore I would like to thank Dr. Clemens Ottermann for providing the glass platelets for the zeta potential measurements and especially Dr. Holger Röhl for his advice and help.

Merck Serono is gratefully acknowledged for their generous material support. I would like to thank Dr. Daniel Schwartz for his support with my work.

From the FU Berlin I deeply thank Prof. Dr. Rainer Haag for the possibility to join in the research about protein adsorption to polyglycerol-coated vials. I would like to thank Tobias Becherer for the preparation of the vials, the QCM-measurements and the great

collaboration and discussions during paper writing. Thanks also to Wei Qiang for preparing the coated and labeled vials.

I want to thank Anton Paar GmbH for the possibility to perform zeta potential measurements on the SurPASS and Dr. Thomas Luxbacher for his support and advice.

From the TU Munich I want to thank Prof. Dr. Ulrich Kulozik for the possibility to perform the contact angle measurements. I also want to thank Wolfgang Holzmüller who gave me great support with the measurements.

I also want to thank several students who helped me with experiments during my research. In particular I want to thank Veronika Fischbacher and Marlene Burisch for doing a great job in the lab. Thanks are also going to Safia Achour-Hayek and Lars Heinzl for their help.

My special thanks go to my colleagues in the groups of Prof. Frieß and Prof. Winter for the good time we spent together and the relaxed atmosphere. I always enjoyed our coffee breaks with lots of cake, the interesting discussions and our social activities. In particular I want to mention Lars, Winnie, Sarah C., Sarah Z., Julia, Philipp, Tim, Eva and Verena. Thank you for the good time we had together, for your support and your friendship. I also want to thank Imke for her general support and advice during these years, Winnie and Philipp for their IT advice and Tim for his technical support. Furthermore, I want to thank Johannes for his kind introduction to the analysis of protein adsorption. My special thanks go to Kristine, who visited me every Wednesday evening, and to Eva, who became my close friends. Thank you for all the time together.

I deeply thank my parents and my brother Nils. Without their encouragement and support I would never have come so far.

Finally, I would like to thank Berni for his never ending support, encouragement and patience over the last years. Thank you for always being there for me and for your love.

Table of Contents

Chapter I

General Introduction and Objectives of the Thesis

1	General Introduction.....	1
1.1	Protein Adsorption to Solid Surfaces and Related Risks.....	1
1.2	Primary Packaging Materials for Parenteral Drugs	2
1.2.1	Glass	2
1.2.2	Siliconization of Glass.....	3
1.2.3	Further Materials, Coatings and Surface Modifications used for Parenteral Packaging.....	5
1.3	Mechanisms and Driving Forces for Protein Adsorption	6
1.4	Factors Influencing Protein Adsorption.....	8
2	Objectives of the Thesis	10
3	References	11

Chapter II

IgG1 and Lysozyme Adsorption to Type I Borosilicate Glass Vials and Siliconized Vials

1	Introduction	18
2	Materials and Methods	19
2.1	Materials.....	19
2.1.1	Chemicals	19
2.1.2	Protein Formulation	20
2.1.2.1	Monoclonal IgG1	20
2.1.2.2	Hen Egg White Lysozyme.....	20
2.1.3	Vials and Closure Systems	21
2.1.4	Vial Fragments.....	21
2.1.5	Glass Powder	21
2.1.6	Siliconized Glass Powder	22
2.1.7	Siliconized and Non-coated Fiolax [®] Glass Slides	22
2.2	Methods.....	22
2.2.1	Adsorption Process	22
2.2.2	HP-SEC	23
2.2.2.1	Non-native HP-SEC	23
2.2.2.2	Native HP-SEC.....	23
2.2.3	Surface Tension Measurements.....	24

2.2.4	UV-Spectroscopy.....	24
2.2.5	Fluorescence Microscopy	24
2.2.6	Electrophoretic Mobility Measurements	24
2.2.6.1	Experiments with IgG1	24
2.2.6.2	Experiments with Lysozyme	25
2.2.7	Streaming Potential Measurements	25
2.2.8	Contact Angle Measurements.....	25
2.2.9	Fluorescence Spectroscopy.....	26
2.2.10	Light Obscuration	26
2.2.11	Visible Particle Inspection.....	26
2.2.12	Turbidity Measurements.....	26
2.2.13	Static Light Scattering	26
2.2.14	Isoelectric Focusing.....	27
2.2.15	Specific Surface Area Analysis	27
2.2.16	Calculation of the Change in Electrokinetic Charge Density.....	27
2.2.17	Calculation of the Change in Interfacial Tension.....	28
3	Results and Discussion	29
3.1	IgG1 Adsorption to Type I Borosilicate Glass Vials and Siliconized Vials.....	29
3.1.1	Charge Characterization and Electrostatic Interactions of IgG1 and Siliconized Glass	29
3.1.2	Investigation of Adsorption of IgG1 to Borosilicate Glass and Siliconized Glass by Static Contact Angle Measurements.....	31
3.1.3	Influence of Formulation pH and Ionic Strength on IgG1 Adsorption to Siliconized Glass Vials.....	34
3.1.3.1	Adsorbed IgG1 Quantity as a Function of pH.....	34
3.1.3.2	Influence of Ionic Strength on IgG1 Adsorption.....	36
3.1.4	Electrostatic Interactions within the Adsorption Interface	38
3.1.5	Influence of Non-ionic Surfactants on IgG1 Adsorption	40
3.1.6	Influence of Sugars and Polyols on IgG1 Adsorption.....	43
3.1.7	Long-term Adsorption of IgG1 to Borosilicate Glass Vials and Siliconized Glass Vials	46
3.2	Lysozyme Adsorption to Borosilicate Glass Vials and Siliconized Glass Vials	52
3.2.1	Charge Characterization of Lysozyme and the Glass Surface.....	52
3.2.2	Influence of pH on Lysozyme Adsorption	53
3.2.3	Influence of Ionic Strength on Lysozyme Adsorption	55
3.2.4	Isotherm Considerations	58
4	Conclusion.....	61
5	References	63

Chapter III

Polyglycerol Coatings of Glass Vials for Protein Resistance

1 Introduction	74
2 Materials and Methods	75
2.1 Chemicals.....	75
2.2 Synthesis and Analytics	76
2.2.1 Azide Functionalized HPG(OMe) (4c).....	77
2.2.2 Amine Functionalized HPG(OMe) (4d).....	77
2.2.3 Triethoxysilyl Modified HPG(OMe) (4)	77
2.3 Glass Coating Procedure.....	78
2.4 Protein Solutions	79
2.5 Protein Adsorption Testing	79
2.6 Stability Testing of the HPG(OH)-Coating toward pH Change via QCM-D.....	80
2.7 Protein Stability after Storage	81
2.8 Tests of Significance	82
3 Results	82
3.1 Effect of Different Polyglycerol Coatings on IgG1 and hGH Adsorption	82
3.2 Influence of Sterilisation on Polyglycerol Coatings	84
3.3 Long-Term Effect of Polyglycerol Coating on Protein Adsorption	84
3.4 Effect of HPG(OH)-Coating on IgG1 Stability in Solution.....	85
3.5 Stability Testing of the HPG(OH)-Coating toward pH Change via QCM-D.....	87
4 Discussion.....	89
5 Conclusion.....	92
6 References	93

Chapter IV

Adsorption of IgG1 and its F(ab')₂ and Fc Fragment to Type I Borosilicate Glass Vials and Siliconized Vials – Influence of pH and Ionic Strength

1 Introduction	98
2 Materials and Methods	99
2.1 Chemicals.....	99
2.2 IgG1 Antibody	99
2.3 Fc Fragments.....	100
2.4 F(ab') ₂ Fragments	100
2.5 Vials and Closure Systems.....	101
2.6 Adsorption Process	101
2.7 UV-Spectroscopy	102

2.8	HP-SEC.....	102
2.9	Determination of the Molar Extinction Coefficient of Fc and F(ab') ₂ Fragments.....	102
2.10	Micro BCA-Assay.....	103
2.11	SDS-PAGE.....	103
2.12	Isoelectric Focusing	104
3	Results and Discussion	104
3.1	Adsorption of IgG1, F(ab') ₂ and Fc Fragment.....	104
3.1.1	Adsorption to Borosilicate Glass Vials	104
3.1.2	Adsorption to Siliconized Glass Vials.....	109
3.2	Simultaneous Adsorption of F(ab') ₂ / Fc Fragments and Orientation Considerations.....	109
4	Conclusion.....	112
5	References	114

Chapter V

	Summary of the Thesis.....	117
--	----------------------------	-----

List of Abbreviations

AI	adsorption index
AUC	area under the curve
BET	Brunauer, Emmett, Teller
bis-ANS	8-anilino-1-naphthalene-sulfonate
BSA	bovine serum albumine
c	concentration
CD	cyclodextrin
c_{eq}	equilibrium concentration
CMC	critical micelle concentration
COC	cyclic olefin copolymer
COP	cyclic olefin polymer
$\Delta_{ads}\sigma_{ek}$	change of electrokinetic charge density upon adsorption
d	pathlength of the cuvette
d_h	hydrodynamic diameter
ε	molar extinction coefficient
ε_o	permittivity of the free space
ε_r	permittivity of the medium
η	viscosity of the solution
EDTA	ethylene diamine tetraacetate
EMBOSS	european molecular biology open software suite
F	Faraday constant
F(ab')	fragment, antigen binding
F(ab') ₂	fragment, antigen binding, dimer
Fc	fragment, crystallizable
FDA	Food and Drug Administration
Γ	mass protein per surface area
γ_l	surface tension of the liquid phase
Γ_{max}	maximum surface concentration
Γ_{pl}	adsorption plateau value
$\Gamma_{pl}(pH)_{max}$	adsorption plateau value at pH of maximum adsorption
γ_s	surface tension of the solid phase
γ_{sl}	interfacial tension between the solid and the liquid phase

<i>G</i>	Gibbs energy
<i>H</i>	enthalpy
HCl	hydrochloric acid
hGH	human Growth Hormone
HLB	hydrophilic lipophilic balance
HP- β -CD	hydroxypropyl- β -cyclodextrin
HPG(OH)	hyperbranched polyglycerol
HPG(OMe)	hyperbranched methoxylated polyglycerol
<i>I</i>	ionic strength
IEF	isoelectric focusing
IEP	isoelectric point
IgG	immunoglobulin G
κ^{-1}	Debye length
K_m	median binding affinity
λ	wavelength of the light
LPG(OMe)	linear methoxylated polyglycerol
μ_e	electrophoretic mobility
MW	molecular weight
MWCO	molecular weight cut off
mPEG	poly(ethylene glycol) methyl ether
<i>n</i>	number of amino acids in a protein sequence, heterogeneity index
N_A	Avogadro's number
NaCl	sodium chloride
NaOH	sodium hydroxide
OEG	oligo (ethylene glycol)
P 188	poloxamer 188
<i>p</i>	level of significance
<i>p</i>	pressure
PBS	phosphate buffered saline
PDMS	poly(dimethylsiloxane)
PEG	poly(ethylene glycol)
PG	polyglycerol
Ph. Eur.	European Pharmacopoeia
pI	isoelectric point

PICVD	Plasma Impulse Chemical Vapor Deposition
pK_a	dissociation constant
PS 80	polysorbate 80
QCM-D	quartz crystal microbalance with dissipation
R	gas constant, correlation coefficient
RNase	ribonuclease
σ_{ek}	electrokinetic charge density
S	entropy
SAM	self-assembled monolayer
SDS	sodium dodecyl sulfate
SDS-PAGE	sodium dodecyl sulfate polyacrylamide gel electrophoresis
SE-HPLC	size exclusion high performance liquid chromatography
τ'	adhesion tension of a surfactant or protein solution
τ°	adhesion tension of water or saline
$[\tau' - \tau^\circ]$	adsorption index
θ	contact angle
T	temperature
ζ	zeta potential
z	valency of the ions

Chapter I

General Introduction and Objectives of the Thesis

1 GENERAL INTRODUCTION

1.1 Protein Adsorption to Solid Surfaces and Related Risks

Adsorption of proteins to solid surfaces is a phenomenon observed in a variety of fields and processes. Due to their surface-activity, protein molecules are able to interact with various surfaces. The specific properties of protein, surface and the surrounding liquid determine the extent to which adsorption may occur. For therapeutic protein formulations, adsorption is a critical point during processing, storage, and even during patient administration of the finished product. Glass and plastics, two of the most common materials for processing materials and storage containers, are well-known to adsorb significant quantities of protein [1-3]. This may lead to a loss in protein content, especially for low-concentrated protein solutions where the relative percentage loss is particularly high. Protein adsorption is a well-known phenomenon e.g. for insulin [1, 4], secretin [5] and Factor VIII [6]. Handling the loss of the biologic in the final dosage form is the main challenge for drug manufacturers. One strategy to overcome this problem is the overfilling of containers, either by applying a higher filling volume, a higher concentration or both [7]. This allows maintaining the necessary dosage after passivation of the surface with the drug product. The disadvantage of this strategy is the higher cost, especially for expensive protein based drugs [7]. Optimization of the protein formulation in regard to adsorption prevention presents an alternative approach. Excipients such as surfactants [2] or carbohydrates [8] may be added to reduce adsorptive losses, and the formulation may be adapted in terms of pH value and ionic strength. However, these adjustments must not endanger long-term stability and biocompatibility of the formulation. Furthermore, the proper selection of containers for processing, transport and storage is a possible approach to decrease the loss of protein content or activity due to

adsorption. Various container materials such as glass, plastics, and coated materials are offered, but up to now, no material provides universal adsorption prevention for all protein drugs.

Besides the loss of protein, structural alterations in the protein due to adsorption were reported [9-11]. Additionally, protein adsorption was observed to potentially initiate protein aggregation [12] which poses the risk of immunogenic reactions toward the drug product [13]. Thus, investigating the factors influencing protein adsorption and the involved mechanisms is important to find suitable approaches for the above mentioned issues.

1.2 Primary Packaging Materials for Parenteral Drugs

For parenteral drugs, the primary packaging material has to fulfill higher requirements compared to topical or oral drug formulations. The Food and Drug Administration (FDA) of the United States of America published a Guidance for Industry concerning "Container closure systems for packaging human drugs and biologics" [14]. According to this document, suitability of a packaging system comprises the protection of, and compatibility with the dosage form, safety and proper performance function. Adsorption of the active drug substance and a related potency loss may constitute a compatibility problem if unacceptable quality changes take place [14]. Therefore, stability testing is usually performed in the packaging system intended for final use. The majority of small volume injectable formulations is stored in vials, followed by syringes, ampoules and cartridges, whereas bottles and bags are used for larger volumes [15]. Still, one of the most commonly used materials is glass, but also plastic vials and different coatings and surface modifications for special applications are available on the market.

1.2.1 Glass

For parenteral drugs, mainly type I borosilicate glass is used. This glass has a high chemical resistance, low leachability and a low thermal expansion coefficient [15], is formable and tight toward gases and liquids. Furthermore, the production of glass containers is possible in a highly reproducible quality. The thermal stability of this material allows a time and cost saving sterilization and depyrogenation by dry heat at high temperatures, which is a major advantage compared to plastics such as cyclic olefin copolymers (COC) or polypropylene. Although the glass surface is basically chemically resistant, reactions with water, acids and alkalines may lead to leaching and extraction of glass components. Borosilicate glass is mainly composed of silicon dioxide and boric oxide with low levels of other oxides which

are not contributing to network formation, such as sodium and aluminum oxides [15]. At acidic conditions, network modifying ions from the glass, e.g. Na^+ , K^+ or Ca^+ are exchanged against protons from an aqueous solution [16]. This loss of hydronium ions during leaching leads to rising pH values in the product solution and potential instabilities of biomolecules. Alkaline attack of the glass surface which is also known as etching [17] leads to the disintegration of the SiO_2 network and finally to decomposition of the glass [16]. Water leads to a leaching of ions and ion exchange between the solution and the glass [16]. Finally, glass flaking may occur due to the delamination of glass which is embedded at the inner glass surface [15]. These flakes consist of alkali borates which recondensed during the final glass preparation after migration to the inner surface and evaporation [15]. This glass instability gained considerable attention by the authorities [18] as well as glass container manufacturers [19] and caused several product recalls in the last years [20]. Several factors are associated with the risk of delamination, some of them presented in an advisory of the US FDA [18]: (a) the manufacturing process of vials and canes may strongly influence the glass chemical resistance [21]. Vials manufactured by molding show a higher resistance than vials formed from glass tubing [17]; (b) alkaline formulations and certain buffers $\text{pH} \geq 7$, e.g. phosphate, citrate or tartrate buffers increase the risk of delamination [15]; (c) long storage times, (d) terminal sterilization and (e) surface treatment with sulfate, e.g. ammonium sulfate were shown to increase the chance of delamination [17]. Vial forming processes at lower heating rate and temperature to reduce the migration of alkali ions to the glass surface are one possible approach to generate surfaces with a potentially lower propensity for delamination [17]. Furthermore, coating of the inner vial surface with SiO_2 can avoid delamination [19]. Due to the variety of product formulations and processing conditions, no general test will serve for individual risk assessment but container testing and additional container screening during stability studies will be necessary [19].

1.2.2 Siliconization of Glass

The use of silicones in pharmaceutical manufacturing as antifoams, tubing material and for the siliconization of container surfaces has been well established for many years. Already in 1949, the siliconization of pharmaceutical containers was patented by Goldman [22]. Coatings with silicone provide advantages such as a good drainage of the solution from the vial wall and thus a better dosage [23], an easy movement of rubber closures e. g. in feeding machines, and reduction of the force for plunger movement in syringes [15]. One of the most common silicone fluids applied for the coating of parenteral packaging components is

Polydimethylsiloxane (PDMS) (Figure I-1a). Endcapped with a trimethylsiloxy-group, some Polydimethylsiloxanes meet the requirements of Dimethicone NF [24], Dimethicone Ph. Eur. [25] (Figure I-1b), or the monograph “Silicone oil used as a lubricant” Ph. Eur. [26].



Figure I-1: Chemical structure of (a) polydimethylsiloxane (PDMS) and (b) Dimethicone (trimethylsiloxy-endcapped PDMS).

Mundry summarized the typical steps of a siliconization process and the most important influencing factors using silicone oil emulsions [27]: Before siliconization, the containers are cleaned by flushing with water for injections and dried with pressurized air. Subsequently, the silicone oil emulsion is applied by spraying or flushing. Excess aerosol or emulsion is sucked up and the silicone oil is baked in a heating tunnel. This step simultaneously includes the sterilization and depyrogenation of the containers. Important variables for this process comprise the type of the silicone oil, the concentration and composition of the silicone oil emulsion, the temperature and time of the baking step, as well as the glass of the containers. In this regard, especially the glass composition and hydrolytic resistance are of importance [27]. Instead of spraying of the silicone oil (emulsion), dipping or wiping may also be applied [28]. Baking of applied silicone fluid with dry heat removes hydration moisture from the surface and ensures a good association of the coating with the substrate surface [28]. Applying silicone oil emulsions, heating is necessary to destruct the contained emulsifier and thus enable a spreading of the PDMS on the surface [27]. During heat-curing, the emulsifiers are removed by pyrolysis or hydrolysis and water evaporates [27]. Trimethylsiloxy-endblocked PDMS fluids are typically considered chemically inert and stable concerning decomposition at temperatures below 150 °C, but certain metals and higher temperatures may influence their decomposition and reactivity [28]. Formaldehyde and low-molecular weight siloxanes may be generated at > 150 °C when silicone oil is heated to about 200 °C [29]. Heat-curing at temperatures below 250 °C for less than 2 h for substrates coated with silicone fluids is therefore recommended by some PDMS suppliers to reduce the formation of formaldehyde [28], whereas in industrial processes, higher temperatures at reduced baking times are applied as well. From a literature review, Mundry concluded that silicone oil emulsions and curing temperatures between 300-350 °C for 10-30 min. should be applied to obtain optimal siliconization results [27]. Due to the low reactivity of silicones and their

stability, sterilization by dry heat and steam autoclaving as well as gassing by ethylene oxide and radiation in low doses is possible [28]. Using silicone oil coatings implies the risk of silicone (micro)droplets in the product solution [15, 30]. In therapeutic protein formulations, this may increase the risk of product-droplet interactions [15] and potential protein aggregation [31]. Minimizing the applied amount of silicone oil is therefore essential [28]. Due to their growing relevance as coated packaging material for injectables, siliconized glass vials were chosen for adsorption studies with IgG1 and lysozyme.

1.2.3 Further Materials, Coatings and Surface Modifications used for Parenteral Packaging

Besides glass vials, plastic vials of cyclic olefins such as cyclic olefin copolymer (COC) and cyclic olefin polymer (COP) have been developed for the packaging of injectables [15]. Compared to polypropylene and polyethylene, these materials provide advantages like high transparency, the absence of extractable metal ions and low levels of organics which may be extracted [32]. Although plastic containers exhibit advantages compared to glass vials e.g. a resistance to breakage and a reduced release of leachables (for COC and COP) [15], their use is not very common. Some reasons are the higher costs of these vials [32] and the challenges arising from their transfer into an aseptic environment: In contrast to glass vials which are conveyed through a heating tunnel directly into an aseptic area, plastic vials are obtained pre-sterilized (e.g. by irradiation) and have to be transferred aseptically [15]. Furthermore, the low weight of these vials compared to glass vials makes their transport on conveyers and their handling difficult, and the potential of product-container interactions over shelf-life periods of several years is still rising concerns [15].

Another option to improve the properties of the packaging materials is the coating of a glass or plastic container. One common coating is the siliconization as presented in section 1.2.2. Coating of glass vials with thin layers of SiO₂ by Plasma Impulse Chemical Vapor Deposition (PICVD) strongly reduces the interaction between the vial surface and the drug [16]. Besides these marketed products, there is great effort on the development of further protein repellent surface coatings to reduce the adsorption of proteins. Poly- or oligoethylene glycol (PEG/OEG)-based coatings are one of the most popular and best investigated coatings [33-35]. The excellent protein repellent effects of these coatings were ascribed to a steric repulsion or excluded volume mechanism [36] or the formation of a structurally stable interfacial water layer [34]. Further investigated surface modifications include coatings with polyglycerols [37-39], zwitterionic self-assembled monolayers and polymers [40, 41],

carbohydrate-derived polymers [42] and dextran [43]. Besides the ability to prevent the adsorption of proteins, a variety of other factors decide about the feasibility of a coating for industrial primary packaging materials for injectables. These include the possibility for sterilization, stability of the coating over 2-3 years, non-toxic properties of the coating and low costs [7]. Furthermore, the coating quality must be verifiable to 100% [7]. These requirements are met only by a minority of promising coatings. Polyglycerols with different side groups constitute a new and innovative coating material. Glass vials coated with these materials as a potential candidate were therefore investigated for their adsorption preventing properties.

1.3 Mechanisms and Driving Forces for Protein Adsorption

Proteins are amphiphilic, surface-active molecules which may adsorb to liquid-gas and solid-liquid interfaces. The mechanism of protein adsorption to and desorption from a solid surface involves several steps, which are schematically depicted in Figure I-2 and were thoroughly described by Norde [44]. Convection and diffusion transport the protein from solution toward the sorbent surface (1), where the molecules may adsorb (2). The rate constant for this deposition is thereby influenced by the surface coverage and any barriers opposing attachment e.g. due to electrostatic repulsion. Once the protein attached on the surface, it structurally relaxes (3), optimizing its interaction with the surface [44]. Changes in the protein's secondary structure may occur upon adsorption [10, 45]. Finally, adsorbed molecules may

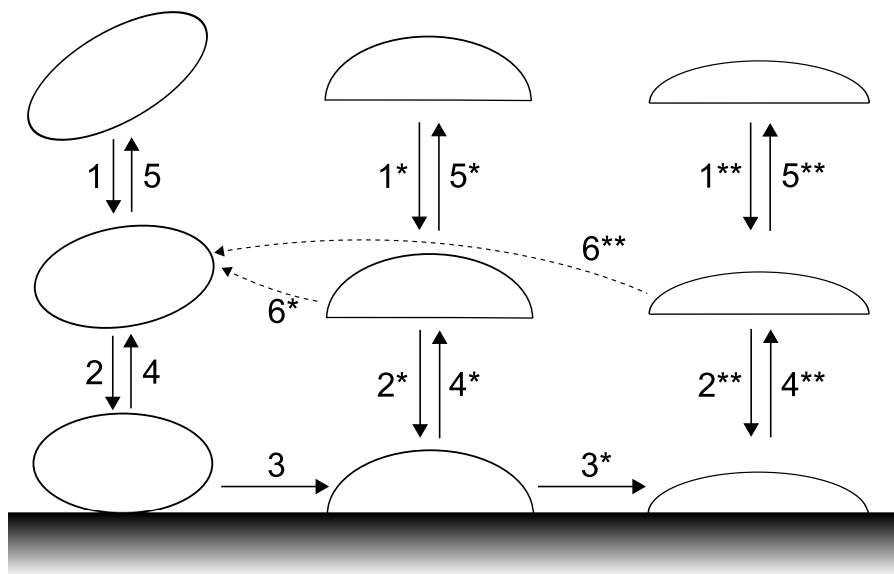


Figure I-2: Schematic process of protein adsorption to a solid surface adapted from Norde [44]. The relaxation degree of the adsorbed protein molecules is indicated by the asterisks.

detach **(4)** and are transported back toward the solution **(5)** [44]. Protein adsorption to solid surfaces was found to be almost irreversible [46, 47] or only partially reversible [48] upon rinsing with buffer. The reversibility of adsorption largely depends on the system studied. After desorption from the sorbent surface, the detached molecules may potentially restructure to their native state **(6)** [44].

At constant pressure p and temperature T , protein adsorption requires a decrease of the systems' Gibbs energy G independent of the adsorption mechanism and kinetics [49]. The change of the Gibbs energy G due to the adsorption process can be written as

$$\Delta_{\text{ads}}G = \Delta_{\text{ads}}H - T\Delta_{\text{ads}}S < 0$$

where H and S represent the enthalpy and entropy [44]. Analysis of the adsorption induced change in Gibbs energy caused by different interaction types thus represents one possible approach to investigate the reasons for protein adsorption [49]. In the following, the most important factors determining protein adsorption, **(A)** electrostatic interactions, **(B)** hydration changes, **(C)** dispersion interactions and **(D)** structural rearrangements, will be briefly presented.

(A) One important driving force for adsorption is the interaction between electrical double layers [44] which is also known as electrostatic interactions. The sorbent surface and the protein are usually electrically charged. Coions and counterions surround them in an aqueous medium and an electrical double layer is formed from this countercharge and the surface charges of protein or sorbent [44]. Upon adsorption, when the protein comes close to the surface, a superposition of their electrical double layers takes place and the position of the counterions is readjusted [50]. It is clear that this interaction is especially favorable when protein and sorbent surface bear net charges of different sign and electrostatically attract each other.

(B) Besides electrostatic interactions, changes in the state of hydration may be another driving force for adsorption [44]. Major parts of the protein's outer surface are composed of charged and polar protein residues since the solvation of these groups compared to hydrophobic protein parts is more easy [51], whereas apolar protein side-chains are by trend buried inside the protein molecule [52]. The hydration of surface exposed apolar protein patches can be avoided by aggregate formation or adsorption of the protein to a non-aqueous interface,

leading to a rise in entropy and thus a lowering of the Gibbs energy [49]. Dehydration of hydrophobic protein patches can thus constitute a driving force for protein adsorption. According to Norde, $\Delta_{ads}G$ by dehydration is higher than by a redistribution of charges for the majority of hydrophobic surfaces, which is why adsorption to hydrophobic surfaces can be observed for all proteins even when the conditions are electrostatically unfavorable [50].

(C) Dispersion interactions are another possible driving force for protein adsorption to solid surfaces. In materials, intermolecular long-range van der Waals forces emerge from dipole interactions and consist of three contributing forces, namely the Keesom force, the London force and the Debye force [53]. Except for the Keesom force which can also be repulsive, van der Waals forces are attractive [53]. The adsorption induced change in Gibbs energy due to dispersion interactions depends on the protein dimensions and the space between sorbent surface and protein [44].

(D) Finally, structural rearrangements of the protein may act as a driving force for adsorption [44]. Main parts of a protein's interior consist of hydrophobic protein parts [51]. Upon contact of a protein with a non-aqueous surface, the importance of intramolecular hydrophobic interactions, which stabilize α -helices or β -sheets, decreases and apolar patches which were previously located inside the protein core may orientate toward the non-aqueous sorbent surface [44]. Conformational changes upon adsorption such as decreased α -helical structures for BSA [54] or a decreased content of β -sheets combined with increased fractions of random coil and α -helices for IgG on a hydrophobic surface were reported [10]. It was postulated that an increasing entropy due to structural rearrangements is the main reason for spontaneous protein adsorption [55].

1.4 Factors Influencing Protein Adsorption

Protein adsorption to solid sorbent surfaces is a complex process which is mainly determined by the properties of the protein and the sorbent surface. For therapeutic proteins, the adsorption conditions and the composition of the formulation also play an important role.

Norde established the classification of proteins according to their structural stability upon adsorption to surfaces [56]: "Hard" proteins adsorb only under electrostatically attractive conditions to polar surfaces and the structural changes involved are low. "Soft" proteins undergo stronger structural changes upon adsorption, potentially with a decrease of ordered structures, and the increase in conformational entropy allows adsorption to polar surfaces

even under electrostatically adverse conditions. However, this entropy gain by adsorption as a driving force applies only for globular proteins, whereas for polymers of loose structures, adsorption involves entropy losses [56]. Besides this structural aspect, the adsorption behavior of a protein depends on its hydrophilicity or hydrophobicity, and the net charge, which was already discussed in the previous chapter. At this point it has to be added that adsorption was frequently observed not only at attractive electrostatic, but also at repulsive conditions [57, 58]. This is where not only the net charge, but also the charge distribution of the components becomes important for adsorption. Kamiyama & Israelachvili suggested that the number of ionic bonds between discrete, oppositely charged groups on sorbent and adsorbate determines adsorption [57]. Furthermore, the protein IEP was found to essentially determine adsorption, as for a variety of proteins and sorbent surfaces a rough correspondence with the pH of maximum adsorption was found [59-62]. Amongst others, this trend was ascribed to a low intermolecular repulsion at the pI and high adsorption rates, not allowing reorientation of the molecules [63] and increasing structural perturbations in the molecules away from the pI [62]. Besides these aspects, the orientation of the molecules at a surface may be related to the adsorbed amount [64]. Furthermore, the sorbent properties such as the hydrophilicity and hydrophobicity, the surface charge, density and roughness, or the movement of surface bound polymer chains may influence adsorption which will not be further discussed here.

Besides the two components protein and sorbent surface, the formulation conditions are an important factor influencing the adsorption of therapeutically applied proteins. These include the pH and ionic strength of the solution, buffer composition, surfactants, polyols and sugars. The pH value of a solution determines the net charge of the protein and the sorbent and thus the electrostatic attractive or repulsive forces in between the protein molecules and between protein and sorbent surface. High salt concentrations may screen these electrostatic interactions and thus influence the adsorbed amount [65]. Some surfactants can reduce the protein adsorption to surfaces [2, 66] or remove already adsorbed protein [67]. Besides, protein adsorption was also shown to be influenced by polyols and sugars [8, 66]. IgG1 adsorption to siliconized vials was investigated considering these formulation relevant classes of excipients.

2 OBJECTIVES OF THE THESIS

The aim of this thesis was to investigate the adsorption of a monoclonal IgG1 antibody and the model protein lysozyme to vials as primary packaging material. In this work, the main focus was set on siliconized glass vials as commercially used coated vials, on non-coated glass vials, and new polyglycerol-coated glass vials which are not yet on the market. The first main objective was to investigate the influence of different formulation parameters such as pH value, ionic strength, surfactants, sugars and polyols on the adsorption of IgG1 to siliconized vials (chapter II). Electrostatic and hydrophobic interactions as driving force were evaluated. Furthermore, the protein adsorption during long-term storage over several months was taken into account. Finally, the adsorption behavior of the model protein lysozyme onto glass vials and siliconized vials was investigated. The second main goal was to evaluate the suitability of new polyglycerol coated vials as protein repellent packaging material at different formulation conditions considering also different vial sterilization methods and long-term storage (chapter III). Finally, the role of the Fc and F(ab')₂ fragment for the adsorption of the IgG1 antibody should be investigated (chapter IV). The focus was set on the adsorption of the separated fragments and a correlation with possible molecular orientations. In summary, this thesis should evaluate the main factors influencing the adsorbed protein amount especially of IgG1 and the protein repellent potential of different glass coatings.

3 REFERENCES

- [1] C. Petty, N.L. Cunningham, Insulin adsorption by glass infusion bottles, poly(vinyl chloride) infusion containers, and intravenous tubing, *Anesthesiology*, 40 (1974) 406-410.
- [2] M.R. Duncan, J.M. Lee, M.P. Warchol, Influence of surfactants upon protein/peptide adsorption to glass and polypropylene, *Int. J. Pharm.*, 120 (1995) 179-188.
- [3] H. Grohganz, M. Rischer, M. Brandl, Adsorption of the decapeptide Cetrorelix depends both on the composition of dissolution medium and the type of solid surface, *Eur. J. Pharm. Sci.*, 21 (2004) 191-196.
- [4] J.C. McElnay, D.S. Elliott, P.F. D'Arcy, Binding of human insulin to burette administration sets, *Int. J. Pharm.*, 36 (1987) 199-203.
- [5] J. Ogino, K. Noguchi, K. Terato, Adsorption of Secretin on Glass Surfaces, *Chem. Pharm. Bull. (Tokyo)*, 27 (1979) 3160-3163.
- [6] McLeod, Walker, Zheng, Hayward, Loss of factor VIII activity during storage in PVC containers due to adsorption, *Haemophilia*, 6 (2000) 89-92.
- [7] D. Haines, L. Burzio, M. Bicker, R. Hormes, H. Koller, J. Buki, Method of preparing a macromolecule deterrent surface on a pharmaceutical package, United States Patent US 8,025,915, September 27 2011.
- [8] J.R. Wendorf, C.J. Radke, H.W. Blanch, Reduced protein adsorption at solid interfaces by sugar excipients, *Biotechnol. Bioeng.*, 87 (2004) 565-573.
- [9] A. Kondo, J. Mihara, Comparison of Adsorption and Conformation of Hemoglobin and Myoglobin on Various Inorganic Ultrafine Particles, *J. Colloid Interface Sci.*, 177 (1996) 214-221.
- [10] A.W.P. Vermeer, M.G.E.G. Bremer, W. Norde, Structural changes of IgG induced by heat treatment and by adsorption onto a hydrophobic Teflon surface studied by circular dichroism spectroscopy, *Biochim. Biophys. Acta, Gen. Subj.*, 1425 (1998) 1-12.
- [11] S.T. Tzannis, W.J. Hrushesky, P.A. Wood, T.M. Przybycien, Irreversible inactivation of interleukin 2 in a pump-based delivery environment, *Proc. Natl. Acad. Sci. U. S. A.*, 93 (1996) 5460-5465.
- [12] E.Y. Chi, J. Weickmann, J.F. Carpenter, M.C. Manning, T.W. Randolph, Heterogeneous nucleation-controlled particulate formation of recombinant human platelet-activating factor acetylhydrolase in pharmaceutical formulation, *J. Pharm. Sci.*, 94 (2005) 256-274.
- [13] A.S. Rosenberg, Effects of protein aggregates: an immunologic perspective, *AAPS J.*, 8 (2006) E501-507.
- [14] CDER/CBER, Guidance for industry: Container closure systems for packaging human drugs and biologics: chemistry, manufacturing, and controls documentation, in, U.S.

- Department of Health and Human Services Food and Drug Administration, Center for Drug Evaluation and Research (CDER), Center for Biologics Evaluation and Research (CBER), Rockville, MD, 1999, pp. 41.
- [15] G.A. Sacha, W. Saffell-Clemmer, K. Abram, M.J. Akers, Practical fundamentals of glass, rubber, and plastic sterile packaging systems, *Pharm. Dev. Technol.*, 15 (2010) 6-34.
- [16] S. AG, SCHOTT Type I plus [Online]: SCHOTT AG, Available: www.schott.com/pharmaceutical_packaging/german/download/flyer_type_i_plus.pdf [Accessed July 28 2013].
- [17] R.D. Ennis, R. Pritchard, C. Nakamura, M. Coulon, T. Yang, G.C. Visor, W.A. Lee, Glass Vials for Small Volume Parenterals: Influence of Drug and Manufacturing Processes on Glass Delamination, *Pharm. Dev. Technol.*, 6 (2001) 393-405.
- [18] US Food and Drug Administration, Advisory to Drug Manufacturers: Formation of Glass Lamellae in Certain Injectable Drugs [Online], 2011, Available: http://www.fda.gov/Drugs/DrugSafety/ucm248490.htm#_ftn6 [Accessed July 24 2013].
- [19] Two ways to Minimize the Delamination Risk of Glass Containers, in: Newsflash Pharmaceutical Packaging, SCHOTT Schweiz AG, 2012.
- [20] US Food and Drug Administration, Available: <http://www.fda.gov/Safety/Recalls/default.htm> [Accessed July 24 2013].
- [21] R. Iacocca, M. Allgeier, Corrosive attack of glass by a pharmaceutical compound, *J. Mater. Sci.*, 42 (2007) 801-811.
- [22] R. Goldman, Drain-clear container for aqueous-vehicle liquid pharmaceutical preparations, United States Patent US 2,504,482, April 18 1950.
- [23] A. Colas, Silicones in Pharmaceutical Applications [Online], 2001, Available: <http://www.dowcorning.com/content/publishedlit/51-993a-01.pdf> [Accessed January 23 2013].
- [24] Dimethicone, in: USP36-NF31, 1998
- [25] 0138 Dimethicone, in: European Pharmacopoeia, 2011
- [26] 3.1.8 Silicone oil used as a lubricant, in: European Pharmacopoeia, 2011
- [27] T. Mundry, 1999, Einbrennsilikonisierung bei pharmazeutischen Glaspackmitteln - Analytische Studien eines Produktionsprozesses, Thesis, Humboldt-Universität zu Berlin.
- [28] A. Colas, J. Siang, K. Ulman, Silicones in pharmaceutical applications. Part 5: Siliconization of Parenteral Packaging Components [Online], 2006, Available: <http://www3.dowcorning.com/content/publishedlit/52-1090-01.pdf> [Accessed May 19 2013].

-
- [29] L. Shin-Etsu Chemical Co., Technical data: Shin-Etsu silicone, Silicone Fluid KF-96 [Online], 2004, Available: www.silicone.jp/e/catalog/pdf/kf96_e.pdf [Accessed July 26 2013].
- [30] D.K. Sharma, P. Oma, S. Krishnan, Silicone microdroplets in protein formulations- Detection and enumeration, *Pharm. Technol.*, 33 (2009) 74-79.
- [31] L.S. Jones, A. Kaufmann, C.R. Middaugh, Silicone oil induced aggregation of proteins, *J. Pharm. Sci.*, 94 (2005) 918-927.
- [32] W. Dirk, A question of use [Online], 2011: SAMEDAN LTD Pharmaceutical Publishers, Available: <http://www.samedanltd.com/magazine/15/issue/157/article/3018> [Accessed May 20 2013].
- [33] K.L. Prime, G.M. Whitesides, Self-assembled organic monolayers: model systems for studying adsorption of proteins at surfaces, *Science*, 252 (1991) 1164-1167.
- [34] P. Harder, M. Grunze, R. Dahint, G.M. Whitesides, P.E. Laibinis, Molecular Conformation in Oligo(ethylene glycol)-Terminated Self-Assembled Monolayers on Gold and Silver Surfaces Determines Their Ability To Resist Protein Adsorption, *J. Phys. Chem. B*, 102 (1998) 426-436.
- [35] S. Pasche, J. Vörös, H.J. Griesser, N.D. Spencer, M. Textor, Effects of Ionic Strength and Surface Charge on Protein Adsorption at PEGylated Surfaces, *J. Phys. Chem. B*, 109 (2005) 17545-17552.
- [36] J.D. Andrade, V. Hlady, Protein adsorption and materials biocompatibility: A tutorial review and suggested hypotheses, in: *Biopolymers/Non-Exclusion HPLC*, Springer Berlin Heidelberg, 1986, pp. 1-63.
- [37] M. Weinhart, T. Becherer, N. Schnurbusch, K. Schwibbert, H.-J. Kunte, R. Haag, Linear and Hyperbranched Polyglycerol Derivatives as Excellent Bioinert Glass Coating Materials, *Adv. Eng. Mater.*, 13 (2011) B501-B510.
- [38] K. Höger, T. Becherer, W. Qiang, R. Haag, W. Frieß, S. Küchler, Polyglycerol coatings of glass vials for protein resistance, *Eur. J. Pharm. Biopharm.*, 85 (2013) 756-764.
- [39] C. Siegers, M. Biesalski, R. Haag, Self-Assembled Monolayers of Dendritic Polyglycerol Derivatives on Gold That Resist the Adsorption of Proteins, *Chem. Eur. J.*, 10 (2004) 2831-2838.
- [40] Y. Chang, S.-C. Liao, A. Higuchi, R.-C. Ruaan, C.-W. Chu, W.-Y. Chen, A Highly Stable Nonbiofouling Surface with Well-Packed Grafted Zwitterionic Polysulfobetaine for Plasma Protein Repulsion, *Langmuir*, 24 (2008) 5453-5458.
- [41] S. Chen, J. Zheng, L. Li, S. Jiang, Strong Resistance of Phosphorylcholine Self-Assembled Monolayers to Protein Adsorption: Insights into Nonfouling Properties of Zwitterionic Materials, *J. Am. Chem. Soc.*, 127 (2005) 14473-14478.

-
- [42] H. Urakami, Z. Guan, Living Ring-Opening Polymerization of a Carbohydrate-Derived Lactone for the Synthesis of Protein-Resistant Biomaterials, *Biomacromolecules*, 9 (2008) 592-597.
- [43] R.A. Frazier, G. Matthijs, M.C. Davies, C.J. Roberts, E. Schacht, S.J.B. Tendler, Characterization of protein-resistant dextran monolayers, *Biomaterials*, 21 (2000) 957-966.
- [44] W. Norde, Proteins at solid surfaces, in: A. Baszkin, W. Norde (Eds.), *Physical Chemistry of Biological Interfaces*, Marcel Dekker Inc., Basel 2000, pp. 115-135.
- [45] P. Roach, D. Farrar, C.C. Perry, Interpretation of Protein Adsorption: Surface-Induced Conformational Changes, *J. Am. Chem. Soc.*, 127 (2005) 8168-8173.
- [46] N. Dixit, K.M. Maloney, D.S. Kalonia, Application of quartz crystal microbalance to study the impact of pH and ionic strength on protein-silicone oil interactions, *Int. J. Pharm.*, 412 (2011) 20-27.
- [47] E. Brynda, M. Houska, F. Lednický, Adsorption of human fibrinogen onto hydrophobic surfaces: The effect of concentration in solution, *J. Colloid Interface Sci.*, 113 (1986) 164-171.
- [48] M. Rabe, D. Verdes, M. Rankl, G.R.J. Artus, S. Seeger, A Comprehensive Study of Concepts and Phenomena of the Nonspecific Adsorption of β -Lactoglobulin, *ChemPhysChem*, 8 (2007) 862-872.
- [49] C.A. Haynes, W. Norde, Globular proteins at solid/liquid interfaces, *Colloids Surf., B*, 2 (1994) 517-566.
- [50] W. Norde, Adsorption of proteins at solid-liquid interfaces, *Cells Mater.*, 5 (1995) 97-112.
- [51] J.S. Laurence, C.R. Middaugh, Fundamental Structures and Behaviors of Proteins, in: W. Wang, C.J. Roberts (Eds.), *Aggregation of Therapeutic Proteins*, John Wiley & Sons, Inc., Hoboken, New Jersey, 2010.
- [52] B. Alberts, A. Johnson, J. Lewis, The Shape and Structure of Proteins, in: *Mol. Biol. Cell*, Garland Science, New York, 2002, <http://www.ncbi.nlm.nih.gov/books/NBK26830/>.
- [53] R.H. French, Origins and Applications of London Dispersion Forces and Hamaker Constants in Ceramics, *J. Am. Ceram. Soc.*, 83 (2000) 2117-2146.
- [54] A. Kondo, S. Oku, K. Higashitani, Structural changes in protein molecules adsorbed on ultrafine silica particles, *J. Colloid Interface Sci.*, 143 (1991) 214-221.
- [55] W. Norde, J. Lyklema, Why proteins prefer interfaces, *J. Biomater. Sci., Polym. Ed.*, 2 (1991) 183-202.
- [56] W. Norde, My voyage of discovery to proteins in flatland ...and beyond, *Colloids Surf., B*, 61 (2008) 1-9.

-
- [57] Y. Kamiyama, J. Israelachvili, Effect of pH and salt on the adsorption and interactions of an amphoteric polyelectrolyte, *Macromolecules*, 25 (1992) 5081-5088.
- [58] X. Zhu, H. Fan, D. Li, Y. Xiao, X. Zhang, Protein adsorption and zeta potentials of a biphasic calcium phosphate ceramic under various conditions, *J. Biomed. Mater. Res., Part B*, 82B (2007) 65-73.
- [59] W. Norde, F. MacRitchie, G. Nowicka, J. Lyklema, Protein adsorption at solid-liquid interfaces: Reversibility and conformation aspects, *J. Colloid Interface Sci.*, 112 (1986) 447-456.
- [60] J. Buijs, P.A.W. van den Berg, J.W.T. Lichtenbelt, W. Norde, J. Lyklema, Adsorption Dynamics of IgG and Its F(ab')₂ and Fc Fragments Studied by Reflectometry, *J. Colloid Interface Sci.*, 178 (1996) 594-605.
- [61] P. Bagchi, S.M. Birnbaum, Effect of pH on the adsorption of immunoglobulin G on anionic poly(vinyltoluene) model latex particles, *J. Colloid Interface Sci.*, 83 (1981) 460-478.
- [62] P. Van Dulm, W. Norde, J. Lyklema, Ion participation in protein adsorption at solid surfaces, *J. Colloid Interface Sci.*, 82 (1981) 77-82.
- [63] M.G.E.G. Bremer, J. Duval, W. Norde, J. Lyklema, Electrostatic interactions between immunoglobulin (IgG) molecules and a charged sorbent, *Colloids Surf., A*, 250 (2004) 29-42.
- [64] J. Buijs, J.W.T. Lichtenbelt, W. Norde, J. Lyklema, Adsorption of monoclonal IgGs and their F(ab')₂ fragments onto polymeric surfaces, *Colloids Surf., B*, 5 (1995) 11-23.
- [65] K.L. Jones, C.R. O'Melia, Protein and humic acid adsorption onto hydrophilic membrane surfaces: effects of pH and ionic strength, *J. Membr. Sci.*, 165 (2000) 31-46.
- [66] J. Mathes, 2010, Protein Adsorption to Vial Surfaces: Quantification, Structural and Mechanistic Studies, Thesis, Ludwig-Maximilians Universität München.
- [67] M. Feng, A.B. Morales, A. Poot, T. Beugeling, A. Bantjes, Effects of Tween 20 on the desorption of proteins from polymer surfaces, *J. Biomater. Sci., Polym. Ed.*, 7 (1995) 415-424.

Chapter II

IgG1 and Lysozyme Adsorption to Type I Borosilicate Glass Vials and Siliconized Vials

Parts of this chapter as is are intended for publication:

Kerstin Höger, Johannes Mathes, Wolfgang Frieß

IgG1 adsorption to siliconized glass vials – influence of pH, ionic strength and nonionic surfactants

Abstract

It was the aim of this study to investigate the adsorption of IgG1 and the model protein lysozyme to type I borosilicate glass vials and siliconized vials. In detail, the influence of the formulation parameters pH value, ionic strength and excipients such as nonionic surfactants, sucrose, mannitol and HP- β -CD on the adsorbed amount of IgG1 was determined. The pH-dependent adsorption trends were attributed to the varying importance of electrostatic and hydrophobic interactions as driving forces for adsorption. The influence of these forces was evaluated by determining the zeta potential of protein and sorbent surface by electrophoretic mobility measurements and the calculation of the charge transfer between the protein-sorbent interface and the formulation. Furthermore, IgG1 adsorption during long-term storage of the formulation in vials was considered by correlating the protein's physical and chemical stability and the adsorbed amount for up to 6 months. pH- and ionic strength dependence of adsorption to glass vials and siliconized vials and the influence of protein and sorbent surface charge were further investigated for the model protein lysozyme.

1 INTRODUCTION

Protein adsorption is a common phenomenon in a multitude of different fields in nature and plays an important role in many biological processes, but it often causes problems in analytical and industrial processes. For pharmaceutical protein formulations, nonspecific protein adsorption gives rise to major concerns when the protein drug molecules get in contact with process materials such as filters, tubings, bags or the final primary packaging. With more than 50% of the market, vials are the most frequently used small volume containers for injectable formulations, followed by syringes and cartridges which account for 25-30% of the products [1]. Besides unmodified vials, siliconized glass vials play the major roles despite the efforts in bringing plastics forward. The lubricating properties of silicone oil are used to facilitate manufacturing processes and product functionalities, such as to provide easy transport of rubber closures in feeding machines, to reduce the plunger friction in syringes [1], to allow complete drainage of a liquid formulation from vials and better dosage [2]. Polydimethylsiloxane is the most commonly used silicone oil due to its good wetting properties, physicochemical stability and biocompatibility. Nevertheless, an increased potential for protein aggregation was found in the presence of silicone oil [3]. A basic understanding of the interaction mechanism of proteins with a siliconized surface is therefore essential for the use of siliconized containers and the prevention of adverse effects. The formulation stability of proteins in presence of silicone oil droplets has been investigated frequently, including analysis of protein loss, potentially due to protein adsorption to silicone oil droplets, and its reduction by surfactants [4] as well as studies on the influence of buffer composition on monomer loss [5]. Protein adsorption to silicone-coated solid surfaces was investigated by quartz crystal microbalance in presence of surfactants [6, 7] and varying pH and ionic strength [8]. Nevertheless, there are few studies investigating protein adsorption to siliconized glass surfaces as present in siliconized syringes or vials.

In general, the sorbent itself influences the adsorption process by the transfer of ions, by overlapping of the electrical double layers of the surface and the adsorbing protein, as well as by surface dehydration [9]. As observed for various proteins and surfaces, the electrostatic interactions between surface and protein as well as amongst protein molecules and thus adsorption are strongly influenced by the formulation pH and ionic strength [8, 10]. Consequently, determination of the electrokinetic properties, which allow conclusions about the charge state of protein and surface, can be used to interpret and predict the adsorption behavior of a protein in terms of electrostatic interactions. Additionally, the effect of ion incorporation into the protein-sorbent interface can be investigated by calculation of the

charge transfer $\Delta_{\text{ads}}\sigma_{\text{ek}}$ between the adsorption layer and the surrounding solution [11] and correlated with the adsorption behavior.

In pharmaceutical protein formulations, polyols and sugars as well as nonionic surfactants are typically added to stabilize the protein in solution [12-14]. Furthermore, some surfactants were shown to prevent adsorption to solid surfaces [15] and to remove already adsorbed protein molecules from various surfaces [16, 17], depending on the properties of the surface, the protein, and the surfactant. Finally, the concentration of the surfactant in solution influences the adsorbed protein amount [18, 19].

This study investigates the adsorption of an IgG1 antibody to siliconized vials and borosilicate glass vials as commercially relevant primary packaging materials with focus on the formulation parameters pH, ionic strength, nonionic surfactants, polyols and sugars. Furthermore, adsorption after long-term storage was investigated. The zeta potential of the protein and the siliconized surface and the charge uptake $\Delta_{\text{ads}}\sigma_{\text{ek}}$ were determined in dependence of the pH and used to interpret the adsorption behavior of IgG1 in terms of electrostatic interactions. Additionally, the effect of ionic strength on the protein adsorption was investigated and related to the interactions between the surface and the protein and in between the protein molecules. Furthermore, the adsorption suppressing effect of two formulation relevant nonionic surfactants on siliconized vials was analyzed. Finally, determination of an ‘adsorption index’ from protein and buffer contact angles was evaluated as a predictive tool for IgG1 adsorption. Besides adsorption experiments with IgG1, the adsorption of the model protein lysozyme to borosilicate glass vials and siliconized vials was investigated with focus on pH, ionic strength and electrostatic conditions. Thus, the study should provide a better mechanistic understanding of protein adsorption on relevant pharmaceutical containers and conditions and enable to select the appropriate formulation composition to minimize protein adsorption.

2 MATERIALS AND METHODS

2.1 Materials

2.1.1 Chemicals

NaH_2PO_4 and sucrose were purchased from Merck Chemicals (Darmstadt, Germany). Na_2HPO_4 , sodium-dodecyl sulfate (SDS) and Nile Red were obtained from Sigma-Aldrich Chemie GmbH (Munich, Germany). NaCl, NaOH and HCl were purchased from VWR

International (Darmstadt, Germany). NaOH used for experiments with lysozyme was from AppliChem GmbH (Darmstadt, Germany), polysorbate 80 Ph. Eur. (PS 80) was purchased from Caelo (Hilden, Germany) and poloxamer 188 Ph. Eur. (P 188) was from BASF (Ludwigshafen, Germany). Dow Corning 365, 35% Dimethicone NF Emulsion (polydimethylsiloxane (PDMS)) was from Dow Corning Corp. (MI, USA). D-(+)-Mannitol was from Riedel-de-Haen (Honeywell Specialty Chemicals Seelze GmbH, Seelze, Germany) and hydroxypropyl- β -cyclodextrin (Cavasol W7 HP Pharma) was obtained from Wacker Chemie AG (Burghausen, Germany).

2.1.2 Protein Formulation

2.1.2.1 Monoclonal IgG1

A 2 mg/ml IgG1 antibody solution in 10 mM phosphate buffer containing 145 mM NaCl (pH 7.2) was kindly donated by Merck Serono (Darmstadt, Germany). The formulation was dialyzed into 10 mM phosphate buffer using a Vivaflow® 50 tangential flow cartridge (Sartorius-Stedim Biotech, Goettingen, Germany) with a 30 kDa MWCO polyethersulfone membrane and the protein concentration was determined by UV-spectroscopy. Variable ionic strengths of the solutions were obtained by adding NaCl, followed by pH adjustment with 1 M NaOH or HCl. A consistent ionic strength of 170 mM at different solution pH values was obtained finally by adding adequate amounts of NaCl to the dialyzed solution. Electrophoretic mobility measurements were performed with 6 mg/ml antibody dialyzed into a 10 mM NaCl solution. For adsorption of IgG1 onto siliconized glass particles, the concentration of IgG1 formulated in 10 mM phosphate buffer pH 4-9 was adjusted so that an equilibrium concentration of about 2 mg/ml resulted after the adsorption process. Ultrapure water (PurelabPlus UV/UF system, ELGA, Celle, Germany) was applied for all buffers and all solutions were filtered through a 0.2 μ m polyethersulfone membrane filter (Pall GmbH, Dreieich, Germany). All excipients and chemicals used were of analytical grade.

2.1.2.2 Hen Egg White Lysozyme

Hen egg white lysozyme chloride was purchased as dialyzed, white, amorphous powder from Dalian Greensnow Egg Products Development Co., Ltd. (Dalian, China). To remove excessive chloride from the powder, the lyophilisate was dissolved and dialyzed against 10 mM phosphate buffer using Vivaflow® 50 tangential flow cartridges (Sartorius-Stedim Biotech, Goettingen, Germany) with a 5 kDa MWCO polyethersulfone membrane. pH and

ionic strength adjustments were performed as for IgG1 (section 2.1.2.1). The protein solutions were filtered through a 0.2 μm polyethersulfone membrane filter (Pall GmbH, Dreieich, Germany) before use. For adsorption experiments on glass particles, the concentration of lysozyme formulated in 10 mM PBS pH 4-11 was adjusted so that an equilibrium concentration of about 10 mg/ml resulted after the adsorption process.

2.1.3 Vials and Closure Systems

Adsorption experiments were performed in pre-siliconized (Dow Corning 365) and baked 2R Fiolax[®] glass vials and non-coated Fiolax[®] borosilicate glass vials which were kindly provided by SCHOTT AG (Mainz, Germany). The vials were washed with ultrapure water of 80 °C in a vial washing machine FAW 500 (Bausch & Stroebel GmbH & Co. KG, Ilshofen, Germany). Siliconized vials were autoclaved at 121 °C, 2 bar for 15 minutes, non-coated glass vials were heat sterilized at 250 °C for 1 h. After filling, the vials were closed with Fluorotec[®] stoppers and sealed with Flip-Off[®] seals (West Pharmaceutical Services, Eschweiler, Germany). The inner surface area of a vial covered with protein formulation was calculated as 13.4 cm² for a filling volume of 3.5 ml [18].

2.1.4 Vial Fragments

Vial fragments for the contact angle measurements were generated from 6R Fiolax[®] borosilicate glass vials, pre-siliconized (Dow Corning 365) and baked 6R Fiolax[®] Clear glass vials as well as 6R TopLyo[™] vials. Siliconized and non-siliconized glass vials were pre-processed as described in section 2.1.3. TopLyo[™] vials were pretreated as bare glass vials. Flinders of at least 1 x 1 cm were cut off the cylinder of the vial with a DREMEL[®] 300 series rotary tool (DREMEL Europe, Breda, The Netherlands). The flinders were cleaned from adherent glass dust with pressurized air.

2.1.5 Glass Powder

Borosilicate glass powder was prepared by shattering Fiolax[®] glass vials and milling in a Pulverisette[®] 5 laboratory planetary mill (Fritsch GmbH, Idar-Oberstein, Germany). The particle fraction $\leq 45 \mu\text{m}$ was collected by fractionation in a sieve tower. Subsequently, the particles were washed with ultrapure water, dried at 90 °C and heat sterilized at 250 °C.

Particles for experiments with lysozyme were again washed extensively before use until the washing media reached a pH of about 7. For electrophoretic mobility measurements, a non-

sedimenting particle fraction was used that was obtained from the supernatant of a particle suspension after 2 h sedimentation.

For experiments with IgG1, the previously washed and sterilized glass powder was again cleaned before use by immersion in 1 M NaOH and subsequent washing in water. Subsequently, the particles were heat sterilized at 200 °C for 1 h. For electrophoretic mobility measurements, the non-sedimenting glass particle fraction after centrifugation dispersed in 10 mM NaCl was used.

2.1.6 Siliconized Glass Powder

For siliconization, 1 g of glass powder prepared for experiments with IgG1 was incubated with 3 ml of a 0.5% PDMS emulsion for 30 min. After evaporation of the fluid at 150 °C the powder was cured at 200 °C for 1 h. The fraction $\leq 25 \mu\text{m}$ was collected and washed by suspending and centrifuging in water. For electrophoretic mobility measurements, the non-sedimenting glass particle fraction after centrifugation dispersed in 10 mM NaCl was used.

2.1.7 Siliconized and Non-coated Fiolax[®] Glass Slides

Coated and non-coated Fiolax[®] glass slides of the same glass composition as Fiolax[®] borosilicate glass vials with the dimension of 20 x 10 mm were kindly prepared by Schott AG (Mainz, Germany). Siliconized slides were obtained by immersion of Fiolax[®] glass slides in Dow Corning 365.

2.2 Methods

2.2.1 Adsorption Process

The adsorption process on vials followed the procedure described by Mathes & Friess [10]. The pre-processed 2R vials were filled with 3.5 ml of a 2 mg/ml IgG1 solution or 10 mg/ml lysozyme solution, closed, sealed, and incubated at 25 °C for 24 h (n=3). The vials were emptied and rinsed four times with the corresponding formulation buffer. For the desorption of bound protein, 3.5 ml of 10 mM PBS containing 145 mM NaCl and 0.05% sodium dodecyl sulfate (SDS), pH 7.2, were filled into each vial. The vials were closed and stored overnight at 25 °C.

For the adsorption of IgG1 to siliconized glass particles, the particles were incubated in protein solutions of different pH value for 24 h while gently shaken repeatedly (n=3). After centrifugation, the supernatant was removed and the particles were washed four times by

resuspending and centrifuging with 10 mM NaCl solution of the same pH as the formulation buffer. The non-sedimenting glass particle fraction in the supernatant after centrifugation at 1000 g for 1 min, dispersed in 10 mM NaCl of the formulation pH, was used for electrophoretic mobility measurements. Lysozyme containing particle suspensions were repeatedly homogenized on a laboratory vortex mixer during the 24 h incubation time. For further processing, the supernatant containing not sedimented particles was collected 2 h after the last mixing step. This particle fraction was washed with NaCl solution as described above.

2.2.2 HP-SEC

2.2.2.1 Non-native HP-SEC

Quantitative analysis of the desorbed protein was performed via HP-SEC on an Agilent 1100 HPLC device with an Agilent 1200 fluorescence detector (Agilent Technologies GmbH, Boeblingen, Germany) using a TSKgel SW_{XL} guard column and a 3000SW_{XL} SEC-column (Tosoh Bioscience GmbH, Stuttgart, Germany) with a flow rate of 0.75 ml/min for sample separation. 400 µl of the protein solution were injected and the intrinsic protein fluorescence was detected at $\lambda_{\text{ex}}/\lambda_{\text{em}}$ 280 nm/334 nm. Desorption buffer was used as mobile phase. A calibration line of 0.1-10 µg/ml IgG1 or 0.05-20 µg lysozyme, respectively, was included in each HPLC batch. Agilent ChemStation Software Rev. B 02.01 was used for manual integration of the chromatograms.

2.2.2.2 Native HP-SEC

Protein aggregates and fragments in the protein solutions were quantified via HP-SEC (equipment see 2.2.2.1) with UV-detection at λ_{ex} 280 nm. 10 mM PBS containing 145 mM NaCl, pH 7.2, served as eluent. Protein aggregates, monomer and fragments were separated on a TSKgel SW_{XL} guard column (Tosoh Bioscience GmbH, Stuttgart, Germany) and a YMC-Pack Diol-300 SEC-column (YMC Europe GmbH, Dinslaken, Germany) at a flow rate of 0.5 ml/min, applying an injection volume of 100 µl with a sample concentration of 2 mg/ml. Agilent ChemStation Software Rev. B 02.01 was used for manual integration of the chromatograms. The content of monomer, aggregates and fragments was calculated in percent of the total protein content of the reference.

2.2.3 Surface Tension Measurements

Surface tension measurements were performed on a Kruess tensiometer K100 MK2 (Kruess GmbH, Hamburg, Germany) with a Wilhelmy plate at 25 °C. The critical micelle concentration (CMC) was determined by an automatic titration of a concentrated surfactant solution in 10 mM PBS pH 7.2 with pure buffer (n=2). The surface tension was measured concentration dependent and the CMC was calculated using the Kruess laboratory desk software 3.0. Surface tension values for calculation of the adhesion tension were determined with a curved Wilhelmy plate. A sample volume of 0.9 ml was filled in a steel vessel and the surface tension was recorded for 10 min (n ≥ 2).

2.2.4 UV-Spectroscopy

UV-spectroscopy for protein quantification was performed on a NanoDrop 2000 spectrophotometer (PEQLab Biotechnology GmbH, Erlangen, Germany) at 280 nm, applying an extinction coefficient of 1.40 cm²/mg, typical for antibodies. For lysozyme, an extinction coefficient of 2.65 cm²/mg was applied [20].

2.2.5 Fluorescence Microscopy

The silicone coating on the glass particles was visualized by fluorescence microscopy (Biozero BZ-8000, Keyence GmbH, Neu-Isenburg, Germany). The particles were stained with 0.01 mg/ml Nile Red in acetone. Bright view or a TexasRed filter system with $\lambda_{\text{ex}}/\lambda_{\text{em}}$ 560 nm/630 nm with 10-fold magnification was used to visualize the particle shape or the silicone coating, respectively. The exposure time for the fluorescence was set to 1/200 s so that fluorescence was only visible for the siliconized glass powder but not for the non-siliconized reference.

2.2.6 Electrophoretic Mobility Measurements

2.2.6.1 Experiments with IgG1

The electrophoretic mobility of glass particles, siliconized glass particles and IgG1 molecules (6 mg/ml) in 10 mM NaCl was determined by dynamic light scattering with a Zetasizer Nano ZS (Malvern Instruments GmbH, Herrenberg, Germany). All measurements were performed at constantly 50 mV in disposable zeta cells. A viscosity as of water was assumed for the solutions. The pH was adjusted automatically by a Malvern MPT-2 autotitrator in a range of pH 2-10 with 0.1 M NaOH and 0.1 M HCl. For siliconized and non-coated glass particles

with a large ratio of the particle size to the Debye length κ^{-1} , the Helmholtz-Smoluchowski equation was applied for computation [21]. The ζ -potential of IgG1 was calculated according to the Hueckel approximation for small particles. Values of non-coated glass powder were obtained as an average of three measurements per pH value of one sample ($n=1$). For siliconized particles and IgG1, at least two samples with three measurements each per pH value were titrated and used for the calculation of the electrokinetic charge density ($n=2$). Zeta potentials of protein-covered siliconized particles were measured directly in 10 mM NaCl solutions of defined pH values ($n\geq 2$).

2.2.6.2 Experiments with Lysozyme

Zeta potential titrations of bare glass particles ($n=2$) and lysozyme (10 mg/ml) ($n=3$) in 10 mM NaCl were determined in a pH range of 2-12 adjusted with 0.25 M NaOH or 0.25 M HCl at constantly 50 mV (equipment and calculations compare section 2.2.6.1). The electrokinetic mobility of lysozyme-covered glass particles was measured directly in 10 mM NaCl solutions of defined pH values at 150 mV ($n=3$).

2.2.7 Streaming Potential Measurements

Streaming potential measurements were performed on a SurPASS Electrokinetic Analyzer (Anton Paar GmbH, Graz, Austria) and an adjustable gap cell with planar slides of 20 x 10 mm. Streaming potentials were measured in 1 mM KCl. Each glass sample was titrated in the range from pH 3 to pH 9 with 0.05 M NaOH or HCl, respectively, starting the titrations at neutral pH. Values were obtained as an average of four measurements per pH value. Zeta potentials were calculated from the measured streaming potentials based on the Helmholtz-Smoluchowski equation.

2.2.8 Contact Angle Measurements

Contact angles of the protein solutions or buffer on glass flinders were measured with a DSA 100 (A. Krüss Optronic GmbH, Hamburg, Germany). The glass fragments were placed horizontally on the sample table in a small transparent plastic chamber to avoid evaporation. Using a pipette, a 3 μ l droplet of the sample solution was carefully placed on the deepest point of the curvature of the flinders ($n \geq 3$). The droplet was video recorded for 700 seconds at a record rate of 0.36 frames per second. Contact angles after 10 min were calculated from the videos by manual adjustment of the base line and circle fitting using the Krüss software DSA 3.

2.2.9 Fluorescence Spectroscopy

Fluorescence spectra of protein and buffer were recorded with a Varian Cary Eclipse fluorescence spectrophotometer (Varian Deutschland GmbH, Darmstadt, Germany) in a 10 x 10 mm fluorescence quartz cuvette at 25 °C. Extrinsic fluorescence was measured in the presence of 5 μ M bis-ANS at λ_{ex} 385 nm and λ_{em} 420 – 700 nm. A protein concentration of 0.05 mg/ml was applied, corresponding to an absorption of 0.07 at the excitation wavelength, as an absorption < 0.1 at λ_{ex} is required to avoid the inner filter effect [22]. Before the measurements, the system was blanked with the corresponding buffer solution. Random noise of the extrinsic fluorescence spectra was smoothed by moving average through 12 points.

2.2.10 Light Obscuration

Subvisible particle analysis was performed via light obscuration with a PAMAS SVSS-35 (PAMAS GmbH, Rutesheim, Germany). Three fractions of 0.3 ml of each sample with 0.3 ml pre-run volume were analyzed [23]. The system was flushed with ultrapure water before each measurement until less than 100 particles per ml in total and no particles $\geq 10 \mu\text{m}$ were detected. PAMAS PMA software was used for data analysis and the amount of particles is given in cumulative particles per ml protein solution.

2.2.11 Visible Particle Inspection

The solutions were inspected visually in front of a dark background and a light source for visible particles.

2.2.12 Turbidity Measurements

Turbidity of the solutions was measured using a Nephla laboratory turbidimeter (Hach Lange GmbH, Düsseldorf, Germany). Light scattering was detected at an angle of 90 ° in turbidity glass cuvettes, applying a filling volume of 1.7 ml. Each sample was measured twice after rotating the cuvette in the holder.

2.2.13 Static Light Scattering

The size distribution of siliconized particle fractions was analyzed on a Horiba LA-950 system (Retsch Technology GmbH, Haan, Germany) by static light scattering according to the Mie Theory. For the measurements, the siliconized glass powder was suspended in 10 mM

NaCl solution and the particle size was determined based on particle volume. Data analysis and calculations were performed using the LA-950 software.

2.2.14 Isoelectric Focusing

The isoelectric point of IgG1 was determined by isoelectric focusing (IEF) using precast SERVALYT PRECOTES[®] 6-9 IEF plates with a thickness of 300 μm . 10 μl per sample with a concentration of 0.5 mg/ml adjusted by dilution with ultrapure water and SERVA Liquid Mix IEF marker 3-10 (SERVA Electrophoresis GmbH, Heidelberg, Germany) were applied to the gel. Electrophoresis was performed at 2000 V and 6 mA at 5 °C. The gels were stained with SERVA Blue W (SERVA Electrophoresis GmbH, Heidelberg, Germany).

2.2.15 Specific Surface Area Analysis

The specific surface area of the siliconized particles was determined with an Autosorb 1 system (Quantachrome, GmbH & Co. KG, Odelzhausen). The sample was outgassed for at least 15 h at 25 °C before the physisorption of krypton. Specific surface area analysis of non-siliconized particles used for adsorption experiments with lysozyme was performed by nitrogen gas sorption with a NOVA 4000e system (Quantachrome GmbH & Co. KG, Odelzhausen).

2.2.16 Calculation of the Change in Electrokinetic Charge Density

Derived from the theory of diffuse double layers, the electrokinetic charge density σ_{ek} of siliconized particles, protein molecules and protein covered siliconized particles was calculated from the ζ -potential by Eq. (1) [21]:

$$\sigma_{\text{ek}} = -\sqrt{8\varepsilon_0\varepsilon cRT} \sinh(zF\zeta/2RT) \quad (1)$$

ε_0 represents the dielectric permittivity of vacuum and ε the relative dielectric constant of the medium. The concentration of the z-z electrolyte is given by c , R is the gas constant, T the absolute temperature and F the Faraday constant. For ε a value of water was assumed. According to the principle of electroneutrality, the charge uptake $\Delta_{\text{ads}}\sigma_{\text{ek}}$ due to adsorption is given by Eq. (2) [11, 24]:

$$\Delta_{\text{ads}}\sigma_{\text{ek}} = \sigma_{\text{ek}}(\text{IgG/silicon. glass}) - \sigma_{\text{ek}}(\text{silicon. glass}) - \sigma_{\text{ek}}(\text{IgG1}) \cdot \Gamma \cdot A \quad (2)$$

σ_{ek} represents the charge density per unit surface area at the slipping layer of the complex IgG1/siliconized glass (IgG1/silicon. glass), of the siliconized glass particles (silicon. glass) or the IgG1 molecule (IgG1) in solution [11]. Γ equals the mass of IgG1 adsorbed per unit surface area and A the surface area per unit mass protein according to Eq. (3) [11]:

$$A = \frac{4\pi r^2 \cdot N_A}{M_w} \quad (3)$$

The term $4\pi r^2$ represents the surface area of one IgG1 molecule of approximately 335 nm^2 when a hydrodynamic radius r of 5.16 nm and a spherical shape of the molecules is assumed [10]. A molecular weight M_w of 152 kDa for IgG1 was applied and N_A equals the Avogadro's number. Values of Γ for the calculation of $\Delta_{\text{ads}}\sigma_{\text{ek}}$ were taken as an approximation from the pH-dependent adsorption at an ionic strength of 40 mM .

2.2.17 Calculation of the Change in Interfacial Tension

When a drop of a liquid is placed on a surface, its shape will depend on the properties of the liquid, the surface and the surrounding air [25]. The relationship between the contact angle θ and the surface tension of the liquid γ_l , the surface tension of the solid γ_s and the interfacial tension between solid and liquid γ_{sl} is described by the equation of Young:

$$\gamma_l \cdot \cos \theta = \gamma_s - \gamma_{sl} \quad (4)$$

From this equation, the adhesion tension τ of a protein or surfactant solution (index \prime) or of pure water / saline (index $^\circ$) can be derived [26]:

$$\tau' = \gamma'_l \cdot \cos \theta' \quad (5)$$

$$\tau^\circ = \gamma^\circ_l \cdot \cos \theta^\circ \quad (6)$$

Vogler defined the difference in adhesion tension between a protein and its solvent solution $[\tau' - \tau^\circ]$ as the adsorption index (AI) [26].

$$\tau' - \tau^\circ = \gamma'_l \cdot \cos \theta' - \gamma^\circ_l \cdot \cos \theta^\circ \quad (7)$$

For calculation of the adhesion tension and the adsorption index, static contact angles and surface tensions after an equilibration time of 10 min were used.

3 RESULTS AND DISCUSSION

3.1 IgG1 Adsorption to Type I Borosilicate Glass Vials and Siliconized Vials

3.1.1 Charge Characterization and Electrostatic Interactions of IgG1 and Siliconized Glass

At first, in order to understand the charge effects on protein adsorption, the zeta potential of IgG1 as well as of siliconized and non-coated glass was determined as a function of pH. The siliconized particles used for adsorption experiments exhibited a specific surface area of $0.79 \pm 0.012 \text{ m}^2/\text{g}$ as determined by krypton sorption in two independent BET measurements. The correlation coefficient of the measurements was $R > 0.9978$. The silicone coating was visualized by staining with Nile Red (Figure II-1a). Static light scattering showed a bimodal size-frequency distribution of the siliconized glass powder (Figure II-2a). Although the powder had been fractionated through a $25 \mu\text{m}$ sieve, some oversized particles were found. For the electrokinetic mobility measurements, a fraction with particle sizes of largely $< 1 \mu\text{m}$ was used (Figure II-2b) (section 2.1.6).

Electrophoretic mobility measurements were applied for zeta potential measurements of solvated IgG1 and suspended silicone-coated and non-coated glass particles. Additionally, streaming potential measurements of siliconized and non-coated planar glass slides served as

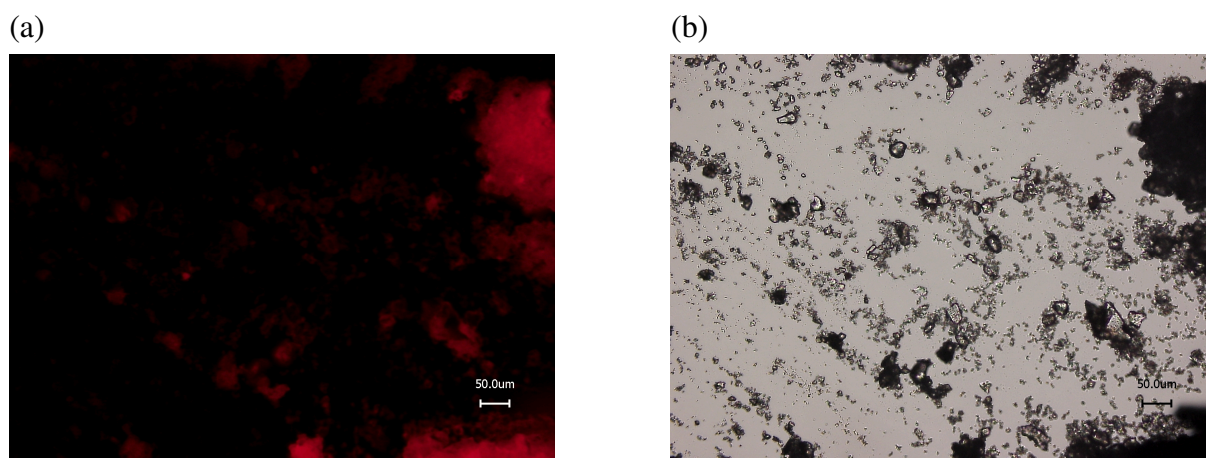


Figure II-1: Siliconized glass particles at 10-fold magnification (a) stained with Nile Red at $\lambda_{\text{ex}}/\lambda_{\text{em}}$ 560/630 nm and an exposure time of 1/200 s and (b) at bright view.

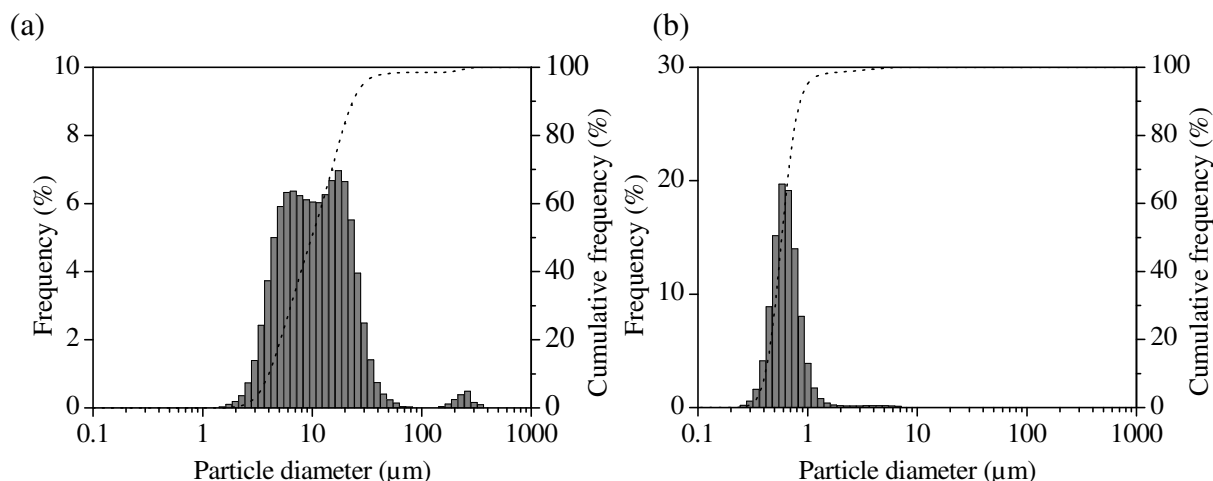


Figure II-2: Frequency distribution of siliconized particles fractionated through a 25 μm sieve (a) and of the non-sedimenting particle fraction (b).

a reference method. For the IgG1 in solution, a titration curve typical for proteins was obtained with a pI of 7.8 (Figure II-3a). The PDMS-coated glass particles exhibited a more positive zeta potential in the examined pH-range compared to non-coated glass particles.

Starting at approx. 13 mV at pH 2, the zeta potential of siliconized glass decreased to a pI of 3.4 and continued to a minimum of about -32 mV at pH 8.4. The non-coated glass particles with a pI of less than 2 showed a negative surface charge in the whole pH range between 2 and 10 due to the dissociation of silanol groups at the glass surface. The zeta potential determined from streaming potential measurements for the planar siliconized glass surface was qualitatively in good agreement with the data for the siliconized particles. A pI of 3.6 was

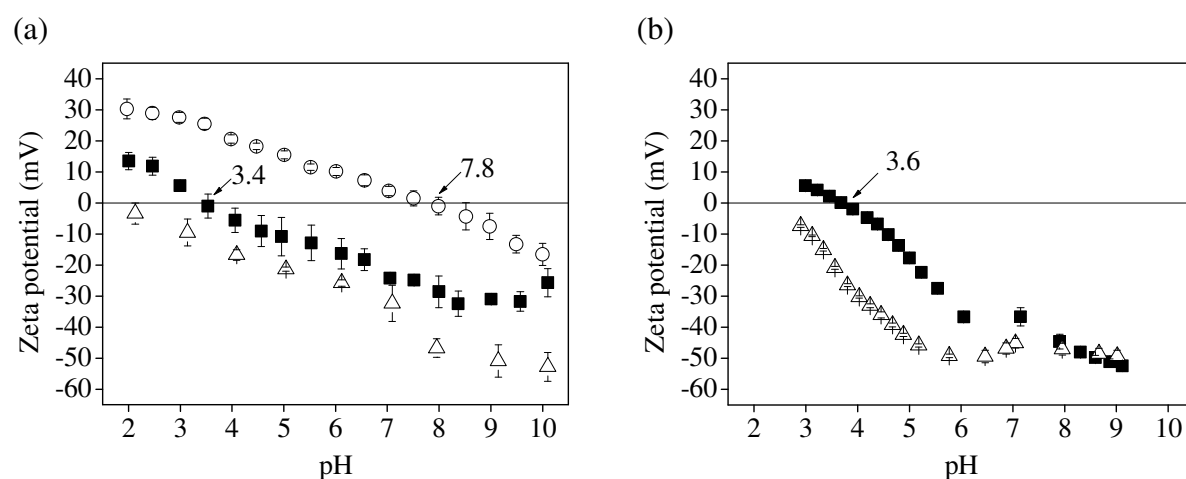


Figure II-3: Zeta potential of glass (Δ), siliconized glass (\blacksquare) and IgG1 (\circ); (a) determined by electrokinetic mobility measurements of coated and non-coated glass particles and IgG1 in 10 mM NaCl solution; (b) determined by streaming potential measurements of coated and non-coated planar glass slides in 1 mM KCl solution.

determined for siliconized glass slides (Figure II-3b). In the tested pH range of 3 to 9, the pI of uncoated glass slides was not reached. With increasing pH, the titration curves reached a minimum of about -49 to -52 mV. Discrepancies of the zeta potentials obtained from electrophoretic mobility measurements and streaming potential measurements may be due to the different measurement techniques and surface morphologies as well as the slightly higher electrolyte concentration used for electrophoretic mobility measurements.

In literature, the pI of silica is found at approx. 2 [10, 27] but may vary in a range between $\text{pH} < 1.5$ and approx. 6, depending on the concentration and type of salt in the solution [27, 28]. In contrast, the pI of pure silicone oil droplets in solution was found near pH 5.0 [29]. Song et al. determined the pI of PDMS-coated glass slides in low concentrated NaCl solution and phosphate buffer at approximately pH 4.5 - 5 [30] and Roth et al. found a pI of PDMS-coated silicon wafers at approx. 4 - 4.5 [31]. Thus the pI determined for our PDMS-coated glass particles is slightly lower than the pI reported in literature. After silylation of the glass surface with PDMS, a small fraction of silanol groups was found remaining at the surface [32]. Thus, the dissociation of residual silanol groups and the adsorption of ions from solution determine the zeta potential of a PDMS-coated surface. Consequently, the pI of the coated surface will be located between the pI of the uncoated surface and of pure silicone oil in solution. The lower pI of our siliconized glass surfaces compared to literature indicates that a rather thin silicone layer was formed and that a fraction of silanol groups characterizes the surface.

3.1.2 Investigation of Adsorption of IgG1 to Borosilicate Glass and Siliconized Glass by Static Contact Angle Measurements

The adsorption of proteins is influenced by the sorbent surface characteristics such as hydrophobicity, electrical state and the specific surface area [24]. Numerous studies showed that hydrophobic surfaces in general adsorb more protein than hydrophilic ones [33-36]. Several approaches were made to align the protein adsorption to sorbent surface properties, e.g. to surface energy [37]. Vogler suggested that the surface energy does not directly control the biological response on a surface, but rather the water reactivity and structure which then influences reactions such as cell adhesion and protein adsorption [26]. Therefore, he correlated an index of solid-liquid interfacial tensions [$\tau' - \tau^\circ$], which quantifies adsorption, to the wettability τ° of a surface and found a linear correlation [26, 38]. According to Vogler's theory of the 'adsorption map', values of [$\tau' - \tau^\circ$] > 0 or [$\tau' - \tau^\circ$] ≤ 0 can be assigned to

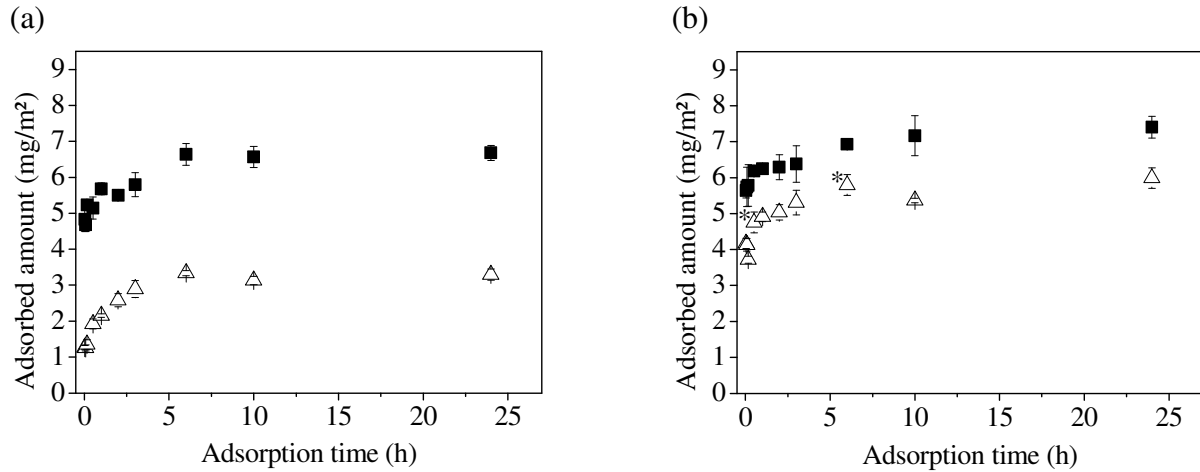


Figure II-4: Adsorption kinetics of IgG1 to borosilicate glass vials (a) and siliconized glass vials (b) at pH 4 (■) and pH 7.2 (Δ); incubation at 25 °C, 2 mg/ml in 10 mM phosphate buffer with 170 mM ionic strength (n=3, *n=2).

surfaces supporting or repelling adsorption, respectively [26] and the map can be used to predict the adsorption behavior on surfaces [38].

To evaluate whether the siliconized and the bare glass surface support the adsorption of IgG1 according to this theory, the adsorption index (AI) [$\tau' - \tau^\circ$] and the adhesion tension τ° for both surfaces was determined for 2 mg/ml IgG1 solutions and the corresponding buffer according to Eq. (6) and (7). Measurements were performed with solutions of pH 4 as the adsorbed amount and thus the sensitivity of the measurements was expected to be higher than at pH 7.2 (Figure II-4a, b). In contrast to Vogler et al. who determined advancing and receding contact angles [38], static contact angles were determined in our experimental setup. As a compromise between sufficiently long adsorption time and reasonable measurement duration, contact angles and surface tensions were recorded 10 min after placing the droplet onto the surface. After this time, adsorption reached more than 70% of the plateau value on both siliconized and bare glass vials (Figure II-4a, b) so that changes of the contact angle due to adsorption could be expected. Figure II-5a shows the adsorption map for IgG1 in 10 mM PBS pH 4. The borders of the depicted parallelogram represent the practically possible adsorption indices [$\tau' - \tau^\circ$] calculated from the measured surface tension of the protein solution and practically (for surfactants) observed maximal possible ($\theta' \rightarrow 120^\circ$) or minimal ($\theta' \rightarrow 0^\circ$) values of the contact angle of the protein solution [38]. The corresponding τ° values were calculated from the measured surface tension γ_1° and the theoretical contact angle θ° of the corresponding solvent. The intersecting line indicates the situation of identical contact angles of the protein solution and the pure solvent ($\theta' = \theta^\circ$) [38]. For borosilicate

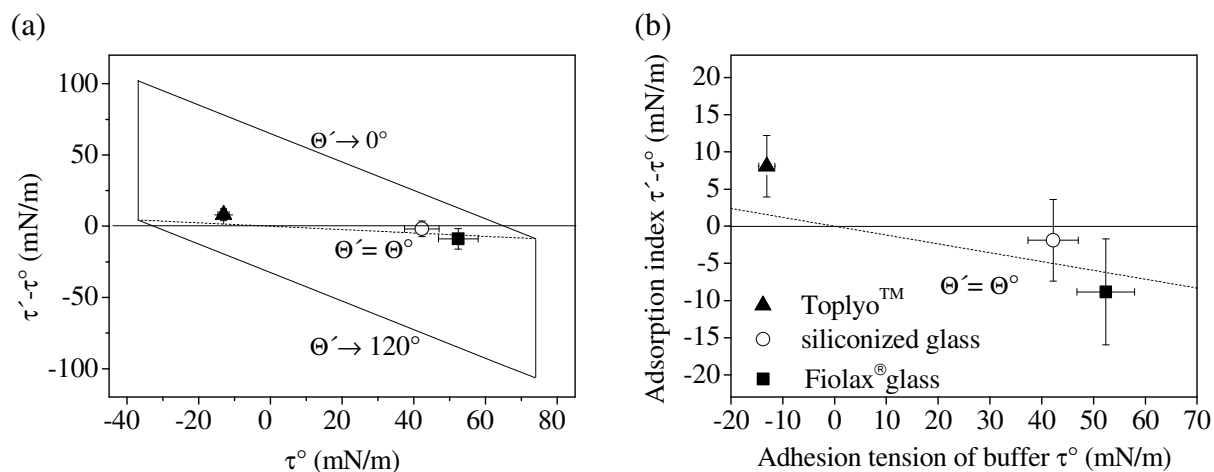


Figure II-5: Adsorption map of IgG1 2 mg/ml in 10 mM phosphate buffer with 170 mM ionic strength, pH 4, including TopLyoTM vials, siliconized vials and borosilicate glass vials; (a) with adsorption boundaries; (b) enlarged section with calculated values.

glass vials and siliconized glass vials, the AI was in the negative range slightly above or below the ($\theta' = \theta^\circ$) line (Figure II-5b) without a significant difference between the contact angles of protein solution and pure solvent. Thus, the contact angle measurements did not indicate adsorption. In contrast, the AI of TopLyoTM vials was positive with a significant difference between θ' and θ° ($p < 0.05$). As mentioned above, this may indicate that only the TopLyoTM vials were hydrophobic enough to support adsorption. However, significant adsorption of IgG1 was found also on siliconized and bare glass vials (Figure II-4a, b). To explain this kind of discrepancy, Vogler proposed that on hydrophilic surfaces, adsorption occurs rather by association of the solute with an incorporated aqueous layer than by physicochemical binding to the surface involving a change of the interfacial tension [26].

In conclusion, the prediction of IgG1 adsorption to siliconized and bare glass vials by calculation of the adsorption index is not feasible for our experimental setup. A clear interpretation of the obtained results depicted in Figure II-5 is difficult due to the high standard deviations of the contact angles and thus of τ° and the AI. This may derive from the measurement technique applied for the contact angle measurements. Most surfaces such as glass show hysteresis of the contact angles due to roughness and chemical heterogeneities, so that advancing as well as receding contact angles are necessary to thoroughly characterize the wettability of a solid surface [38]. However, our experimental setup enabled only static measurements. The manual application of the droplet on the surface and the curvature of the fragment itself may also have influenced the droplet shape.

3.1.3 Influence of Formulation pH and Ionic Strength on IgG1 Adsorption to Siliconized Glass Vials

3.1.3.1 Adsorbed IgG1 Quantity as a Function of pH

The influence of pH on IgG1 adsorption to siliconized glass vials was investigated between pH 2 and 12 (Figure II-6). Adsorption experiments were performed at a concentration of 2 mg/ml IgG1, at which adsorption plateau values (Γ_{pl}) for IgG1 on siliconized vials were reached (Figure II-7). The pH-dependent adsorption exhibited a bell-shaped curve as commonly found for protein adsorption at solid-liquid interfaces [10, 39, 40] with an adsorption maximum at a pH of 4 to 5 with about 5.0-5.2 mg/m² (Figure II-6). A second maximum was found around the pI of the protein (7.8) at pH 7 to 9 with adsorption values of about 4.5 mg/m². With further increasing pH the adsorption level dropped sharply. At pH 12, no adsorption could be detected. Thus, for the IgG1 antibody the adsorption maximum was not located at the pI of the protein but at acidic pH conditions. As shown by electrophoretic mobility measurements, the pIs of the siliconized surface and the antibody are both located within the investigated pH range (Figure II-3a). As a consequence, repulsive or attractive electrostatic interactions between the protein and the surface as well as intermolecular repulsive forces may contribute to the adsorption process at different pH values. In the pH range between the pI of siliconized glass of approx. 3.4 and the pI of the antibody of approx. 7.8, protein and sorbent were oppositely charged. At pH 4 to 5 the two partners carried substantial charge of similar absolute value but opposite algebraic sign, resulting in a strong electrostatic attraction. At lower solution pH, the protein net charge and thus the

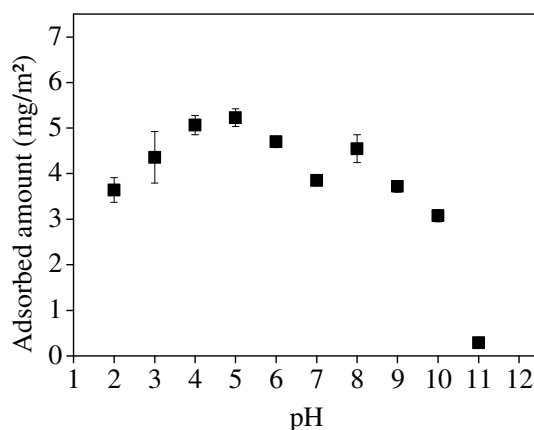


Figure II-6: Adsorption of IgG1 to siliconized glass vials depending on formulation pH; incubation time 24 h at 25 °C, 2 mg/ml in 10 mM phosphate buffer with 170 mM ionic strength (n=3).

intermolecular repulsion increased, leading to reduced IgG1 adsorption. Electrostatic repulsion between protein and sorbent at pH values below the pI of siliconized glass finally resulted in significantly reduced adsorbed amounts. Nevertheless, considerable adsorption was still found below pH 3.4 which can be attributed to hydrophobic protein-surface interactions. At pH values above the adsorption maximum, the decreased protein charge led to reduced adsorption due to the low electrostatic attraction.

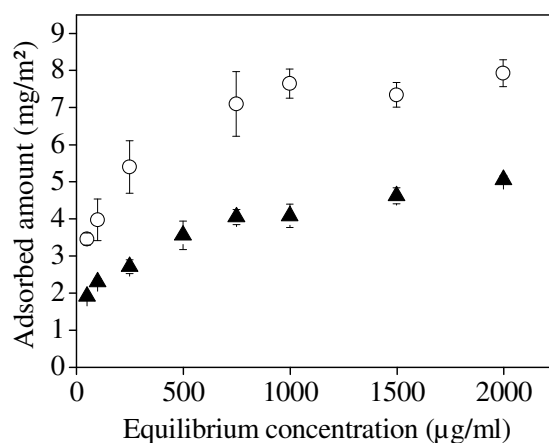


Figure II-7: Adsorption isotherm of IgG1 at pH 4.0 (O) and pH 7.2 (▲) on siliconized glass vials in 10 mM phosphate buffer with 170 mM ionic strength adjusted with NaCl and incubation at 25 °C (n=3).

Adsorption maxima at pH values below the pI of the protein were also reported by Salgin et al. and Mathes & Friess [10, 41]. In contrast, Norde et al. observed a coincidence of the adsorption maximum with the region of the protein pI [42]. It was suggested that structural perturbations in the protein molecules lead to reduced adsorbed amounts at pH values away from the pI [42, 43]. Furthermore, high adsorbed amounts of IgG around the pI were explained by a low intermolecular repulsion and high adsorption rates in this pH region [39]. In the mentioned literature studying the pH-dependence of protein adsorption, in most cases a single adsorption maximum was observed, e.g. for the adsorption of monoclonal IgG1 to hydrophilic borosilicate glass vials [10]. In contrast, the adsorption profile for IgG1 on hydrophobic siliconized glass vials showed a second local maximum around the pI of the protein at pH 7-9. Due to the low protein charge at this pH, electrostatic interactions with the surface contributed only marginally to adsorption. On the other hand, hydrophobic interactions with the siliconized surface were increased, and on hydrophobic surfaces, the decrease in Gibbs energy due to surface dehydration dominates over the changes by electrostatic effects [44]. Therefore, adsorption of proteins to surfaces exhibiting hydrophobic domains can be observed in general even when the electrostatic conditions are unfavorable

[44]. Thus, the second adsorption maximum supposedly resulted from hydrophobic interactions of IgG1 with the hydrophobic siliconized glass surface, whereas the first adsorption maximum was driven by the predominance of attractive electrostatic interactions. At pH values above 7.8, both the antibody and the surface owned an increasingly negative net charge. The growing repulsion in between the protein molecules as well as between protein and sorbent led to a sharp drop of the adsorbed amount resulting in less than 0.5 mg/m² IgG1 at pH 11-12. Similar adsorption trends were also described in literature [45, 46]. Despite adverse electrostatic conditions, considerable amounts adsorbed, potentially due to the transfer of ions between the protein-sorbent interface and the solution [47]. Furthermore, a decrease in Gibbs energy by the dehydration of hydrophobic surface patches due to protein adsorption [48] or structural rearrangements of the protein [47] were possible driving forces for adsorption.

3.1.3.2 Influence of Ionic Strength on IgG1 Adsorption

The contribution of electrostatic interactions to IgG1 adsorption at different pH values was further investigated by analyzing the adsorbed amount at different ionic strengths up to 1 M adjusted with NaCl. Γ_{pl} were determined exemplary at pH 4.0 and 7.2, representing a pH close to the adsorption maximum and a common formulation pH in the range of the second maximum, respectively (compare section 3.1.3.1). At pH 4.0 an increase of the ionic strength up to 1 M resulted in rising adsorption values (Figure II-8) whereas a marginal decrease in adsorption was observed at pH 7.2. For the interpretation of the observed trend toward electrostatic interactions, the role of ions in the adsorption process has to be considered. At

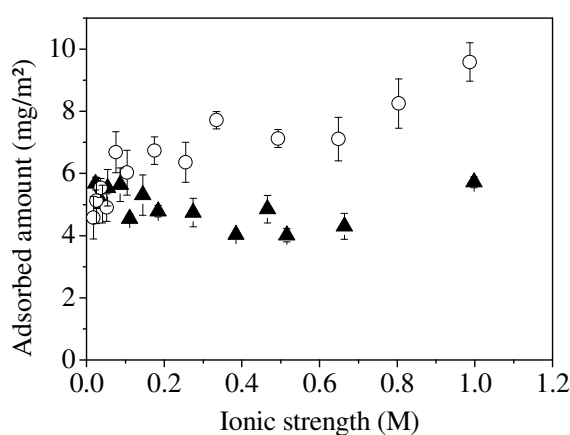


Figure II-8: Adsorption of IgG1 in dependence of ionic strength at pH 4.0 (○) and 7.2 (▲); incubation time 24 h at 25 °C, 2 mg/ml in 10 mM phosphate buffer, ionic strength adjusted with NaCl (n=3).

high salt concentrations, the screening of intermolecular repulsive forces can increase the adsorption whereas the shielding of attractive electrostatic interactions between protein and sorbent may reduce the adsorption [46]. Increasing adsorbed amounts with rising ionic strength at pH 4.0 thus indicated the shielding of predominantly intermolecular repulsive forces that limited the packing density on the surface, rather than a screening of electrostatic attractive forces. At pH 7.2, the electrostatic attraction toward the hydrophobic surface but also the intermolecular repulsion was negligible due to the low net charge of the protein. The weak effect of ionic strength on IgG1 adsorption at pH 7.2 thus underlined the minor importance of electrostatic interactions for the adsorption process and suggested superiority of hydrophobic interactions with the siliconized surface. A similar trend was also found for IgG1 adsorption to hydrophobic COP plastic vials at pH 7.2 and was ascribed to the predominance of dispersion forces and hydrophobic interactions for adsorption and the minor importance of electrostatic interactions between the protein molecules [10].

In section 3.1.3.1, the pH of maximum adsorption was determined at the basis of an adsorption profile at an ionic strength of $I = 170$ mM and correlated with zeta potential measurements performed at much lower ionic strength. However, the ionic strength dependent adsorption study showed that predictions of the adsorbed amount at a certain ionic strength over a large pH range are difficult. Therefore, the pH-dependent adsorption was additionally determined at a lower ionic strength of $I = 40$ mM to allow a better comparison with results of the zeta potential measurements.

Compared to the adsorption profile obtained at $I = 170$ mM, the curve at $I = 40$ mM was shifted toward higher pH values in the range of pH 2-7 with the adsorption maximum at

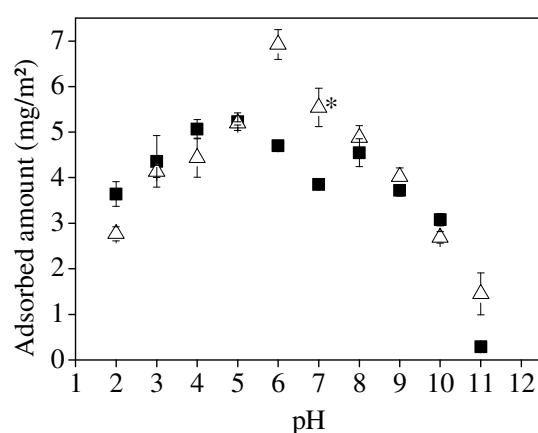


Figure II-9: Adsorption of IgG1 to siliconized glass vials depending on formulation pH at 40 mM (Δ) or 170 mM (■) ionic strength adjusted with NaCl; incubation time 24 h at 25 °C, 2 mg/ml in 10 mM phosphate buffer (n=3, *n=2).

pH 6-7 instead of pH 4-5 (Figure II-9). At pH values above pH_{\max} , the adsorption curves at both ionic strengths virtually matched so that the second maximum observed at $I = 170$ mM was reduced to a shoulder. At pH 12, adsorption could not be quantified anymore. A shift of the adsorption maximum toward higher pH values at decreased ionic strength was also described for IgG on silica [49, 50] as well as on borosilicate glass vials [10]. The new adsorption maximum at pH 6-7 resulted from a charge state of IgG1 allowing sufficient attractive electrostatic interactions with the surface but comparably low intermolecular repulsion so that a dense occupation of the surface with protein molecules was possible. Around the pI of IgG1, the influence of ionic strength on adsorption was low due to the dominance of hydrophobic and dispersion interactions with the surface and low intermolecular repulsive forces. At acidic pH values, the reduced adsorption at decreased ionic strength confirmed the trend observed previously in Figure II-8.

3.1.4 Electrostatic Interactions within the Adsorption Interface

When a protein adsorbs to a sorbent, the electrical fields of both components overlap [51]. Charge redistribution takes place, which was thoroughly investigated by Norde and Lyklema [44, 48]. If the charges of sorbent and protein do not compensate each other, the accumulation of net charge in the contact region between both components leads to an energetically unfavorable, high electrostatic potential [44]. To prevent such an excess of net charge, an exchange of low-molecular-weight-ions between the adsorption layer and the surrounding solution may take place [44]. However, the unfavorable chemical effect of the incorporation of ions counteracts adsorption [48]. Thus, maximum adsorption affinity is found when no ions are additionally incorporated into the contact region [44]. Determination of the pH-dependent charge transfer $\Delta_{\text{ads}}\sigma_{\text{ek}}$ between the solution and the protein-sorbent interface thus is a helpful tool to interpret the location of $\Gamma_{\text{pl}}(pH)_{\max}$. $\Delta_{\text{ads}}\sigma_{\text{ek}}$ can be calculated from the zeta potentials of the protein, the sorbent and the protein-sorbent complex as well as the adsorbed amount per unit surface area $\Gamma_{\text{pl}}(pH)$ [11] as defined in section 2.2.16, Eq. (2). Zeta potentials of protein covered particles were determined in the pH range of 4-9 and compared to that of solvated protein and siliconized particles (Figure II-10). The values of the protein-particle complex were expected to lie in between the curves of the uncoated particles and the protein due to a partial coverage of the negatively charged siliconized surface with positively charged protein molecules. In fact, the resulting curve with a pI of 7.7 strongly resembled the curve of the protein with a pI of 7.8. The similar pIs of the protein and the protein-covered particles indicated a vast compensation of the negative charge of the sorbent surface by adsorbed

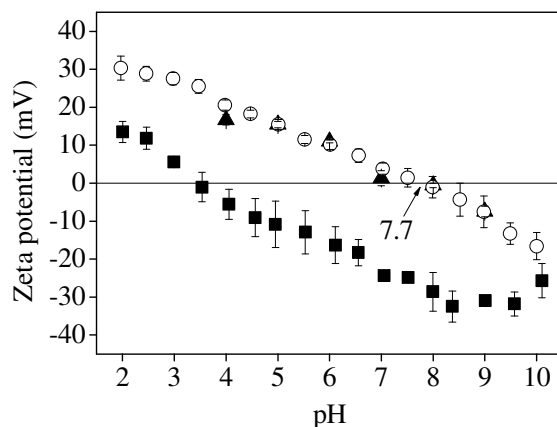


Figure II-10: Zeta potential of siliconized glass particles (■), IgG1 (○) and siliconized particles with adsorbed IgG1 (▲) in 10 mM NaCl solution.

counterions [11] or by the positive charges of the protein. $\Delta_{\text{ads}}\sigma_{\text{ek}}$ was calculated from the zeta potentials determined in 10 mM NaCl solutions. $\Gamma_{\text{pl}}(pH)$ were taken as an approximation from the pH-dependent adsorption at an ionic strength of $I = 40$ mM (Figure II-9).

In Figure II-11, $\Delta_{\text{ads}}\sigma_{\text{ek}}$ for the adsorption of IgG1 to siliconized glass particles is depicted. With increasing pH, the curve rose from negative to positive $\Delta_{\text{ads}}\sigma_{\text{ek}}$ values. Intersection with the x-axis at approx. pH 7.0 indicated energetically favorable adsorption conditions at this pH with a minimum incorporation of additional ions into the adsorption layer. Negative values of $\Delta_{\text{ads}}\sigma_{\text{ek}}$ in the pH range from 4.0 to 7.0 indicated an additional uptake of negatively charged ions to compensate the positive charges of the adsorbed protein, whereas further cations were incorporated above pH 7.0 [11]. If charge neutrality in the interface is assumed to be the driving factor for protein adsorption, maximum adsorption affinity for IgG1 adsorption in

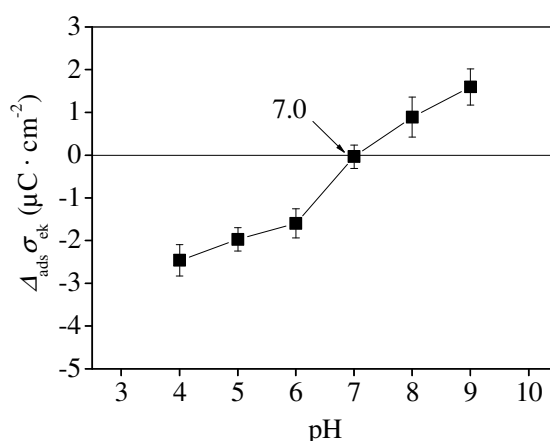


Figure II-11: Charge transfer ($\Delta_{\text{ads}}\sigma_{\text{ek}}$) between the adsorbed layer and the surrounding liquid; $\Delta_{\text{ads}}\sigma_{\text{ek}}$ calculated according to Eq. (2); $\Gamma_{\text{pl}}(pH)$ taken from pH-dependent adsorption at 40 mM ionic strength. Standard deviations were calculated by applying the Gaussian error propagation.

10 mM NaCl was expected at pH 7.0. Decreasing the ionic strength from 170 mM to 40 mM already shifted the adsorption maximum from pH 4-5 to pH 6-7. Thus, a further shift toward pH 7 in 10 mM NaCl solution and a correspondence of the adsorption maximum with $\Delta_{\text{ads}}\sigma_{\text{ek}} = 0$ may be expected. A correlation of the adsorption maximum at low ionic strength with the pH of minimal charge uptake into the protein-sorbent interface was also observed by Mathes & Friess [10]. Elgersma reported a coincidence of the adsorption maximum with the pI of protein-covered particles for bovine serum albumin on different latices [11], whereas Buijs et al. determined the maximum adsorption of F(ab')₂ at pH values between the pI of the protein and the protein-particle complex [52]. Thus, a clear correlation between the adsorption maximum, the pH of minimal charge uptake and the pI of the protein-sorbent complex was not generally found but is a conceivable concept.

3.1.5 Influence of Non-ionic Surfactants on IgG1 Adsorption

In the following, the influence of polysorbate 80 (PS 80) and poloxamer 188 (P 188) on IgG1 adsorption to siliconized and non-siliconized vials at pH 4.0 and 7.2 was investigated. Both non-ionic surfactants are approved for parenteral use. As protein stabilization against aggregation by surfactants was shown to depend on the molar ratio of surfactant and protein [53, 54], the detergents were added to the IgG1 formulation at surfactant:protein molar ratios of 1:10 up to a surfactant excess of 1000:1.

On siliconized glass vials, both surfactants effectively suppressed IgG1 adsorption. At pH 7.2

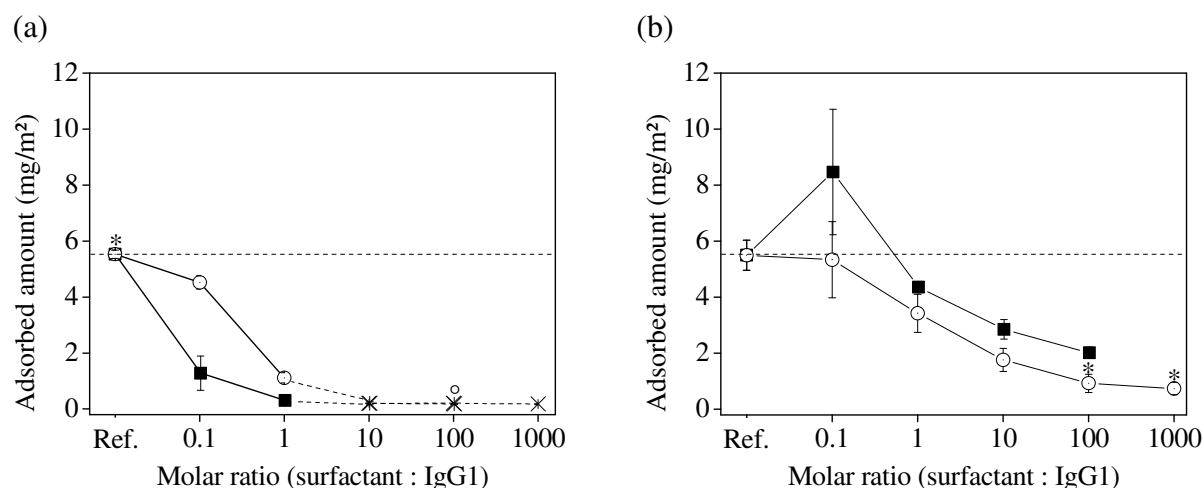


Figure II-12: Influence of polysorbate 80 (O) and poloxamer 188 (■) on adsorption of IgG1 to siliconized glass vials at pH 7.2 (a) and pH 4.0 (b); 2 mg/ml in 10 mM phosphate buffer with 170 mM ionic strength; incubation time 24 h at 25 °C. Values depicted with (x) could not be quantified anymore (n=3, *n=2, °n ≥ 1).

and molar ratios of 10:1 and higher, adsorption was reduced by at least 95% to values which could not be quantified any more (Figure II-12a). In contrast, a molar ratio of 100:1 PS 80 or P 188 was necessary at pH 4.0 to reduce adsorption by approx. 83% or 63%, respectively (Figure II-12b). No results could be obtained for a molar ratio of 1000:1 P 188 so that the maximum effect could not be determined.

Most nonionic surfactants are supposed to mainly interact with the sorbent surface [55] and their adsorption preventing effect was ascribed to the formation of a detergent layer at the sorbent surface [16]. However, a direct interaction of nonionic surfactants with specific protein sites was observed in some cases [55]. Therefore, an interaction of the nonionic surfactants with hydrophobic protein sites may be considered, preventing hydrophobic interactions with other proteins [53] or surfaces. Interestingly, low concentrations of P 188 led to increased adsorption at pH 4.0. A similar effect was described previously for protein adsorption in presence of SDS [56]. The authors related this phenomenon to a binding of the surfactant to the protein, leading to an increased adsorption by changes in the protein structure, or to an increased hydrophobicity of the protein-surfactant complex. Moreover, it was suggested that surfactants at low concentration may increase the surface hydrophobicity and thus the protein adsorption [55]. Both mechanisms were assumed to contribute to the observed effect on siliconized glass vials.

At pH 7.2, strong hydrophobic interactions were supposed to dominate adsorption of the marginally charged protein to the negatively charged but hydrophobic siliconized glass surface (see section 3.1.3.1). Shielding of hydrophobic protein sites and of the sorbent surface by nonionic surfactants efficiently reduced the adsorption of IgG1 at this pH. At pH 4.0, the adsorption was reduced to a much lower extent than at pH 7.2. This indicated an only marginal suppression of the strong electrostatic interactions between protein and sorbent at this pH by PS 80 and P 188.

At pH 7.2, P 188 was found superior to PS 80 in suppressing IgG1 adsorption, whereas the inverse trend was observed at pH 4.0. It was shown that the ability of nonionic surfactants to prevent protein adsorption decreased with an increased content of hydrophilic domains of the detergent [15]. PS 80 with an HLB value of 15 is more hydrophobic than P 188 which exhibits an HLB value above 24 (Table II-1). Therefore, PS 80 was expected to interact stronger with hydrophobic protein surface residues than P 188 and to suppress adsorption with higher efficiency. However this trend was only observed at pH 4.0. Furthermore, PS 80 and P 188 exhibit great differences in their critical micelle concentration (CMC). For PS 80, the CMC in PBS pH 7.2 was determined at a concentration of 0.0017% (w/v), corresponding to a

molar ratio of surfactant:protein of about 1:1 (Table II-2). P 188 exhibits a CMC of 0.4032-1.0032% in water [57, 58], corresponding to a surfactant:protein ratio higher than 10:1. Values for the CMC of P 188 were derived from literature as a determination at 25 °C in PBS by surface tension measurements was not possible. At pH 7.2, maximum adsorption suppression was reached close to the CMC of both surfactants whereas no clear correlation was found for adsorption at pH 4.0. Overall, no general correlation was found between the CMC and the concentration of maximum adsorption suppression. It also needs to be considered that P 188 may show a slower adsorption at the water / silicone oil interface than PS 80 due to its lower diffusion coefficient [6]. This makes a faster formation of a detergent film at the buffer/vial interface by PS 80 and a superior prevention of IgG1 adsorption conceivable.

Both surfactants were found efficient in suppressing IgG1 adsorption to siliconized glass vials at a standard ionic strength of 170 mM. Furthermore, as described in section 3.1.3.2, a

Table II-1: Surfactant characteristics of polysorbate 80 and poloxamer 188.

	Polysorbate 80 (PS 80)	Poloxamer 188 (P 188)
^a CMC (in % (w/v))	^d 0.0017±0.00058	^e 0.4032-1.0032% [57, 58]
^b HLB value	15 [59]	> 24 [57, 58]
^c MW (g/mol)	1310	8600 [60]

^acritical micelle concentration (CMC)

^bhydrophilic lipophilic balance (HLB)

^cmolecular weight

^dCMC determined in 10 mM PBS, 145 mM NaCl pH 7.2 at 25 °C

^eCMC determined in water, values derived from literature

Table II-2: Molar ratios of surfactant and protein and corresponding concentrations in percent (w/v).

Molar ratio surfactant:protein^a	Corresponding surfactant concentration in percent (w/v)	
	Polysorbate 80 (PS 80)	Poloxamer 188 (P 188)
1:10	0.00017	0.0011
1:1	0.0017	0.011
10:1	0.017	0.11
100:1	0.17	1.1
1000:1	1.7	11

^aactual molar ratios in experiments may deviate slightly from the theoretical value

reduction of the protein adsorption can be reached by adjusting the ionic strength, depending on solution pH. Consequently, the effect of PS 80 and P 188 on IgG1 adsorption to siliconized vials was additionally investigated at a minimum ionic strength of 17 or 23 mM in 10 mM phosphate buffer at pH 4.0 and 7.2, respectively, at a fixed surfactant:protein ratio of 10:1.

Decreasing the ionic strength at pH 7.2 led to a slight increase of adsorption without surfactants as was already discussed in section 3.1.3.2, and also the adsorption suppressing effect of PS 80 and P 188 was slightly reduced at low ionic strength (Figure II-13a). At pH 4.0, adsorption in surfactant-free solutions was decreased at low ionic strength. This trend was also observed in presence of the surfactants and PS 80 proved to be slightly superior to P 188 in suppressing adsorption (Figure II-13b). Also at low ionic strength, the adsorption reduction by surfactants in percent was stronger at pH 7.2, where hydrophobic interactions dominated the adsorption process, than at pH 4.0. Thus, the influence of ionic strength on the overall adsorption trend was maintained in presence of the nonionic surfactants and adsorption prevention can be enhanced by an appropriate combination of both parameters.

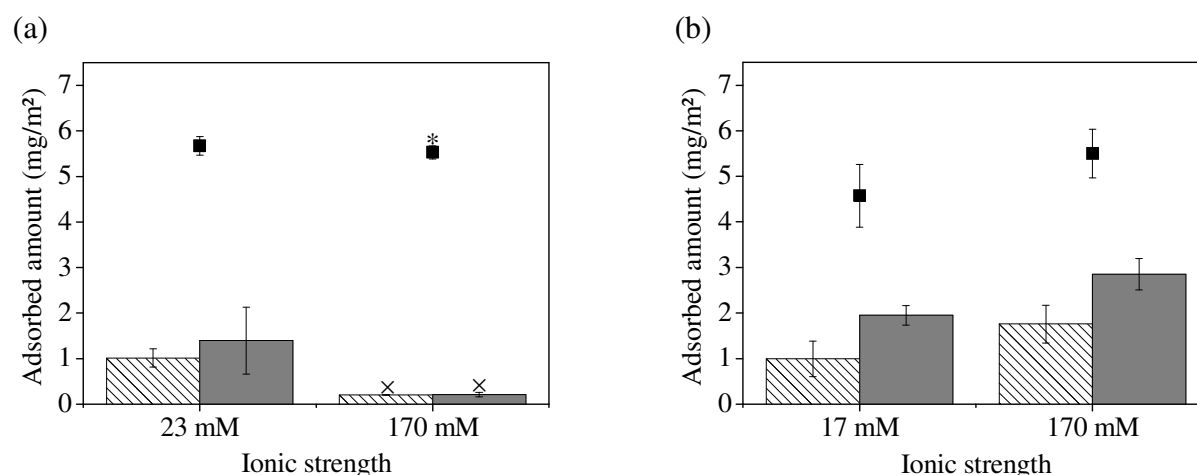


Figure II-13: Effect of variable ionic strength on IgG1 adsorption to siliconized glass vials in absence of surfactants (■) and with additional polysorbate 80 (patterned) or poloxamer 188 (grey) at pH 7.2 (a) and pH 4.0 (b); applied surfactant:protein molar ratio 10:1; incubation time 24 h at 25 °C, 2 mg/ml in 10 mM phosphate buffer, ionic strength adjusted with NaCl; values marked with (x) could not be quantified any more (n=3, *n=2).

3.1.6 Influence of Sugars and Polyols on IgG1 Adsorption

In the previous section, the effect of surfactants on IgG1 adsorption was investigated. Besides this group of excipients, sugars and polyols are widely used as nonspecific stabilizers in protein pharmaceuticals [14]. Although not typically used to inhibit protein adsorption, a

benefit by this group of excipients was described under certain conditions [18, 61]. Therefore, its effect on the adsorption of IgG1 to siliconized vials was investigated exemplarily with sucrose, mannitol and the cyclic oligosaccharide hydroxypropyl- β -cyclodextrin (HP- β -CD). In the presence of sugars, proteins are preferentially hydrated [62] due to an increase of the water surface tension by the co-solvent [63, 64], and an unfavorable change of the free energy takes place [62]. Since this change is greater for the denatured state with its increased surface area, the equilibrium in solution is shifted toward the compact native state of the protein [62]. Polyols belong to the group of the solvophobic compounds [63]. These increase the hydrophobic effect and, compared to pure water, the interaction between solvent and nonpolar protein regions becomes even more unfavorable [63]. Thus, thermodynamically unfavorable denaturation of a protein involving a pronounced exposure of hydrophobic protein domains and an increased contact area between protein and solvent should be opposed by glycerol [65]. As for protein-water interfaces, an exclusion of excipients can also be expected for solid surfaces [66]. Cyclodextrins (CDs) are commonly used as solubility enhancers [67]. Due to their cone like structure with a hydrophobic interior and hydrophilic exterior, CDs are water soluble and able to encapsulate whole molecules [67] or parts of bigger guest molecules, such as proteins, in their cavity [68]. Until a few years ago, marketed products for parenteral use containing CDs contained exclusively low-molecular-weight drugs [69-71]. However, a stabilizing effect of some cyclodextrin derivatives against protein aggregation was reported [69, 72].

The effect of mannitol, sucrose and HP- β -CD on IgG1 adsorption to siliconized vials was investigated at pH 7.2 and pH 4.0. Since the efficiency of co-solutes in stabilizing proteins was found to depend on their concentration and a minimum concentration of 300 mM was suggested necessary for a stabilization [73], all excipients were added to the protein formulation in this concentration. At pH 7.2, only HP- β -CD significantly reduced adsorption ($p < 0.05$), whereas almost no effect was observed in presence of mannitol and sucrose (Figure II-14). The effect of various sugars and polyols on the adsorption of BSA, lysozyme and RNase A to hydrophilic and siliconized SiO₂/TiO₂-surfaces was thoroughly investigated by Wendorf et al. who found decreased adsorbed amounts for most of the tested conditions [61]. This trend could not be observed for mannitol and sucrose in our experiment, but our results corresponded well with the findings of Mathes for the adsorption of IgG1 to borosilicate glass vials [18]. Wendorf et al. attributed the observed effect to the stabilization of the native state of the protein on the surface by the excipients, involving a decreased propensity for irreversible adsorption and thus lower irreversible adsorbed amounts [61]. The

stabilizing effect of sugars and polyols on a high concentrated IgG1 formulation of pH 6 was investigated by Matheus [74]. In this study, the chemical stability of the formulation was only marginally improved by sucrose and mannitol, which might explain the unchanged adsorption of IgG1 to siliconized vials at pH 7.2.

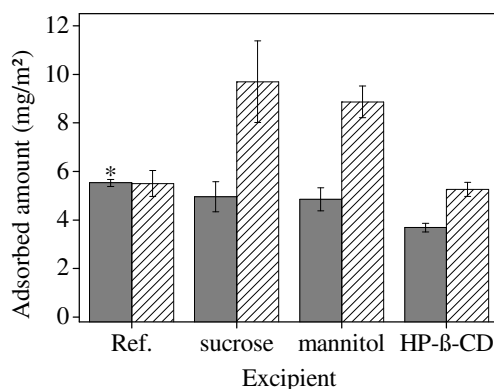


Figure II-14: Influence of 300 mM sucrose, mannitol and HP-β-CD on IgG1 adsorption to siliconized glass vials at pH 7.2 (grey) and pH 4.0 (patterned); 2 mg/ml in 10 mM phosphate buffer with 170 mM ionic strength; incubation time 24 h at 25 °C (n=3, * n=2); reference values as in Figure II-12.

Since a strong pH-dependence could be observed in previous adsorption experiments, the effect of the excipients was additionally investigated at pH 4.0. Both mannitol and sucrose increased the adsorbed amount whereas adsorption was almost unchanged with HP-β-CD (Figure II-14). On the one hand, the influence of potential sugar adsorption to the surface may be considered to explain the observed phenomenon. Binding of carbohydrates to negatively charged mica accompanied by a reduction of the long-range electrostatic double-layer force and reduced surface charge was shown by Claesson et al. [75]. However, this would result in a decreased electrostatic attraction of IgG1 to the surface also at pH 4.0 and thus rather to decreased adsorbed amounts. For some polyols and sugars, a slightly increased adsorption of IgG1 at low excipient concentrations but reduced adsorption at high concentrations of 1 M was also found by Mathes on borosilicate glass vials at pH 4 [18]. In silicone oil-water emulsions, a slightly increased protein loss in solution in presence of sucrose was found by Ludwig et al., potentially due to an increased adsorption to silicone oil droplets [4]. The authors ascribed this to the exclusion of sucrose from the silicone oil-water interface. According to Mahler et al., the exclusion of excipients may lead to a stabilization of proteins in solution but also to a destabilization of proteins at interfaces [66]. Adsorption in a destabilized state may lead to an increased spreading of the molecules on the surface and thus reduced adsorbed amounts, but also an enhanced adsorption via surface exposed hydrophobic

patches may be hypothesized. The stabilizing effect of preferential hydration was shown to depend on the pH value for some proteins due to changed dimensions of the molecules [62]. However, dynamic light scattering measurements revealed only a minor dependence of the hydrodynamic diameter of IgG1 on the pH value [18], so that the different adsorption behavior at different pH values could rather not be ascribed to this aspect. A decrease of intermolecular electrostatic repulsion by the preferential exclusion and thus higher adsorbed amounts at pH 4 may just be speculated.

HP- β -CD significantly reduced adsorption at pH 7.2, but did not affect adsorption at pH 4.0. As mentioned above, cyclodextrins may incorporate hydrophobic protein residues in their interior. Hydrophobic interactions of the protein with the surface may thus be reduced, leading to decreased adsorption values at pH 7.2. Since the influence of HP- β -CD on electrostatic interactions is supposed to be low, the main driving force for adsorption at pH 4.0 and thus the adsorbed amounts were almost unchanged. In conclusion, several aspects might explain the effect of sucrose, mannitol and HP- β -CD on IgG1 adsorption behavior but further studies are necessary to investigate and proof the mechanism.

3.1.7 Long-term Adsorption of IgG1 to Borosilicate Glass Vials and Siliconized Glass Vials

The contact time of pharmaceutical protein formulations with different process materials varies between several hours to days until the product is filled into the final primary packaging in that it is stored for months or years. Most studies investigating protein adsorption comprise only short time intervals of several minutes up to 24 h [33, 76, 77] whereas longer time intervals are considered rarely [78, 79]. Therefore, we investigated the adsorption of IgG1 to vials for up to 6 months as a relevant storage time for protein formulations. The filled vials were stored at 2-8 °C and additionally at 25 °C and 40 °C, corresponding to the temperatures for long-term and accelerated stability studies recommended by the ICH-guideline Q1A(R2). The adsorbed amount was determined after 24 h, 7 days, 1, 3 and 6 months. Besides siliconized vials, also type I borosilicate glass vials were included in the study to investigate the influence of the sorbent surface and the adsorption mechanism on long-term adsorption trends.

During storage for up to 6 months, adsorption from protein solutions pH 7.2 changed slightly at all temperatures on borosilicate and siliconized vials compared to adsorption after 24 h (Figure II-15b, Figure II-16b). Marginal changes were also observed for adsorption to borosilicate glass vials at pH 8.6 (Figure II-15c) and at pH 4.0, 2-8 °C and 25 °C (Figure

II-15a, Figure II-16a). In contrast, an enormous increase in adsorption was observed at pH 4.0 in vials stored at 40 °C for 6 months (Figure II-15a, Figure II-16a).

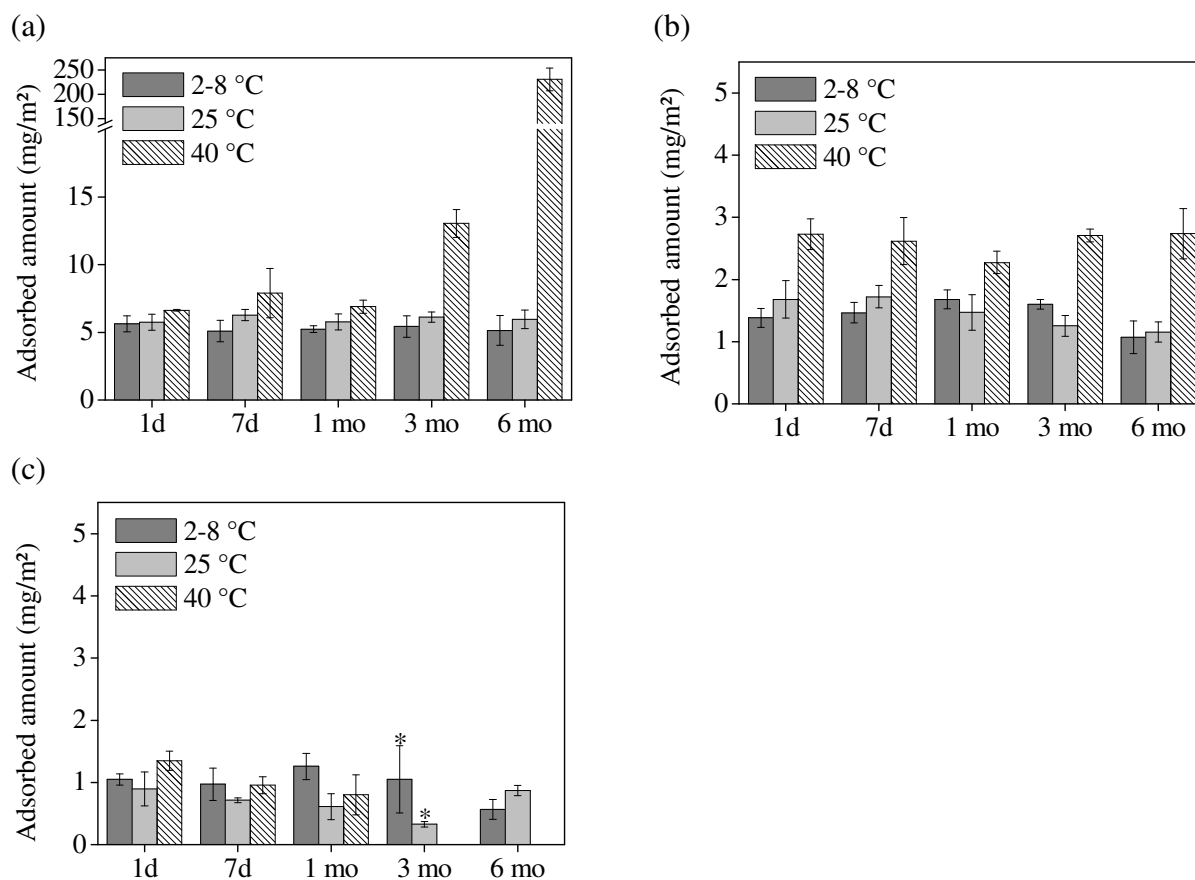


Figure II-15: IgG1 adsorption to type I borosilicate glass vials after 6 months storage at pH 4.0 (a), pH 7.2 (b) and pH 8.6 (c) at 2-8 °C, 25 °C and 40 °C; 2 mg/ml in 10 mM phosphate buffer with 170 mM ionic strength (n=3, *n=2).

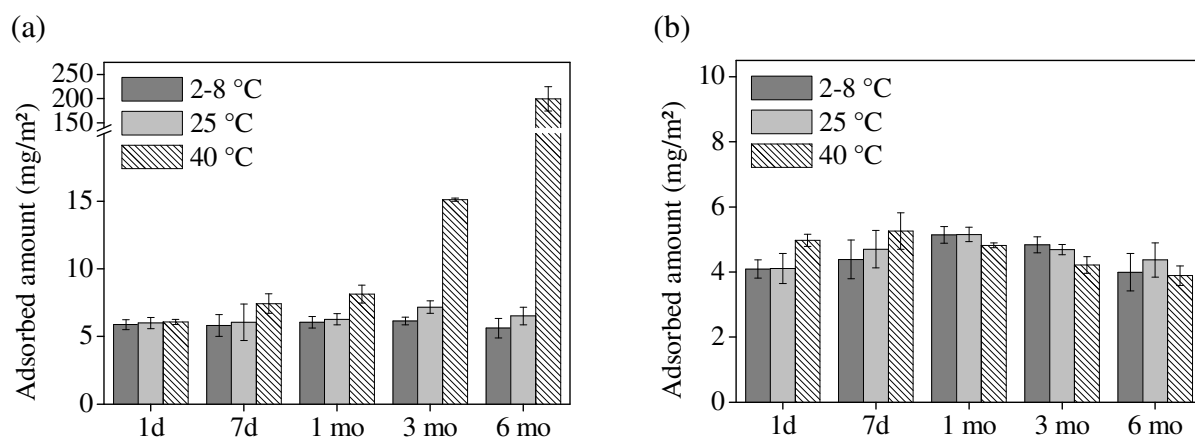


Figure II-16: IgG1 adsorption to siliconized glass vials after 6 months storage at pH 4.0 (a) and pH 7.2 (b) at 2-8 °C, 25 °C and 40 °C; 2 mg/ml in 10 mM phosphate buffer with 170 mM ionic strength (n=3).

As stated in section 3.1.3.1, pH-dependent variations in the adsorbed amount can be ascribed to different driving forces for adsorption. However, the strong increase in adsorption at pH 4.0/40 °C was rather not derived only from a different adsorption mechanism than at pH 7.2 but instead from protein instability. High temperature or an unsuitable pH value may lead to aggregation [80, 81], and also deamidation processes are influenced by these parameters [82]. Therefore, the samples after 6 months storage were investigated for potential instabilities that may influence the adsorption behavior.

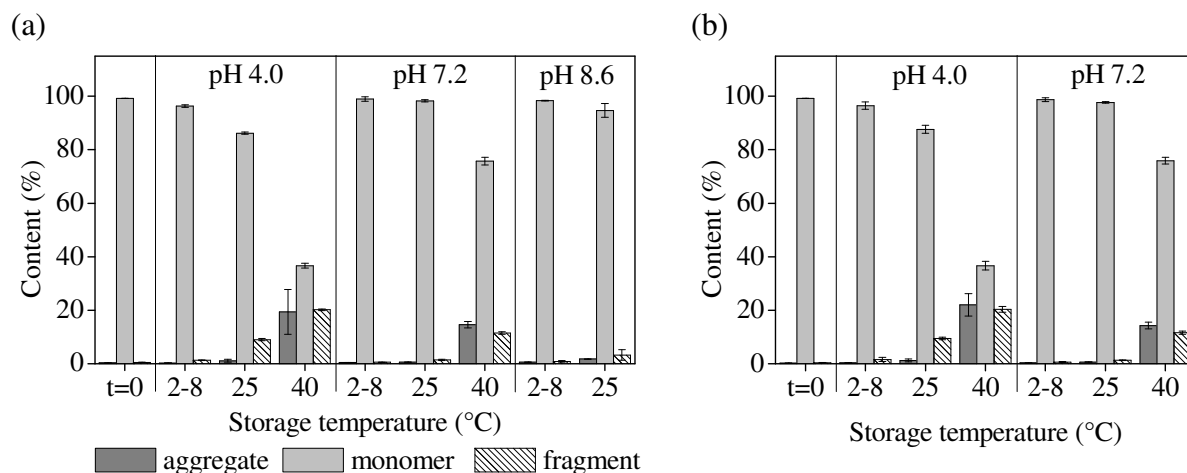


Figure II-17: Content of monomer, aggregates and fragments of IgG1 solutions stored in type I borosilicate glass vials (a) or siliconized glass vials (b) for 6 months (n=3) at different temperatures.

In all formulations stored at 40 °C but especially at pH 4.0, the HP-SEC monomer content was strongly decreased in favor to increased amounts of higher molecular weight aggregates and fragments (Figure II-17a, b). Furthermore, the total amount of protein in these samples of pH 4.0 was reduced, which can be related to protein particles and insoluble aggregates that were too large to be eluted through the column [83]. As SEC is limited to particles of up to approx. 0.02 μm [84], light obscuration was applied to detect particles larger than 1 μm . In all formulations, the number of particles was increased compared to the reference but was extremely high for solutions of pH 4.0/40 °C (Figure II-19a, b). Solutions of pH 7.2 and 8.6 still met the specifications of Ph. Eur. for subvisible particles in parenteral solutions with less than 6000 counts for particles $\geq 10 \mu\text{m}$ and less than 600 counts $\geq 25 \mu\text{m}$ per container [85], whereas solutions of pH 4.0 partially exceeded this threshold. Additionally, the turbidity of all formulations stored at 40 °C was increased (Figure II-19a, b).

The tertiary structure of the protein was investigated by extrinsic fluorescence measurements with bis-ANS. This dye is weakly fluorescent in a polar environment [86] but exhibits a high fluorescence accompanied by a blue shift of the emission maximum upon exposure to a non-

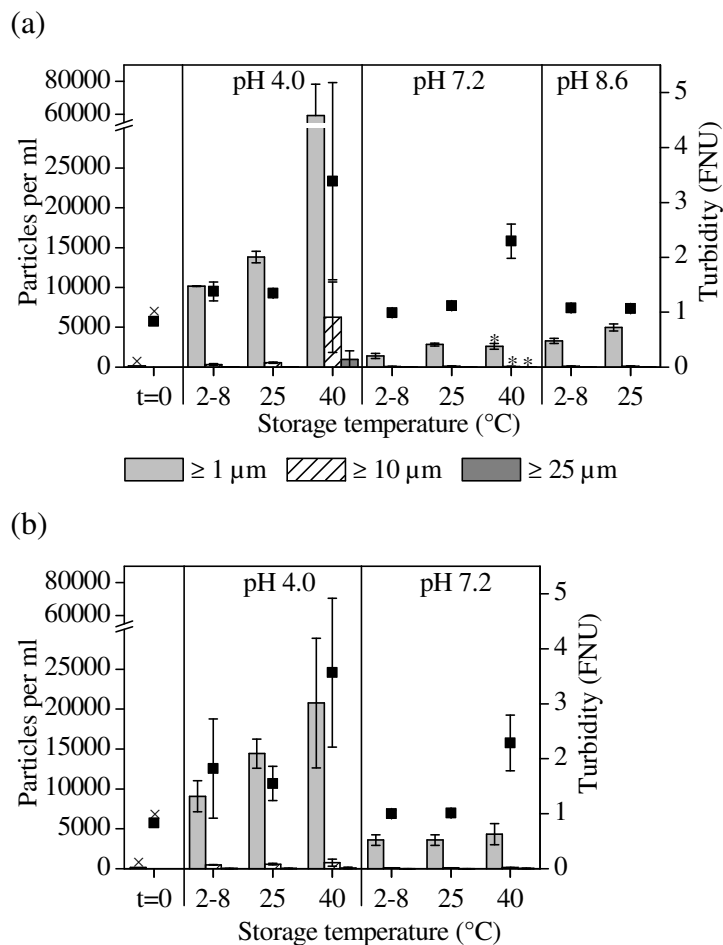


Figure II-19: Turbidity and number of particles determined in IgG1 solutions stored in type I glass vials (a) and siliconized glass vials (b) for 6 months at different temperatures (n=3, *n=2, x n=1).

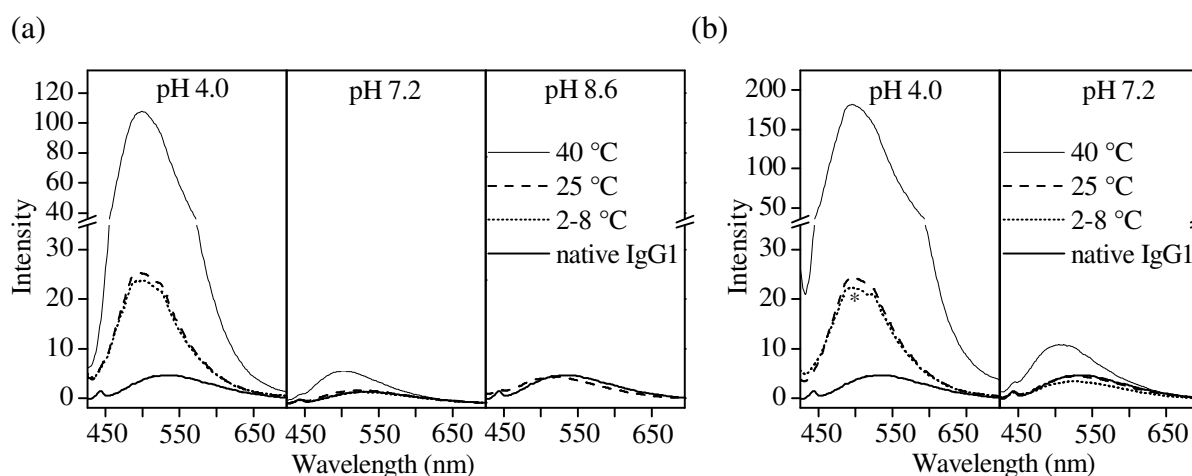


Figure II-18: Extrinsic fluorescence spectra of IgG1 solutions after 6 months storage at pH 4.0, pH 7.2, and pH 8.6 in type I borosilicate glass vials (a) and siliconized glass vials (b) in presence of 5 μM bis-ANS (n \geq 2, *n=1); storage temperatures 2-8 °C, 25 °C and 40 °C; native IgG1 formulated in 170 mM PBS pH 7.2.

After 6 months storage, the pI of IgG1 was unchanged in all formulations stored at 2-8 °C (Figure II-20). Samples of pH 7.2/40 °C and pH 8.6/25 °C showed a strong shift of the pI toward lower pH values. A slight shift at pH 7.2/25 °C was observed for solutions stored in siliconized vials. This trend corresponds with findings in literature, where increased deamidation of asparagine was found at neutral or basic pH values and increased temperature [82]. In formulations of pH 4.0, no change of the protein pI and thus no deamidation occurred independent of the storage temperature.

In general, only slight differences were observed between corresponding formulations stored in siliconized or bare glass vials. The increase in adsorption in solutions of pH 4.0/40 °C correlated with the extent of particulate formation and unfolding whereas this correlation was not this clear at 25 °C and 2-8 °C. Aggregates or monomers with exposed hydrophobic surface residues should show an increased adsorption affinity. A changed surface activity of protein molecules at elevated temperature and an increased adsorption tendency of the denatured molecules was also proposed by Arnebrandt et al. [89]. Furthermore, the adsorption of protein clusters even on a surface with pre-adsorbed protein was previously reported by Rabe et al. for hydrophobic surfaces [90]. On the other hand, protein aggregation induced by interaction of the protein with the sorbent surface was reported in several cases [91, 92]. Initial adsorption, nucleation and subsequent formation of larger aggregates was proposed as a possible mechanism [91]. However, this probably requires a rather large sorbent surface for contact with the protein as this phenomenon was observed only after the addition of non-proteinogenic particles to the solution [91] and the onset and occurrence of aggregation was dependent on the particle number and hydrophobicity [92]. In our case, the surface area of about 13.4 cm² wetted by the protein solution in a 2R vial was rather small. Furthermore, the very similar increase in adsorption at pH 4.0/40 °C on both the hydrophobic siliconized and the hydrophilic borosilicate glass surface rather indicates a largely surface-independent aggregation process at acidic pH and elevated temperature. At pH 7.2, the increased aggregation and unfolding tendency at 40 °C storage could not be clearly correlated with an increase in adsorption (Figure II-15b, Figure II-16b). Whether this applied for pH 8.6 could not be clarified since the protein stability and adsorption at 40 °C was investigated only up to 1 month at this pH. Although no considerable difference in formulation stability was observed between solutions stored in borosilicate and siliconized glass vials, the influence of the temperature on adsorption was slightly different at pH 7.2 (Figure II-15b, Figure II-16b). It may be speculated, that different adsorption kinetics on the hydrophobic and the hydrophilic surface led to this observation.

3.2 Lysozyme Adsorption to Borosilicate Glass Vials and Siliconized Glass Vials

In the previous sections, the adsorption of a monoclonal IgG1 antibody to siliconized vials and also borosilicate glass vials was investigated. Since electrostatic interactions and protein charge were shown to strongly influence the adsorption behavior, further adsorption experiments were performed with a protein with a different isoelectric point. Lysozyme is a small, globular protein with a molecular weight of about 14.4-14.6 kDa [47, 93]. It belongs to the group of ‘hard’ proteins that have a high structural stability [94] and was shown to adsorb to various surfaces by mainly electrostatic and hydrophobic interactions [33, 47, 95].

3.2.1 Charge Characterization of Lysozyme and the Glass Surface

As already performed for monoclonal IgG1 and siliconized particles (compare section 3.1.1), the zeta potential of lysozyme and borosilicate glass was determined to investigate the influence of electrostatic interactions for adsorption. The borosilicate glass particles had a specific surface area of about 0.72 m²/g determined by a BET measurement using nitrogen as adsorbing gas. For the electrokinetic mobility measurements, the non-sedimenting particle fraction was used. Lysozyme exhibited a typical protein titration curve with an isoelectric point at about pH 10.1 (Figure II-21a). In most cases, the pI of lysozyme was reported in a pH range of about pH 11.0 to 11.6 [47, 96-98] but also at approx. pH 9 [99]. Thus, the determined pI of lysozyme is in the range reported in literature. In addition, the theoretical protein charge

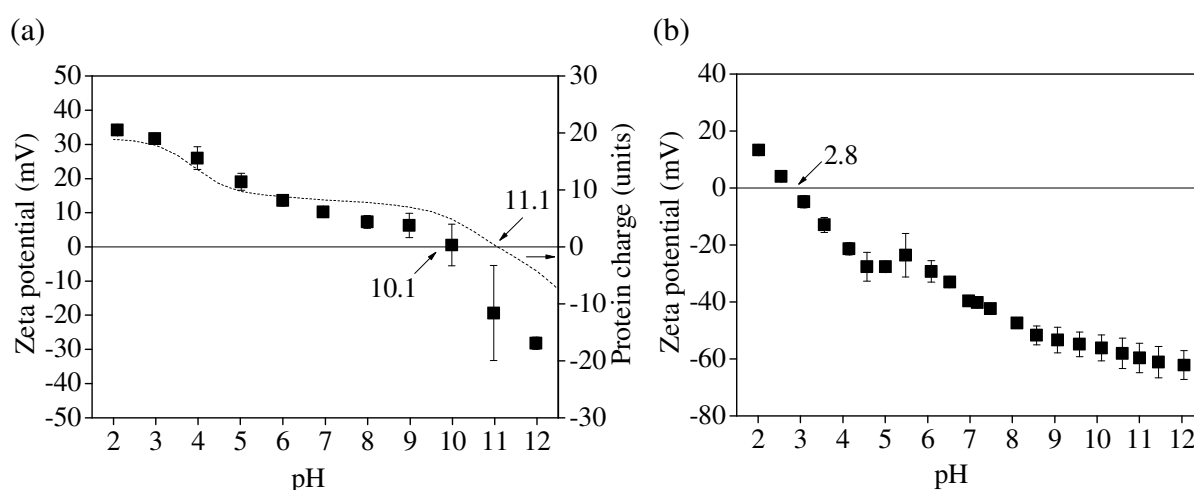


Figure II-21: Zeta potential of lysozyme (■) (n=3) and its theoretical protein charge calculated from the protein sequence (dotted line) (a) and zeta potential of borosilicate glass particles (n=2) (b); zeta potentials determined by electrophoretic mobility measurements in 10 mM NaCl solution.

was calculated from the amino acid composition of the protein with the European Molecular Biology Open Software Suite (EMBOSS) [100] using the hen egg white lysozyme sequence derived from the Research Collaboratory for Structural Bioinformatics (RCSB) protein data bank (ID 1LYZ). The calculated curve showed roughly the same trend as the experimentally obtained one but exhibited a higher pI at approx. pH 11.1 (Figure II-21a). The borosilicate glass surface exhibited a negative zeta potential at pH values above 2.8 (Figure II-21b) due to the dissociation of silanol groups. Thus, the lysozyme molecules and the glass surface were oppositely charged in the pH range between 2.8 and 10.1.

3.2.2 Influence of pH on Lysozyme Adsorption

All experiments were performed at a lysozyme concentration of 10 mg/ml and an adsorption time of 24 h, after which equilibrium adsorption conditions were almost reached (Figure II-22). At first, the pH-dependent adsorption of lysozyme to borosilicate glass vials was investigated (Figure II-23a). A bell-shaped pH-dependency with steadily increasing adsorption from pH 2 to 9 was observed, followed by a strong drop of the curve at pH 10. No values are depicted for formulations of higher pH values since visible precipitation of the protein was observed soon after pH adjustment.

Between pH 3 and the adsorption maximum at pH 9, lysozyme and the glass surface are oppositely charged and thus electrostatically attract each other. With increasing pH, the protein charge and thus the electrostatic attraction toward the negatively charged glass surface progressively decreased. Concurrently, the electrostatic repulsion between the molecules on the surfaces decreased, allowing a denser occupation of the surface. The simultaneous increase of adsorption with decreasing protein charge up to pH 9 thus strongly suggests that

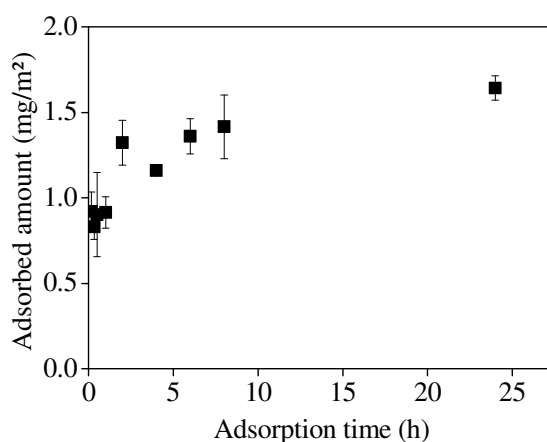


Figure II-22: Adsorption kinetics of lysozyme to type I borosilicate glass vials in 10 mM phosphate buffer with 170 mM ionic strength; incubation time 24 h at 25 °C (n=3).

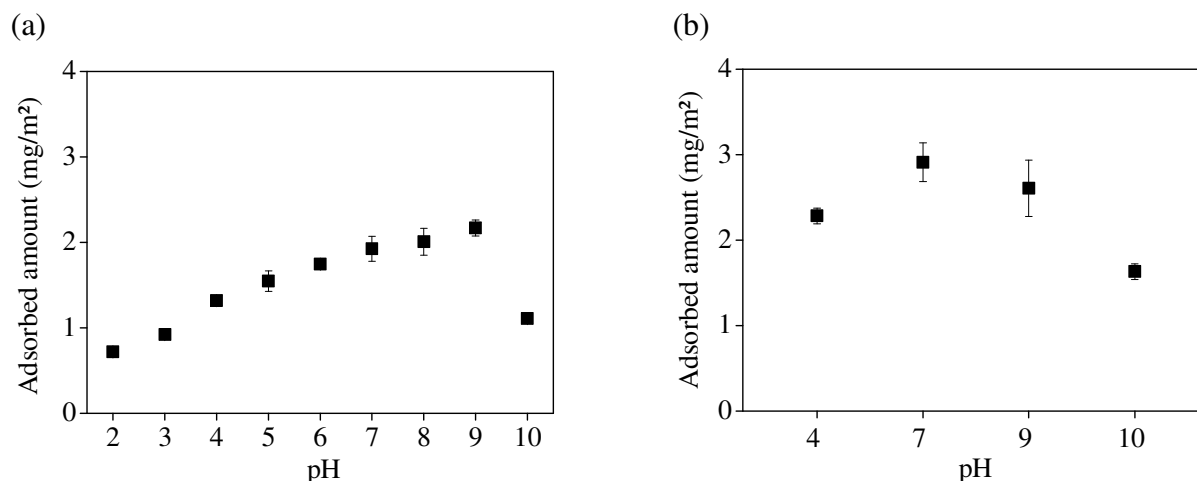


Figure II-23: Adsorption of lysozyme to type I borosilicate glass vials (a) and siliconized glass vials (b) depending on formulation pH in 10 mM PBS with 170 mM ionic strength; incubation time 24 h at 25 °C (n=3).

mainly the intermolecular repulsion on the surface was the limiting factor for lysozyme adsorption. According to this concept, high adsorbed amounts were expected at the pI of lysozyme, where the intermolecular repulsion is virtually zero. However, the adsorbed amount dropped sharply at pH 10. This may indicate that a certain attractive electrostatic interaction with the sorbent surface is necessary for pronounced adsorption. In the state of zero net charge, adsorption presumably took place mainly due to surface dehydration and dispersive interactions with the surface. A similar pH-dependency of lysozyme adsorption with adsorption maxima slightly below the pI of the protein was previously reported for various sorbent materials [94, 101]. The pH-dependent adsorption behavior of lysozyme was ascribed to a decreasing importance of electrostatic interactions for adsorption with increasing pH and the strong influence of lateral electrostatic intermolecular repulsion [102]. Vinu et al. further underlined the dominance of hydrophobic interactions close to the pI of the protein [101].

On siliconized glass vials, adsorption was investigated only at exemplary pH values. A similar pH-dependence as on bare glass vials was observed with the adsorption maximum at slightly lower pH values between 7 and 9 (Figure II-23b). An exact statement is not possible as adsorption was tested at larger pH intervals than on borosilicate vials. In section 3.1.1 it was shown that also the siliconized surface exhibited a negative surface charge over a large pH range. Therefore, similar charge interactions as on borosilicate glass vials were assumed. In general, slightly higher adsorption was found on the hydrophobic surface. This was ascribed to the increased contribution of hydrophobic interactions on these vials because the dehydration of hydrophobic patches due to adsorption is energetically favorable [48].

In contrast to our findings and those described by van der Veen et al., several publications reported a correspondence of the pI with the pH of maximum adsorption for a variety of proteins and surfaces [40, 49]. Some explanations for this phenomenon were already given in section 3.1.3.1. Van der Veen et al. hypothesized, that the adsorption maximum of lysozyme may instead correspond with the pI of the protein/sorbent complex [94]. Such a correlation was previously reported in approximation e.g. for BSA on polystyrene particles [11]. Figure II-24 depicts the zeta potential of the lysozyme-borosilicate glass complex between pH 4 and pH 11. The curve with an isoelectric point at about pH 6.5 is located in between the curves of the bare glass particles and the dissolved lysozyme. This indicates that the negative sorbent surface charges are partially compensated by the positive charges of the protein and adsorbed counterions. However, a correspondence of the pI of the protein-sorbent complex with the adsorption maximum was not found. Net charge neutrality of the protein-covered surface does thus not explain the location of the adsorption maximum. It may be rather concluded, that the adsorption maximum slightly below the protein pI resulted from an equilibrium of low intermolecular repulsion and a sufficient electrostatic attraction toward the (siliconized) glass surface, potentially with a certain contribution of hydrophobic interactions.

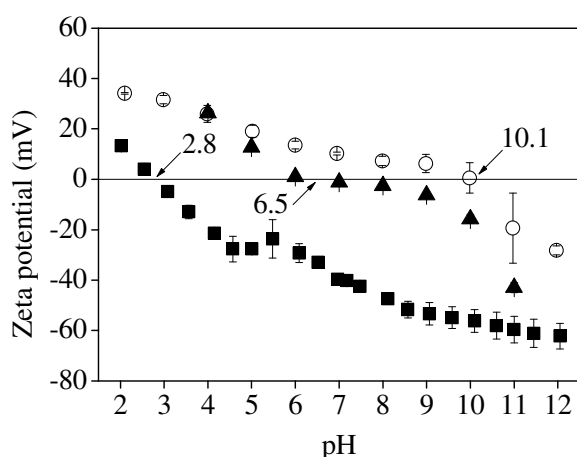


Figure II-24: Zeta potential of borosilicate glass particles (■) ($n=1$), lysozyme (○) and borosilicate glass particles with adsorbed lysozyme (▲) ($n \geq 2$) in 10 mM NaCl solution.

3.2.3 Influence of Ionic Strength on Lysozyme Adsorption

To further investigate the influence of intermolecular and protein-sorbent electrostatic interactions on lysozyme adsorption, the adsorbed amount at increasing ionic strengths up to 1 M was determined on borosilicate glass vials. Experiments were performed at exemplary pH values of 4.0, 7.2, 9.0 and 10.0, representing adsorption conditions of very high and high

positive protein charge, at the adsorption maximum or close to the pI of lysozyme, respectively.

At pH 4.0, adsorption increased with ionic strength (Figure II-25). Due to the positive protein net charge, the lysozyme molecules are electrostatically attracted toward the negatively charged glass surface. With increasing ion concentration, this attraction but also the strong repulsion between the molecules, which opposes the overall adsorption process, is screened. The simultaneous increase of lysozyme adsorption with ionic strength indicates that mainly the intermolecular repulsion determined the adsorbed amount of lysozyme to borosilicate glass vials at high protein charge, as was already suggested in the previous section. At pH 7.2 and pH 9.0, where lysozyme was marginally charged, the adsorbed amount decreased with increasing ionic strength (Figure II-25).

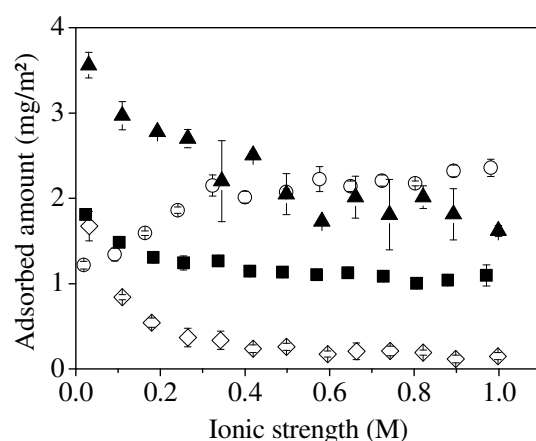


Figure II-25: Adsorption of lysozyme in dependence of ionic strength at pH 4.0 (○), pH 7.2 (■), pH 9.0(▲) and pH 10.0 (◇); incubation time 24 h at 25 °C, 10 mg/ml in 10 mM phosphate buffer, ionic strength adjusted with NaCl (n=3).

This indicates that the shielding effect of ions predominantly reduced attractive electrostatic forces between the protein and the glass surface rather than intermolecular repulsive forces at these pH values. Close to the pI at pH 10.0, adsorption was assumed to be rather independent of electrostatic interactions due to the almost neutral net charge of lysozyme. However, the decrease in adsorption with increasing ionic strength indicated the presence of attractive electrostatic interactions between the protein and the sorbent. Although exhibiting a neutral net charge, a protein molecule may exhibit positively and negatively charged patches on the surface. Kamyama & Israelachvili suggested that the adsorption of amphoteric polyelectrolytes is determined by the distribution of charges on sorbent surface and polymer rather than by the average charge, and by the formation of discrete ionic bonds between oppositely charged groups [103]. Similarly, Yadav et al. proposed that attractive protein-

protein interactions found between overall positively charged monoclonal antibodies resulted from the distribution of surface charges [104]. Ionic strength dependent adsorption of lysozyme thus showed, that also close to the pI of the molecule, attractive electrostatic interactions with the surface influence the adsorbed amount. Decreasing lysozyme adsorption in formulations of $\text{pH} > 5$ with increasing ionic strength was also previously reported for silica [105], glass particles [106] and $\text{SiO}_2/\text{TiO}_2$ surfaces [107]. This was ascribed to reduced electrostatic attractions due to a shielding of lysozyme and sorbent charges [107]. As can be observed in Figure II-25, a further increase of the ionic strength from about 0.4 M to 1.0 M hardly influenced the adsorbed amount at all tested pH values, indicating that a further shielding of electrostatic interactions did not render the adsorption process more favorable.

In a further step, the influence of ionic strength on the location of the adsorption maximum of lysozyme on borosilicate glass vials was investigated. Reduction of the ionic strength from 170 mM to 40 mM led to a shift of the adsorption maximum from pH 9 to about pH 6 to 7 (Figure II-26a). In fact, increased adsorbed amounts in the pH range between about 7 and 10 and a shift of the adsorption maximum toward higher pH values were expected from the previously described experiment. A shift of the maximum in this direction had already been observed for IgG1 in section 3.1.3.2 and was reported in literature for lysozyme [94] and other proteins [10, 49, 50]. It may be assumed that the adsorption maximum at 40 mM ionic strength resulted from a favorable interplay of large enough electrostatic attraction toward the surface and sufficiently low intermolecular repulsion. On siliconized vials, $\Gamma(\text{pH})_{\text{max}}$ at

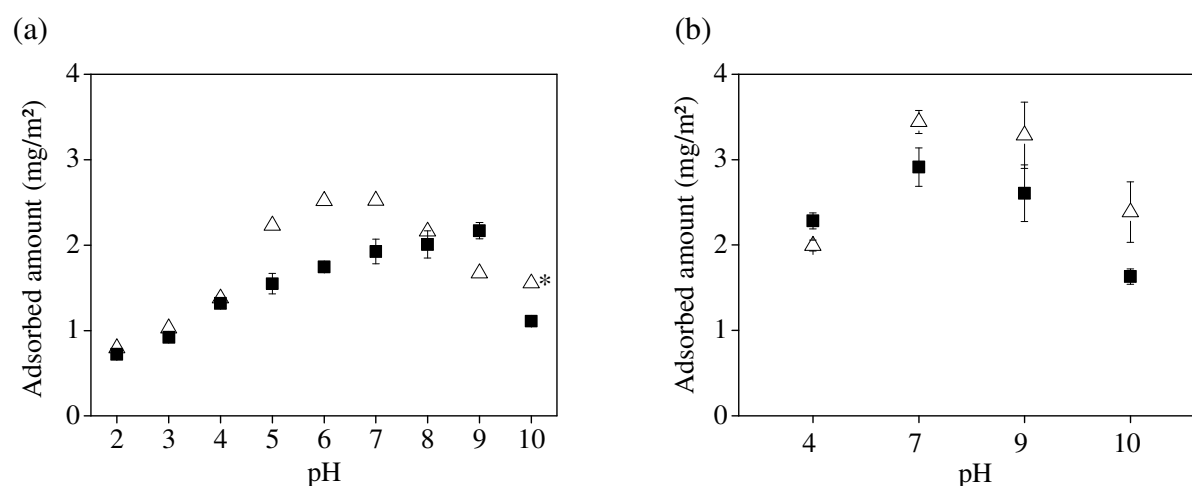


Figure II-26: Adsorption of lysozyme to type I borosilicate glass vials (a) and siliconized glass vials (b) depending on formulation pH at a formulation ionic strength of 40 mM (Δ) or 170 mM (■) adjusted with NaCl; incubation time 24 h at 25 °C (n=3, *n=2).

40 mM ionic strength was located approximately at the same or slightly higher pH than at 170 mM ionic strength, thus confirming the trends reported in literature (Figure II-26b). In conclusion, the adsorption maximum on siliconized vials presumably resulted from a very low intermolecular repulsion combined with sufficiently high electrostatic attraction toward the sorbent surface as suggested for bare glass vials.

3.2.4 Isotherm Considerations

One of the most popular methods to describe protein adsorption affinities to surfaces is an adsorption isotherm in which the adsorbed amount Γ is plotted against the equilibrium concentration c_{eq} . Several mathematical models were developed and are commonly used to analyze protein isotherms [108-110]. One of the first approaches which was often used for protein isotherm interpretations [111, 112] is the equation of Langmuir [113]:

$$\Gamma = \frac{\Gamma_{\text{max}} K c_{\text{eq}}}{1 + K c_{\text{eq}}} \quad (8)$$

Γ represents the adsorbed amount per surface area, Γ_{max} the maximum adsorbed amount and c_{eq} the equilibrium concentration of the protein in solution. K is a constant and was e.g. interpreted as bonding energy coefficient [113]. Originally developed for the description of gas adsorption to solid surfaces [114], the Langmuir equation was mentioned inappropriate to describe the adsorption of proteins from solution due to the difference in adsorption mechanism for small molecules and macromolecules [115]. Furthermore, the Freundlich model was used to describe adsorption isotherms of proteins [116, 117] by the power function

$$\Gamma = K \cdot c_{\text{eq}}^n \quad (9)$$

in which K represents the Freundlich equilibrium constant and n the isotherm power term [109]. This model is used in a strictly empirical sense but may be of theoretical interest to describe the adsorption to surfaces which are energetically heterogeneous [108]. Finally, the Langmuir-Freundlich equation [113]

$$\Gamma = \frac{\Gamma_{\text{max}} (K_m c_{\text{eq}})^n}{1 + (K_m c_{\text{eq}})^n} \quad (10)$$

considers heterogeneous bonding energies with the bonding energy coefficients following a Gaussian-like distribution [113]. K_m represents the median binding affinity and n the

heterogeneity index [118]. Values of $n < 1$ apply for heterogeneous materials whereas homogeneous materials exhibit a value of $n = 1$, leading to a reduction of Eq. 10 to the Langmuir equation (Eq. 8) [118]. Mathematically equivalent to the Langmuir-Freundlich equation is the Hill equation [119]. Assuming a homogeneous surface it allows the interpretation of cooperative adsorption processes due to lateral interactions. In this case, the parameter n expresses the degree of cooperativity, indicating positive cooperativity for values $n > 1$ [119]. Thus, fitting of adsorption isotherms according to Eq. 10 allows no interpretation of the parameter n in terms of surface heterogeneity and adsorption cooperativity at the same time under the same assumptions.

Lysozyme adsorption isotherms were determined in a bulk solution concentration range between 0.005 and 2 mg/ml (Figure II-27a) (here mentioned as isotherm I) and between 0.1 and 20 mg/ml (isotherm II) (Figure II-27b). The isotherms were fitted using the Langmuir, the Freundlich, and the Langmuir-Freundlich equation. Obtained values for the parameters are listed in Table II-3.

None of the models clearly fitted adsorption isotherm I best, just the correlation coefficients obtained were slightly better for the Langmuir and the Langmuir-Freundlich equation than for the Freundlich equation. Transformation of the data by the Scatchard plot (Γ/c_{eq} versus Γ) or the semi-reciprocal plot (c_{eq}/Γ versus c_{eq}) [120] did only show a linear trend for the latter equation (data not shown). This implies that the assumptions of the Langmuir model, (a)

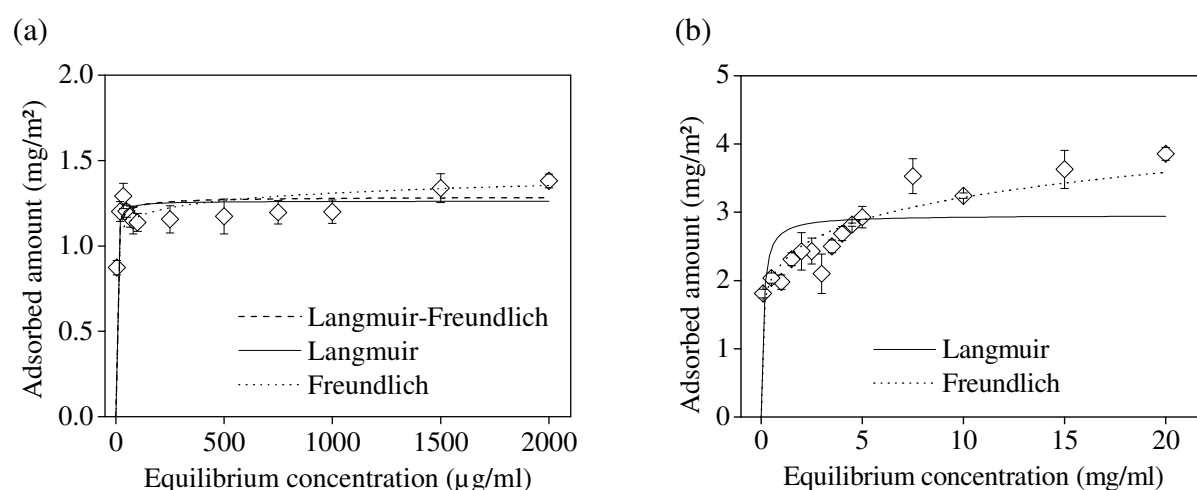


Figure II-27: Adsorption isotherms of lysozyme on borosilicate glass vials at equilibrium concentrations in a range of approximately (a) 0.005-2.0 mg/ml and (b) 0.1-20 mg/ml, determined at pH 7.2 in 10 mM phosphate buffer with 170 mM ionic strength; incubation time 24 h at 25 °C (n=3); isotherms were fitted by nonlinear curve approximation applying the Langmuir, the Freundlich or the Langmuir-Freundlich model.

Table II-3: Results of nonlinear curve fitting of adsorption isotherms of lysozyme on borosilicate glass vials at pH 7.2 applying different fitting models.

	Langmuir model parameters		Freundlich model parameters		Langmuir-Freundlich model parameters		
	Γ_{\max}^a (mg/m ²)	K^a (ml/g)	Γ_{\max}^a (mg/m ²)	n^a	Γ_{\max}^a (mg/m ²)	n^a	K_m^a (ml/g)
c (bulk) (mg/ml)							
0.005-2	1.26	0.49	0.93	0.05	1.29	0.73	0.65
0.1-20	2.95	9.84	2.24	0.16	n.a. ^b	n.a. ^b	n.a. ^b

^aobtained by nonlinear least square fit according to Levenberg-Marquardt algorithm

^bvalues not computable

equilibrium between adsorbed and free molecules, (b) monolayer adsorption, (c) energetic equivalence of adsorption sites, and (d) the absence of intermolecular interactions [121], are not fulfilled for lysozyme adsorption to borosilicate glass vials in the concentration range of isotherm I. Luo & Andrade stated that the Langmuir model is not suitable to describe the adsorption of proteins and ascribed this to the different adsorption mechanisms of macromolecules compared to small molecules: proteins bind via multiple sites, potentially irreversibly, and cooperative interactions play a role [115]. Furthermore, most surfaces are heterogeneous [115]. Therefore, the isotherm was further interpreted by the results obtained from fitting by the Langmuir-Freundlich equation. As mentioned above, the obtained values of $n < 1$ (Table II-3) may indicate heterogeneity of the borosilicate glass surface. Interpretation of n according to the Hill equation, assuming a homogeneous surface, did not indicate positive cooperativity of lysozyme adsorption.

In contrast to isotherm I, the isotherm for bulk concentrations between 0.1 and 20 mg/ml could not be fitted by the Langmuir-Freundlich equation. Best fits were obtained by the Freundlich model (Figure II-27b), which is only used in an empirical sense and reflects a continuous increase of the adsorbed amount with the bulk concentration [108].

The poor fitting of both isotherms by the Langmuir model may be ascribed to the intermolecular interactions between lysozyme molecules as outlined in the previous sections, multilayer adsorption or to the phenomena mentioned by Luo & Andrade as stated above. Adsorption isotherms exhibiting steps, as observed for isotherm II in the range of about 1.5-3.5 mg/ml, were previously reported and considered to derive from conformational changes of the adsorbed protein molecules [122] or a change in the molecular orientation with surface coverage [24].

4 CONCLUSION

IgG1 adsorption to siliconized glass vials was shown to be highly dependent on formulation pH and ionic strength. Determination of the charge characteristics of the protein molecules and the siliconized glass surface was used to interpret the contribution of electrostatic interactions to the adsorption process. Higher amounts of adsorbed protein were found for pH values at which opposing charges of the protein and the surface led to attractive electrostatic conditions. Calculation of the charge transfer between the protein-sorbent interface and the surrounding solution upon adsorption allowed further insight into the electrostatic interactions influencing the adsorption process. The pH of maximum adsorption could be correlated to the minimal ion uptake into the interfacial region between protein and sorbent surface. Electrostatic interactions are thus supposed to govern adsorption at pH values below the pI of IgG1. The occurrence of a second local adsorption maximum around the pI of the protein was ascribed to a pronounced influence of hydrophobic interactions. This assumption was supported by the marginal influence of ionic strength on adsorption at pH 7.2 compared to distinct changes in protein adsorption at pH 4.0. Addition of the nonionic surfactants P 188 and PS 80 resulted in almost complete suppression of adsorption at pH 7.2, and a strong but less pronounced effect at pH 4.0. From these results it can be concluded that electrostatic interactions contribute substantially to IgG1 adsorption to siliconized glass vials especially at acidic pH values. At these conditions, a decrease of the ionic strength is a rather effective additional tool to reduce protein adsorption to packaging materials. Close to the protein's pI, additionally hydrophobic interactions drive adsorption to a remarkable extent. Adsorption of IgG1 decreased only slightly by the addition of sucrose, mannitol or HP- β -CD or even increased. Determination of an 'adsorption index' was found to be not suitable to predict the adsorption behavior of IgG1 to different vial surfaces with the applied experimental setup. In contrast, a clear dependency of the adsorbed amount on the physical and chemical stability of the IgG1 solution could be demonstrated by analyzing the adsorption of IgG1 after long-term storage of the formulation in siliconized and bare glass vials.

Investigation of the pH- and ionic strength dependent adsorption of lysozyme as a model protein to borosilicate glass vials and siliconized vials showed a strong dependence on lateral electrostatic interactions. Adsorption isotherms could be fitted by applying the Langmuir-Freundlich or the Freundlich model, depending on the investigated concentration range of the isotherm. From the adsorption experiments with lysozyme and IgG1 it can be summarized, that especially electrostatic interactions strongly contributed to the adsorption behavior of both proteins to borosilicate glass vials and siliconized vials. This understanding enables a

more rational design of protein formulations to be packaged in (siliconized) vials or prefilled syringes.

5 REFERENCES

- [1] G.A. Sacha, W. Saffell-Clemmer, K. Abram, M.J. Akers, Practical fundamentals of glass, rubber, and plastic sterile packaging systems, *Pharm. Dev. Technol.*, 15 (2010) 6-34.
- [2] A. Colas, Silicones in Pharmaceutical Applications [Online], 2001, Available: <http://www.dowcorning.com/content/publishedlit/51-993a-01.pdf> [Accessed January 23 2013].
- [3] L.S. Jones, A. Kaufmann, C.R. Middaugh, Silicone oil induced aggregation of proteins, *J. Pharm. Sci.*, 94 (2005) 918-927.
- [4] D.B. Ludwig, J.F. Carpenter, J.-B. Hamel, T.W. Randolph, Protein adsorption and excipient effects on kinetic stability of silicone oil emulsions, *J. Pharm. Sci.*, 99 (2010) 1721-1733.
- [5] R. Thirumangalathu, S. Krishnan, M.S. Ricci, D.N. Brems, T.W. Randolph, J.F. Carpenter, Silicone oil- and agitation-induced aggregation of a monoclonal antibody in aqueous solution, *J. Pharm. Sci.*, 98 (2009) 3167-3181.
- [6] J. Li, S. Pinnamaneni, Y. Quan, A. Jaiswal, F. Andersson, X. Zhang, Mechanistic Understanding of Protein-Silicone Oil Interactions, *Pharm. Res.*, 29 (2012) 1689-1697.
- [7] N. Dixit, K. Maloney, D. Kalonia, Protein-Silicone Oil Interactions: Comparative Effect of Nonionic Surfactants on the Interfacial Behavior of a Fusion Protein, *Pharm. Res.*, 30 (2013) 1848-1859.
- [8] N. Dixit, K.M. Maloney, D.S. Kalonia, Application of quartz crystal microbalance to study the impact of pH and ionic strength on protein-silicone oil interactions, *Int. J. Pharm.*, 412 (2011) 20-27.
- [9] W. Norde, J. Lyklema, Thermodynamics of protein adsorption. Theory with special reference to the adsorption of human plasma albumin and bovine pancreas ribonuclease at polystyrene surfaces, *J. Colloid Interface Sci.*, 71 (1979) 350-366.
- [10] J. Mathes, W. Friess, Influence of pH and ionic strength on IgG adsorption to vials, *Eur. J. Pharm. Biopharm.*, 78 (2011) 239-247.
- [11] A.V. Elgersma, R.L.J. Zsom, W. Norde, J. Lyklema, The adsorption of bovine serum albumin on positively and negatively charged polystyrene latices, *J. Colloid Interface Sci.*, 138 (1990) 145-156.
- [12] N.B. Bam, T.W. Randolph, J.L. Cleland, Stability of protein formulations: investigation of surfactant effects by a novel EPR spectroscopic technique, *Pharm. Res.*, 12 (1995) 2-11.
- [13] T. Arakawa, Y. Kita, Protection of bovine serum albumin from aggregation by Tween 80, *J. Pharm. Sci.*, 89 (2000) 646-651.

-
- [14] W. Wang, Instability, stabilization, and formulation of liquid protein pharmaceuticals, *Int. J. Pharm.*, 185 (1999) 129-188.
- [15] M.R. Duncan, J.M. Lee, M.P. Warchol, Influence of surfactants upon protein/peptide adsorption to glass and polypropylene, *Int. J. Pharm.*, 120 (1995) 179-188.
- [16] M. Feng, A.B. Morales, A. Poot, T. Beugeling, A. Bantjes, Effects of Tween 20 on the desorption of proteins from polymer surfaces, *J. Biomater. Sci., Polym. Ed.*, 7 (1995) 415-424.
- [17] S. Welin-Klintström, A. Askendal, H. Elwing, Surfactant and Protein Interactions on Wettability Gradient Surfaces, *J. Colloid Interface Sci.*, 158 (1993) 188-194.
- [18] J. Mathes, 2010, Protein Adsorption to Vial Surfaces: Quantification, Structural and Mechanistic Studies, Thesis, Ludwig-Maximilians Universität München.
- [19] M. Zhang, M. Ferrari, Reduction of albumin adsorption onto silicon surfaces by Tween 20, *Biotechnol. Bioeng.*, 56 (1997) 618-625.
- [20] L.N. Arnaudov, R. de Vries, Thermally Induced Fibrillar Aggregation of Hen Egg White Lysozyme, *Biophys. J.*, 88 (2005) 515-526.
- [21] J. Lyklema, Elektrische Doppelschichten: Elektrostatik und Elektrodynamik, *Chem. Ing. Tech.*, 71 (1999) 1364-1369.
- [22] R.H. Pain, Determining the Fluorescence Spectrum of a Protein, in: *Current Protocols in Protein Science*, John Wiley & Sons, Inc., 2001.
- [23] J.C. Kasper, D. Schaffert, M. Ogris, E. Wagner, W. Friess, Development of a lyophilized plasmid/LPEI polyplex formulation with long-term stability-A step closer from promising technology to application, *J. Controlled Release*, 151 (2011) 246-255.
- [24] C.A. Haynes, W. Norde, Globular proteins at solid/liquid interfaces, *Colloids Surf., B*, 2 (1994) 517-566.
- [25] R. Tadmor, Line Energy and the Relation between Advancing, Receding, and Young Contact Angles, *Langmuir*, 20 (2004) 7659-7664.
- [26] E.A. Vogler, Structure and reactivity of water at biomaterial surfaces, *Adv. Colloid Interface Sci.*, 74 (1998) 69-117.
- [27] M. Kosmulski, Positive Electrokinetic Charge of Silica in the Presence of Chlorides, *J. Colloid Interface Sci.*, 208 (1998) 543-545.
- [28] G.V. Franks, Zeta Potentials and Yield Stresses of Silica Suspensions in Concentrated Monovalent Electrolytes: Isoelectric Point Shift and Additional Attraction, *J. Colloid Interface Sci.*, 249 (2002) 44-51.
- [29] Y. Gu, D. Li, The ζ -Potential of Silicone Oil Droplets Dispersed in Aqueous Solutions, *J. Colloid Interface Sci.*, 206 (1998) 346-349.
- [30] J. Song, J.F.L. Duval, M.A. Cohen Stuart, H. Hillborg, U. Gunst, H.F. Arlinghaus, G.J. Vancso, Surface Ionization State and Nanoscale Chemical Composition of UV-

- Irradiated Poly(dimethylsiloxane) Probed by Chemical Force Microscopy, Force Titration, and Electrokinetic Measurements, *Langmuir*, 23 (2007) 5430-5438.
- [31] J. Roth, V. Albrecht, M. Nitschke, C. Bellmann, F. Simon, S. Zschoche, S. Michel, C. Luhmann, K. Grundke, B. Voit, Surface Functionalization of Silicone Rubber for Permanent Adhesion Improvement, *Langmuir*, 24 (2008) 12603-12611.
- [32] V.M. Litvinov, H. Barthel, J. Weis, Structure of a PDMS Layer Grafted onto a Silica Surface Studied by Means of DSC and Solid-State NMR, *Macromolecules*, 35 (2002) 4356-4364.
- [33] M. Malmsten, Ellipsometry studies of the effects of surface hydrophobicity on protein adsorption, *Colloids Surf., B*, 3 (1995) 297-308.
- [34] K. Wannerberger, S. Welin-Klintström, T. Arnebrant, Activity and Adsorption of Lipase from *Humicola lanuginosa* on Surfaces with Different Wettabilities, *Langmuir*, 13 (1997) 784-790.
- [35] R.J. Marsh, R.A.L. Jones, M. Sferrazza, Adsorption and displacement of a globular protein on hydrophilic and hydrophobic surfaces, *Colloids Surf., B*, 23 (2002) 31-42.
- [36] H. Elwing, S. Welin, A. Askendal, U. Nilsson, I. Lundström, A wettability gradient method for studies of macromolecular interactions at the liquid/solid interface, *J. Colloid Interface Sci.*, 119 (1987) 203-210.
- [37] A. Michiardi, C. Aparicio, B.D. Ratner, J.A. Planell, J. Gil, The influence of surface energy on competitive protein adsorption on oxidized NiTi surfaces, *Biomaterials*, 28 (2007) 586-594.
- [38] E.A. Vogler, D.A. Martin, D.B. Montgomery, J. Graper, H.W. Sugg, A graphical method for predicting surfactant and protein adsorption properties, *Langmuir*, 9 (1993) 497-507.
- [39] M.G.E.G. Bremer, J. Duval, W. Norde, J. Lyklema, Electrostatic interactions between immunoglobulin (IgG) molecules and a charged sorbent, *Colloids Surf., A*, 250 (2004) 29-42.
- [40] P. Bagchi, S.M. Birnbaum, Effect of pH on the adsorption of immunoglobulin G on anionic poly(vinyltoluene) model latex particles, *J. Colloid Interface Sci.*, 83 (1981) 460-478.
- [41] S. Salgin, S. Takaç, T.H. Özdamar, Adsorption of bovine serum albumin on polyether sulfone ultrafiltration membranes: Determination of interfacial interaction energy and effective diffusion coefficient, *J. Membr. Sci.*, 278 (2006) 251-260.
- [42] W. Norde, F. MacRitchie, G. Nowicka, J. Lyklema, Protein adsorption at solid-liquid interfaces: Reversibility and conformation aspects, *J. Colloid Interface Sci.*, 112 (1986) 447-456.
- [43] P. Van Dulm, W. Norde, J. Lyklema, Ion participation in protein adsorption at solid surfaces, *J. Colloid Interface Sci.*, 82 (1981) 77-82.

-
- [44] W. Norde, Adsorption of proteins at solid-liquid interfaces, *Cells Mater.*, 5 (1995) 97-112.
- [45] X. Zhu, H. Fan, D. Li, Y. Xiao, X. Zhang, Protein adsorption and zeta potentials of a biphasic calcium phosphate ceramic under various conditions, *J. Biomed. Mater. Res., Part B*, 82B (2007) 65-73.
- [46] K.L. Jones, C.R. O'Melia, Protein and humic acid adsorption onto hydrophilic membrane surfaces: effects of pH and ionic strength, *J. Membr. Sci.*, 165 (2000) 31-46.
- [47] T. Arai, W. Norde, The behavior of some model proteins at solid-liquid interfaces 1. Adsorption from single protein solutions, *Colloids Surf.*, 51 (1990) 1-15.
- [48] W. Norde, J. Lyklema, Why proteins prefer interfaces, *J. Biomater. Sci., Polym. Ed.*, 2 (1991) 183-202.
- [49] J. Buijs, P.A.W. van den Berg, J.W.T. Lichtenbelt, W. Norde, J. Lyklema, Adsorption Dynamics of IgG and Its F(ab')₂ and Fc Fragments Studied by Reflectometry, *J. Colloid Interface Sci.*, 178 (1996) 594-605.
- [50] H. Xu, J.R. Lu, D.E. Williams, Effect of Surface Packing Density of Interfacially Adsorbed Monoclonal Antibody on the Binding of Hormonal Antigen Human Chorionic Gonadotrophin, *J. Phys. Chem. B*, 110 (2006) 1907-1914.
- [51] W. Norde, J. Lyklema, The adsorption of human plasma albumin and bovine pancreas ribonuclease at negatively charged polystyrene surfaces: III. Electrophoresis, *J. Colloid Interface Sci.*, 66 (1978) 277-284.
- [52] J. Buijs, J.W.T. Lichtenbelt, W. Norde, J. Lyklema, Adsorption of monoclonal IgGs and their F(ab')₂ fragments onto polymeric surfaces, *Colloids Surf., B*, 5 (1995) 11-23.
- [53] N.B. Bam, J.L. Cleland, J. Yang, M.C. Manning, J.F. Carpenter, R.F. Kelley, T.W. Randolph, Tween protects recombinant human growth hormone against agitation-induced damage via hydrophobic interactions, *J. Pharm. Sci.*, 87 (1998) 1554-1559.
- [54] D.K. Chou, R. Krishnamurthy, T.W. Randolph, J.F. Carpenter, M.C. Manning, Effects of Tween 20[®] and Tween 80[®] on the stability of Albutropin during agitation, *J. Pharm. Sci.*, 94 (2005) 1368-1381.
- [55] M. Wahlgren, Karlsson, C. A. C., Welin-Klintstroem, S., Interactions between proteins and surfactants at solid interfaces, *Surfactant Sci. Ser.*, 110 (2003) 321-343.
- [56] M.C. Wahlgren, T. Arnebrant, The concentration dependence of adsorption from a mixture of β -lactoglobulin and sodium dodecyl sulfate onto methylated silica surfaces, *J. Colloid Interface Sci.*, 148 (1992) 201-206.
- [57] A.V. Kabanov, E.V. Batrakova, D.W. Miller, Pluronic[®] block copolymers as modulators of drug efflux transporter activity in the blood-brain barrier, *Adv. Drug Delivery Rev.*, 55 (2003) 151-164.

- [58] E. Batrakova, H.-Y. Han, V. Alakhov, D. Miller, A. Kabanov, Effects of Pluronic Block Copolymers on Drug Absorption in Caco-2 Cell Monolayers, *Pharm. Res.*, 15 (1998) 850-855.
- [59] T.M. Göppert, R.H. Müller, Polysorbate-stabilized solid lipid nanoparticles as colloidal carriers for intravenous targeting of drugs to the brain: Comparison of plasma protein adsorption patterns, *J. Drug Target.*, 13 (2005) 179-187.
- [60] F. B, Poloxamers (1) Lutrol[®] F 68 (Poloxamer 188) [Online], 1999: http://worldaccount.basf.com/wa/NAFTA/Catalog/Pharma/doc4/BASF/exact/lutrol_f_68/.pdf?title=Poloxamers%20%281%29%20Lutrol%20F%2068%20%28Poloxamer%20188%29.&asset_type=pi/pdf&language=EN&urn=urn:documentum:eCommerce_so1_EU:09007bb28001ac1e.pdf, [Accessed March 10 2013].
- [61] J.R. Wendorf, C.J. Radke, H.W. Blanch, Reduced protein adsorption at solid interfaces by sugar excipients, *Biotechnol. Bioeng.*, 87 (2004) 565-573.
- [62] T. Arakawa, S.N. Timasheff, Stabilization of protein structure by sugars, *Biochemistry*, 21 (1982) 6536-6544.
- [63] S.N. Timasheff, Solvent effects on protein stability: Current Opinion in Structural Biology, *Curr. Opin. Struct. Biol.*, 2 (1992) 35-39.
- [64] J.C. Lee, S.N. Timasheff, The stabilization of proteins by sucrose, *J. Biol. Chem.*, 256 (1981) 7193-7201.
- [65] K. Gekko, S.N. Timasheff, Mechanism of protein stabilization by glycerol: preferential hydration in glycerol-water mixtures, *Biochemistry*, 20 (1981) 4667-4676.
- [66] H.-C. Mahler, S. Fischer, T.W. Randolph, J.F. Carpenter, Protein aggregation and particle formation: Effects of formulation, interfaces, and drug product manufacturing operations, in: W. Wang, C.J. Roberts (Eds.), *Aggregation of therapeutic proteins*, John Wiley & Sons, Inc., Hoboken, New Jersey, 2010.
- [67] T. Loftsson, M.E. Brewster, Pharmaceutical applications of cyclodextrins. 1. Drug solubilization and stabilization, *J. Pharm. Sci.*, 85 (1996) 1017-1025.
- [68] T. Serno, R. Geidobler, G. Winter, Protein stabilization by cyclodextrins in the liquid and dried state, *Adv. Drug Delivery Rev.*, 63 (2011) 1086-1106.
- [69] T. Serno, J.F. Carpenter, T.W. Randolph, G. Winter, Inhibition of agitation-induced aggregation of an IgG-antibody by hydroxypropyl- β -cyclodextrin, *J. Pharm. Sci.*, 99 (2010) 1193-1206.
- [70] M.E. Davis, M.E. Brewster, Cyclodextrin-based pharmaceuticals: past, present and future, *Nat. Rev. Drug Discov.*, 3 (2004) 1023-1035.
- [71] J. Peeters, P. Neeskens, J.P. Tollenaere, P. Van Remoortere, M.E. Brewster, Characterization of the interaction of 2-hydroxypropyl- β -cyclodextrin with itraconazole at pH 2, 4, and 7, *J. Pharm. Sci.*, 91 (2002) 1414-1422.

-
- [72] S. Tavornvipas, S. Tajiri, F. Hirayama, H. Arima, K. Uekama, Effects of hydrophilic cyclodextrins on aggregation of recombinant human growth hormone, *Pharm. Res.*, 21 (2004) 2369-2376.
- [73] T. Arakawa, S.J. Prestrelski, W.C. Kenney, J.F. Carpenter, Factors affecting short-term and long-term stabilities of proteins, *Adv. Drug Delivery Rev.*, 10 (1993) 1-28.
- [74] S. Matheus, 2006, Development of High Concentration cetuximab Formulations using Ultrafiltration and Precipitation Techniques, Thesis, Ludwig-Maximilians-Universität München.
- [75] P.M. Claesson, H.K. Christenson, J.M. Berg, R.D. Neuman, Interactions between Mica Surfaces in the Presence of Carbohydrates, *J. Colloid Interface Sci.*, 172 (1995) 415-424.
- [76] T. Wei, S. Kaewtathip, K. Shing, Buffer Effect on Protein Adsorption at Liquid/Solid Interface, *J. Phys. Chem. C*, 113 (2009) 2053-2062.
- [77] Y. Tie, C. Calonder, P.R. Van Tassel, Protein adsorption: Kinetics and history dependence, *J. Colloid Interface Sci.*, 268 (2003) 1-11.
- [78] McLeod, Walker, Zheng, Hayward, Loss of factor VIII activity during storage in PVC containers due to adsorption, *Haemophilia*, 6 (2000) 89-92.
- [79] J. Deere, E. Magner, J.G. Wall, B.K. Hodnett, Mechanistic and Structural Features of Protein Adsorption onto Mesoporous Silicates, *J. Phys. Chem. B*, 106 (2002) 7340-7347.
- [80] E.Y. Chi, S. Krishnan, T.W. Randolph, J.F. Carpenter, Physical Stability of Proteins in Aqueous Solution: Mechanism and Driving Forces in Nonnative Protein Aggregation, *Pharm. Res.*, 20 (2003) 1325-1336.
- [81] W. Wang, Protein aggregation and its inhibition in biopharmaceutics, *Int. J. Pharm.*, 289 (2005) 1-30.
- [82] R.M. Daniel, M. Dines, H.H. Petach, The denaturation and degradation of stable enzymes at high temperatures, *Biochem. J.*, 317 (1996) 1-11.
- [83] S. Zöls, R. Tantipolphan, M. Wiggenghorn, G. Winter, W. Jiskoot, W. Friess, A. Hawe, Particles in therapeutic protein formulations, Part 1: Overview of analytical methods, *J. Pharm. Sci.*, 101 (2012) 914-935.
- [84] S.K. Singh, N. Afonina, M. Awwad, K. Bechtold-Peters, J.T. Blue, D. Chou, M. Cromwell, H.-J. Krause, H.-C. Mahler, B.K. Meyer, L. Narhi, D.P. Nesta, T. Spitznagel, An industry perspective on the monitoring of subvisible particles as a quality attribute for protein therapeutics, *J. Pharm. Sci.*, 99 (2010) 3302-3321.
- [85] 3.1.8 Silicone oil used as a lubricant, in: *European Pharmacopoeia*, 2011
- [86] A.L. Smoot, M. Panda, B.T. Brazil, A.M. Buckle, A.R. Fersht, P.M. Horowitz, The Binding of Bis-ANS to the Isolated GroEL Apical Domain Fragment Induces the Formation of a Folding Intermediate with Increased Hydrophobic Surface Not Observed in Tetradecameric GroEL, *Biochemistry*, 40 (2001) 4484-4492.

- [87] A.O. Grillo, K.L. Edwards, R.S. Kashi, K.M. Shipley, L. Hu, M.J. Besman, C.R. Middaugh, Conformational origin of the aggregation of recombinant human factor VIII, *Biochemistry*, 40 (2001) 586-595.
- [88] K. Ahrer, A. Jungbauer, Chromatographic and electrophoretic characterization of protein variants, *J. Chromatogr., B*, 841 (2006) 110-122.
- [89] T. Arnebrant, K. Barton, T. Nylander, Adsorption of α -lactalbumin and β -lactoglobulin on metal surfaces versus temperature, *J. Colloid Interface Sci.*, 119 (1987) 383-390.
- [90] M. Rabe, D. Verdes, S. Seeger, Surface-induced spreading phenomenon of protein clusters, *Soft Matter*, 5 (2009) 1039-1047.
- [91] E.Y. Chi, J. Weickmann, J.F. Carpenter, M.C. Manning, T.W. Randolph, Heterogeneous nucleation-controlled particulate formation of recombinant human platelet-activating factor acetylhydrolase in pharmaceutical formulation, *J. Pharm. Sci.*, 94 (2005) 256-274.
- [92] V. Sluzky, J.A. Tamada, A.M. Klibanov, R. Langer, Kinetics of insulin aggregation in aqueous solutions upon agitation in the presence of hydrophobic surfaces, *Proc. Natl. Acad. Sci. U. S. A.*, 88 (1991) 9377-9381.
- [93] R. Cegielska-Radziejewska, G. Leńnierowski, J. Kijowski, Properties and application of egg white lysozyme and its modified preparations - a review., *Pol. J. Food Nutr. Sci.*, 58 (2008) 5-10.
- [94] M. van der Veen, W. Norde, M.C. Stuart, Electrostatic interactions in protein adsorption probed by comparing lysozyme and succinylated lysozyme, *Colloids Surf., B*, 35 (2004) 33-40.
- [95] J. Buijs, V. Hlady, Adsorption Kinetics, Conformation, and Mobility of the Growth Hormone and Lysozyme on Solid Surfaces, Studied with TIRF, *J. Colloid Interface Sci.*, 190 (1997) 171-181.
- [96] A. Salis, M.S. Bhattacharyya, M. Monduzzi, Specific Ion Effects on Adsorption of Lysozyme on Functionalized SBA-15 Mesoporous Silica, *J. Phys. Chem. B*, 114 (2010) 7996-8001.
- [97] D.E. Kuehner, J. Engmann, F. Fergg, M. Wernick, H.W. Blanch, J.M. Prausnitz, Lysozyme Net Charge and Ion Binding in Concentrated Aqueous Electrolyte Solutions, *J. Phys. Chem. B*, 103 (1999) 1368-1374.
- [98] Y.J. Yao, K.S. Khoo, M.C.M. Chung, S.F.Y. Li, Determination of isoelectric points of acidic and basic proteins by capillary electrophoresis, *J. Chromatogr. A*, 680 (1994) 431-435.
- [99] L. Palacio, C.C. Ho, P. Prádanos, A. Hernández, A.L. Zydney, Fouling with protein mixtures in microfiltration: BSA-lysozyme and BSA-pepsin, *J. Membr. Sci.*, 222 (2003) 41-51.
- [100] P. Rice, I. Longden, A. Bleasby, EMBOS: The European Molecular Biology Open Software Suite, *Trends Genet.*, 16 (2000) 276-277.

-
- [101] A. Vinu, V. Murugesan, M. Hartmann, Adsorption of Lysozyme over Mesoporous Molecular Sieves MCM-41 and SBA-15: Influence of pH and Aluminum Incorporation, *J. Phys. Chem. B*, 108 (2004) 7323-7330.
- [102] T.J. Su, J.R. Lu, R.K. Thomas, Z.F. Cui, J. Penfold, The Effect of Solution pH on the Structure of Lysozyme Layers Adsorbed at the Silica–Water Interface Studied by Neutron Reflection, *Langmuir*, 14 (1998) 438-445.
- [103] Y. Kamiyama, J. Israelachvili, Effect of pH and salt on the adsorption and interactions of an amphoteric polyelectrolyte, *Macromolecules*, 25 (1992) 5081-5088.
- [104] S. Yadav, T.M. Laue, D.S. Kalonia, S.N. Singh, S.J. Shire, The Influence of Charge Distribution on Self-Association and Viscosity Behavior of Monoclonal Antibody Solutions, *Mol. Pharm.*, 9 (2012) 791-802.
- [105] F.K. Onwu, S.P.I. Ogah, Adsorption of lysozyme onto silica and polystyrene surfaces in aqueous medium, *Afr. J. Biotechnol.*, 10 (2011) 3014-3021.
- [106] F. Hussein, 2007, Untersuchung verschiedener Einflüsse auf die Proteinadsorption an Primärpackmitteln, Thesis, Technische Universität Carolo-Wilhelmina zu Braunschweig.
- [107] J.R. Wendorf, C.J. Radke, H.W. Blanch, The role of electrolytes on protein adsorption at a hydrophilic solid-water interface, *Colloids Surf., B*, 75 (2010) 100-106.
- [108] S. Sharma, G.P. Agarwal, Interactions of Proteins with Immobilized Metal Ions: A Comparative Analysis Using Various Isotherm Models, *Anal. Biochem.*, 288 (2001) 126-140.
- [109] L.C.L. Aquino, E.A. Miranda, I.S. Duarte, P.T.V. Rosa, S.M.A. Bueno, Adsorption of human immunoglobulin G onto ethacrylate and histidine-linked methacrylate, *Braz. J. Chem. Eng.*, 20 (2003) 251-262.
- [110] R.D. Johnson, F.H. Arnold, The temkin isotherm describes heterogeneous protein adsorption, *Biochim. Biophys. Acta, Protein Struct. Mol. Enzymol*, 1247 (1995) 293-297.
- [111] J.E. Lee, S.S. Saavedra, Molecular Orientation in Heme Protein Films Adsorbed to Hydrophilic and Hydrophobic Glass Surfaces, *Langmuir*, 12 (1996) 4025-4032.
- [112] N. Bouropoulos, J. Moradian–Oldak, Analysis of Hydroxyapatite Surface Coverage by Amelogenin Nanospheres Following the Langmuir Model for Protein Adsorption, *Calcif. Tissue Int.*, 72 (2003) 599-603.
- [113] S.-C. Tsai, K.-W. Juang, Y.-L. Jan, Sorption of cesium on rocks using heterogeneity-based isotherm models, *J. Radioanal. Nucl. Chem.*, 266 (2005) 101-105.
- [114] I. Langmuir, The Adsorption of Gases on Plane Surfaces of Glass, Mica and Platinum, *J. Am. Chem. Soc.*, 40 (1918) 1361-1403.
- [115] Q. Luo, J.D. Andrade, Cooperative Adsorption of Proteins onto Hydroxyapatite, *J. Colloid Interface Sci.*, 200 (1998) 104-113.

- [116] T.P. Johnston, Adsorption of Recombinant Human Granulocyte Colony Stimulating Factor (rhG-CSF) to Polyvinyl Chloride, Polypropylene, and Glass: Effect of Solvent Additives, *PDA J. Pharm. Sci. Technol.*, 50 (1996) 238-245.
- [117] H.P. Jennissen, Evidence for negative cooperativity in the adsorption of phosphorylase b on hydrophobic agaroses, *Biochemistry*, 15 (1976) 5683-5692.
- [118] R.J. Umpleby, S.C. Baxter, Y. Chen, R.N. Shah, K.D. Shimizu, Characterization of Molecularly Imprinted Polymers with the Langmuir–Freundlich Isotherm, *Anal. Chem.*, 73 (2001) 4584-4591.
- [119] L.K. Koopal, W.H. van Riemsdijk, J.C.M. de Wit, M.F. Benedetti, Analytical Isotherm Equations for Multicomponent Adsorption to Heterogeneous Surfaces, *J. Colloid Interface Sci.*, 166 (1994) 51-60.
- [120] Q. Lan, A.S. Bassi, J.-X. Zhu, A. Margaritis, A modified Langmuir model for the prediction of the effects of ionic strength on the equilibrium characteristics of protein adsorption onto ion exchange/affinity adsorbents, *Chem. Eng. J. (Amsterdam, Neth.)*, 81 (2001) 179-186.
- [121] T. Zuyi, C. Taiwei, On the Applicability of the Langmuir Equation to Estimation of Adsorption Equilibrium Constants on a Powdered Solid from Aqueous Solution, *J. Colloid Interface Sci.*, 231 (2000) 8-12.
- [122] W. Norde, J. Lyklema, The adsorption of human plasma albumin and bovine pancreas ribonuclease at negatively charged polystyrene surfaces: I. Adsorption isotherms. Effects of charge, ionic strength, and temperature, *J. Colloid Interface Sci.*, 66 (1978) 257-265.

Chapter III

Polyglycerol Coatings of Glass Vials for Protein Resistance

The following chapter has been published in the European Journal of Pharmaceutics and Biopharmaceutics and the reproduction in this thesis is permitted by the journal:

Kerstin Höger^{1*}, Tobias Becherer^{2*}, Wei Qiang², Rainer Haag², Wolfgang Frieß¹, Sarah Kuchler¹

Polyglycerol coatings of glass vials for protein resistance

Eur. J. of Pharm. Biopharm., 85 (2013) 756-764

¹Department for Pharmacy, Pharmaceutical Technology and Biopharmaceutics, Ludwig-Maximilians University, Munich, Germany

²Department for Organic Chemistry, Freie Universität Berlin, Germany

*both authors contributed equally

Polyglycerol synthesis, analytics, vial coating and QCM-measurements were performed by Tobias Becherer. Wei Qiang contributed to vial coating.

Abstract

Proteins are surface active molecules which undergo non-specific adsorption when getting in contact with surfaces such as the primary packaging material. This process is critical as it may cause a loss of protein content or protein aggregation. To prevent unspecific adsorption, protein repellent coatings are of high interest. We describe the coating of industrial relevant borosilicate glass vials with linear methoxylated polyglycerol, hyperbranched polyglycerol and hyperbranched methoxylated polyglycerol. All coatings provide excellent protein

repellent effects. The hyperbranched, non-methoxylated coating performed best. The protein repellent properties were maintained also after applying industrial relevant sterilization methods (≥ 200 °C). Marginal differences in antibody stability between formulations stored in bare glass vials and coated vials were detected after 3 months storage; the protein repellent effect remained largely stable.

Here we describe a new material suitable for the coating of primary packaging material of proteins which significantly reduces the protein adsorption and, thus, could present an interesting new possibility for biomedical applications.

1 INTRODUCTION

Therapeutic antibodies are of great relevance for the treatment of various severe diseases such as cancer or autoimmune diseases [1]. The adsorption of therapeutic proteins on surfaces e.g. in the production line or in the storage containers poses challenges. Possible consequences might be the loss of the protein content [2] but also potential protein aggregation [3] accompanied by the risk of immunological reactions leading to a reduced therapeutic effect or severe adverse effects [4].

Consequently, substantial research efforts are made aiming for reduced protein adsorption to various materials [5]. In general, protein adsorption is driven by the interaction between electrical double layers and changes in the hydration state but also dispersion interactions [6]. To a certain extent, the ionic strength or the pH of the protein formulations may be adapted and excipients can be added [7]. Nevertheless, the mandatory preservation of the protein stability and the necessary physiological acceptability limits such changes [7].

Borosilicate glass is still a common material for the primary packaging of parenteral drugs. Aiming for increased protein resistance, material surface modifications by chemical strategies such as coating with dextran [8], carbohydrate-derived polymers [9], zwitterionic self-assembled monolayers and polymers [10, 11] have been tested. Chapman et al. mentioned several characteristics of functional groups on SAMs that showed good protein repellent properties [12]. Besides containing hydrogen bond accepting and polar groups, they do not incorporate hydrogen bond donors and they exhibit no net charge [12]. Furthermore, flexible aliphatic polyether elements, a branched structure, hydrophilic groups [13] and a stable layer of interfacial water [14] were related to a good protein resistance. Poly(ethylene glycol) (PEG) and oligo(ethylene glycol) (OEG) exhibit excellent protein repelling effects [15, 16] and unify many of those properties. The exact mechanism of the protein repellent

effect of PEG is still ambiguous. Currently, steric repulsion due to the polymer chains [17] and the ability to strongly bind water in the interface [14] are the favored theories. However, the main drawbacks of PEG are its thermal instability at temperatures ≥ 195 °C [13] and its sensitivity toward oxidation [18, 19] putting the coating as well as the drug stability at risk. Good thermal stability of the coating material is important for pharmaceutical industrial applications as basic sterilization processes such as heat sterilization are performed at temperatures ≥ 200 °C. Due to these limitations, the search for alternative materials is still ongoing. In 2004, monolayers of dendritic polyglycerol (PG) derivatives were described to reduce unspecific protein adsorption comparable to PEG [13]. In contrast to PEG, PG exhibits higher thermal and oxidative stability [13]. Decomposition of PEG starts at 195 °C whereas PG is stable up to 226 °C [13]. Besides dendritic PG structures, chemical modifications such as linear poly(methyl glycerol) and linear polyglycerols are also highly effective in terms of cell and protein resistance [20]. Nevertheless, until today, the suitability of those promising polymers for pharmaceutical industrial applications in terms of protein resistance has not been tested.

In this study, the coating procedure of industrial relevant type I glass vials serving as primary packaging material of protein formulations with linear methoxylated (LPG(OMe)), hyperbranched (HPG(OH)) and hyperbranched methoxylated (HPG(OMe)) polyglycerol based monolayers are described. We investigated the effects on protein adsorption using an IgG model antibody and human Growth Hormone (hGH). The impact of pH, ionic strength, and the suitability for industry-relevant sterilization methods (heat sterilization and autoclaving) on the protein resistance is presented. Furthermore, coating stability, long-term storage stability and its influence on the protein structure are described.

2 MATERIALS AND METHODS

2.1 Chemicals

All chemicals and solvents were reagent or HPLC grade, used as received and purchased from Sigma (Steinheim, Germany) unless stated otherwise. Dialysis was performed in regenerated cellulose tubes from Spectrum laboratories (Spectra/ Por[®] 6 Dialysis membrane, molecular weight cut-off (MWCO) 1000 g·mol⁻¹, purchased from Roth, Karlsruhe, Germany). The deionized water used was purified using a Millipore water purification system with a minimum resistivity of 18.0 M Ω ·cm. NaH₂PO₄ and glycine were purchased from Merck Chemicals (Darmstadt, Germany), Na₂HPO₄, Na-dodecylsulfate and bis-ANS were obtained

from Sigma-Aldrich (Munich, Germany). NaCl, NaOH and HCl were bought from VWR International (Darmstadt, Germany), and D-(+)-mannitol was obtained from Riedel-de-Haen (Honeywell Specialty Chemicals Seelze GmbH, Seelze, Germany).

2.2 Synthesis and Analytics

Triethoxysilyl modified polymers, LPG(OMe) (**1**), mPEG (**2**), and HPG(OH) (**3**) were synthesized as reported earlier [20] (Figure III-1A). HPG(OH) (**3a**) (GPC: M_n 2.0 kDa, M_w 3.1 kDa) and LPG(OMe) (GPC: M_n 2.2 kDa, M_w 2.7 kDa) were synthesized by a one-step anionic ring-opening polymerization of glycidol and glycidyl methyl ether, respectively [20-22]. Triethoxysilyl modified HPG(OMe) (**4**) was synthesized via a five-step sequence. Therefore, 5% of the initially present hydroxy groups of HPG(OH) (**3a**) were successively mesylated with methanesulfonyl chloride (**4a**) and converted to the corresponding azide (**4b**) with sodium azide analogously to literature [23]. The residual hydroxy groups were methylated by means of methyl iodide (**4c**). Subsequent catalytic hydrogenation of the azide groups with Pd/C gave the corresponding amine (**4d**) which was coupled to 3-(triethoxysilyl)propyl isocyanate to yield the triethoxysilyl modified HPG(OMe) (**4**) [20]. Amine functionalized HPG(OH) (**3b**) was synthesized according to literature [23].

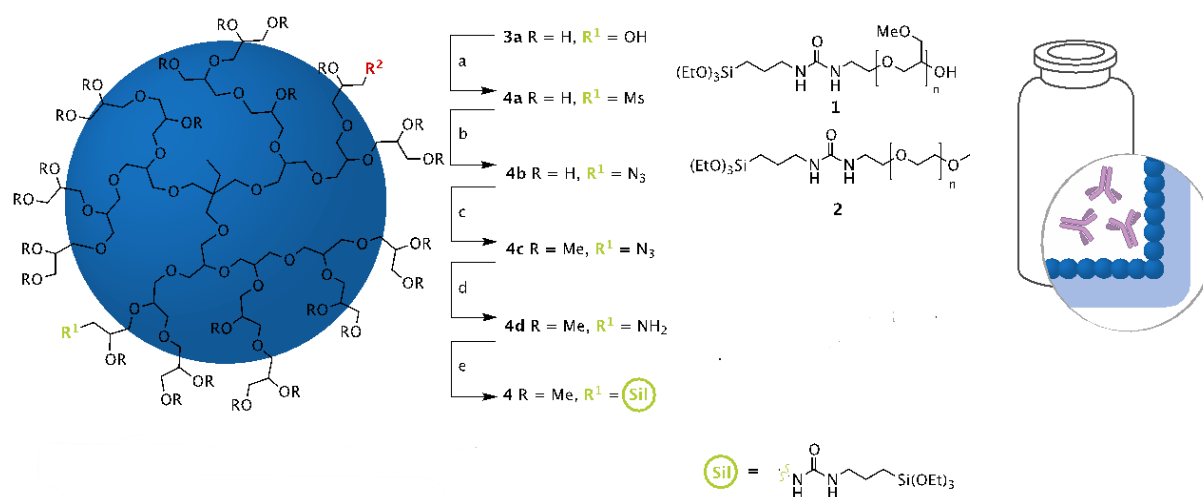


Figure III-1: (A) Synthesis and chemical structures of triethoxysilyl modified polymers: (a) MsCl, Pyridine, rt, 24 h; (b) NaN₃, DMF, 60 °C, 3 d; (c) KOH, DMSO, MeI, rt, 24 h; (d) Pd/C, MeOH, rt, 3 d; (e) 3-(triethoxysilyl)propyl isocyanate, THF, TEA, rt, 20 h; (B) Sketch of coated glass vial filled with antibody solution. (For interpretation of the references to color in this figure legend, the reader is referred to the web version of this article.)

2.2.1 Azide Functionalized HPG(OMe) (4c)

Azide functionalized HPG(OH) (**4b**) (2000 g·mol⁻¹, 12.3 g, 6.2 mmol) was dissolved in dry DMSO (200 mL) under inert gas atmosphere and KOH (41.7 g, 744 mmol, 120 eq. (4 eq./OH)) was added. The resulting suspension was vigorously stirred and cooled in a water bath. After slow addition of methyl iodide (52.8 g, 23.2 mL, 372 mmol, 60 eq. (2 eq./OH)) the mixture was stirred for 24 h under inert gas atmosphere. The reaction was quenched by the addition of water, concentrated under reduced pressure, and subsequently dried in high vacuum. The resulting residue was treated by water, and the compound was repeatedly extracted with DCM. The combined organic layers were dried under reduced pressure to yield a yellow honeylike product (12.7 g, 79%).

¹H NMR (400 MHz; CDCl₃): δ = 3.64-3.43 (m, 200 H, PG-backbone, secondary -OCH₃); 3.34 (s, 43 H, primary -OCH₃); 1.41-1.34 (m, 2 H, CH₂CH₃ of starter); 0.81 (t, 3 H, CH₂CH₃ of starter) ppm. ¹³C NMR (700 MHz; CDCl₃): δ = 79.6-79.2, 78.9-78.5, 72.7-72.6, 72.4-72.2, 72.0-71.0, 70.6-69.3 (PG-backbone); 59.3-59.2 (primary -OCH₃); 58.2-57.9 (secondary -OCH₃); 60.8-60.5 (CHN₃); 52.0, 51.6 (CH₂N₃); 23.7 (CH₂CH₃ of starter); 7.7 (CH₂CH₃ of starter) ppm. IR ν_{max}/cm⁻¹: 3361; 2876; 2098; 1460; 1355; 1274; 1196; 1089; 961; 832; 677.

2.2.2 Amine Functionalized HPG(OMe) (4d)

Azide functionalized HPG(OMe) (**4c**) (2500 g·mol⁻¹, 12.7 g, 4.9 mmol) was dissolved in MeOH. Pd/C (20 wt%, 2.5 g) was added and the mixture was stirred for 3 d under H₂-atmosphere (5 bar) at rt. The reaction mixture was filtered through Celite[®] and concentrated in vacuo to give a yellow honeylike product (11.3 g, 89%).

¹H NMR (400 MHz; CDCl₃): δ = 3.64-3.42 (m, 200 H, PG-backbone, secondary -OCH₃); 3.33 (s, 43 H, primary -OCH₃); 1.36-1.32 (m, 2 H, CH₂CH₃ of starter); 0.81 (t, 3 H, CH₂CH₃ of starter) ppm. ¹³C NMR (700 MHz; CDCl₃): δ = 79.5-79.1, 78.8-78.3, 72.6-72.5, 72.3-72.1, 71.8-70.9, 70.3-69.6 (PG-backbone); 59.2-59.1 (primary -OCH₃); 58.0-57.8 (secondary -OCH₃); 50.9-50.7 (CHNH₂); 43.2-42.7 (CH₂NH₂); 23.7 (CH₂CH₃ of starter); 7.7 (CH₂CH₃ of starter) ppm. IR ν_{max}/cm⁻¹: 3362; 2875; 1643; 1461; 1356; 1262; 1196; 1085; 960; 832; 679.

2.2.3 Triethoxysilyl Modified HPG(OMe) (4)

Triethoxysilyl modified HPG(OMe) (**4**) was synthesized analogously to literature [20]. Therefore amine functionalized HPG(OMe) (**4d**) (2500 g·mol⁻¹, 4 g, 1.5 mmol) was dissolved in dry THF (100 mL) under inert gas atmosphere in a teflon flask. While stirring at rt TEA (0.61 g, 0.83 mL, 6 mmol) and 3-(triethoxysilyl)propyl isocyanate (0.59 g, 0.59 mL,

2.4 mmol) were added successively and the reaction was allowed to proceed for 20 h. The mixture was concentrated under reduced pressure and subsequently dialysed against EtOH to yield **4** as yellow honeylike product (3.5 g, 86%).

^1H NMR (700 MHz; CDCl_3): δ = 5.17 (brs, 2 H, 2 x NH); 3.73 (q, 6 H, $\text{SiOCH}_2\text{CH}_3$); 3.63-3.34 (m, 203 H, PG-backbone, secondary $-\text{OCH}_3$); 3.29 (s, 43 H, primary $-\text{OCH}_3$); 3.08-3.00 (m, 4 H, 2 x CH_2NH); 1.54-1.47 (m, 2 H, $\text{SiCH}_2\text{CH}_2\text{CH}_2\text{NH}$); 1.32-1.26 (m, 2 H, CH_2CH_3 of starter); 0.76 (t, 3 H, CH_2CH_3 of starter); 0.54 (t, 2 H, $\text{SiCH}_2\text{CH}_2\text{CH}_2\text{NH}$) ppm. ^{13}C NMR (700 MHz; CDCl_3): δ = 158.7 (C=O); 79.5-79.2, 78.8-78.5, 72.6-72.3, 71.7-71.0, 70.2-69.8 (PG-backbone, $\text{NHCH}_2\text{CH}_2\text{CH}_2\text{O}$); 59.3-59.1 (primary $-\text{OCH}_3$); 58.4-58.2 (OCH_2CH_3); 58.0-57.7 (secondary $-\text{OCH}_3$); 43.2-42.7 ($\text{NHCH}_2\text{CH}_2\text{CHO}$, $\text{SiCH}_2\text{CH}_2\text{CH}_2\text{NH}$); 23.7 (CH_2CH_3 of starter); 23.0 ($\text{SiCH}_2\text{CH}_2\text{CH}_2\text{NH}$); 18.3 (OCH_2CH_3); 7.7 (CH_2CH_3 of starter) ppm. IR $\nu_{\text{max}}/\text{cm}^{-1}$: 3360; 2878; 1644; 1460; 1356; 1261; 1196; 1085; 956; 915; 832; 683.

^1H and ^{13}C NMR spectra were recorded on a Jeol ECX spectrometer operating at 400 MHz and a Bruker Avance 3 operating at 700 MHz, respectively at concentrations of $100 \text{ mg}\cdot\text{mL}^{-1}$. The chemical shifts are reported in δ (ppm) values and were referenced to indicated solvents. IR spectra were recorded on a Nicolet Avatar 32 FT-IR with Smart iTR accessory. GPC measurements were performed on an Agilent 1100 Series instrument including a refractive index detector. PS standards in THF and Pullulane standards in water have been used for calibration. The measurements were run in THF and in an aqueous sodium nitrate solution (0.1 M), respectively (1 mL min^{-1} , $20 \text{ }^\circ\text{C}$), using an array of Suprema Lux 100, Suprema 1000 and Suprema Lux 3000 columns (dimensions: $8 \times 300 \text{ mm}$, particle size: $10 \mu\text{m}$, PSS, Mainz, Germany).

2.3 Glass Coating Procedure

2R Fiolax[®] glass vials were coated according to a modified procedure described by Weinhart et al. [20]. The vials were cleaned and chemically activated by immersion into freshly prepared piranha solution ($\text{H}_2\text{SO}_4:\text{H}_2\text{O}_2 = 3:1$) for 30 min, followed by thoroughly rinsing with Milli-Q water and ethanol. Subsequently, the vials were filled up to the neck with an ethanolic solution containing the respective triethoxysilyl modified polymer ($0.1\cdot 10^{-3} \text{ M}\cdot\text{cm}^{-2}$ glass surface) and 30% v/v 1 M aqueous acetic acid. The vials were sealed with DuraSeal[®] (Carl Roth, Karlsruhe, Germany) to prevent evaporation and placed in an oven at $40 \text{ }^\circ\text{C}$ for 12 h. After cooling down to room temperature the vials were thoroughly rinsed with ethanol and dried in a stream of N_2 .

For QCM-D measurements, quartz crystal sensors with a silicon dioxide layer (QSX 303, Q-Sense AB, Gothenburg, Sweden) were cleaned and chemically activated by immersion into a 5:1:1 mixture of Milli-Q water, ammonia solution, and H₂O₂ for 7 min at 70°C, rinsed with Milli-Q water and ethanol, and placed in a glass vial containing an ethanolic solution of the respective triethoxysilyl modified polymer ($0.1 \cdot 10^{-3}$ M·cm⁻² glass surface) and 30% v/v 1 M aqueous acetic acid, closed with a cap, and placed in an oven at 40 °C for 12 h. Afterwards the quartz crystal sensors were thoroughly rinsed with ethanol and dried in a stream of N₂.

2.4 Protein Solutions

For adsorption experiments, a 2 mg/ml IgG1 solution in 10 mM phosphate buffer adjusted to varying ionic strength up to 170 mM with NaCl, was used as standard protein formulation. The pH value was adjusted by addition of 1 M NaOH or HCl. Human Growth Hormone (hGH) for adsorption experiments was obtained from Genotropin® MiniQuick 0.6 I.E. and 1.2 I.E. single-use syringes (Pharmacia & Upjohn). After reconstitution of the lyophilisates and dilution with corresponding formulation buffer, the solutions contained 0.8 mg/ml hGH, formulated in 1.5 mM NaH₂PO₄, 0.70 mM Na₂HPO₄, 11.19 mM glycine and 274.25 mM mannitol. All protein solutions were filtered through a 0.2 µm polyethersulfone membrane filter (Pall GmbH, Dreieich, Germany) before use. Ultrapure water (0.055 IS/cm) for all applications was obtained from a Purelab Plus UV/UF system (ELGA LabWater, Celle, Germany).

2.5 Protein Adsorption Testing

Adsorption experiments were performed in 2R Fiolax® type I borosilicate glass vials uncoated or coated with HPG(OH), HPG(OMe), LPG(OMe) or mPEG. Prior to testing, all vials were washed with ultrapure water at 80 °C. For standard adsorption testing, the vials were filled with 3.5 ml of a 2 mg/ml IgG1 solution or 1 ml of 0.8 mg/ml hGH solution, closed with Fluorotec® stoppers, sealed with Flip-Off® seals (West Pharmaceutical Services Deutschland GmbH & Co. KG) and incubated at 25 °C for 24 h (Figure III-1B). The inner surface area of a vial covered with protein formulation was calculated as 13.4 cm² or 5.06 cm² for a filling volume of 3.5 ml or 1 ml, respectively. After incubation, the vials were emptied using a syringe. Subsequently, each vial was rinsed four times with the corresponding formulation buffer. For desorption of bound protein, 3.5 ml (1 ml for vials with hGH) of 10 mM PBS containing 145 mM NaCl and 0.05% SDS (pH 7.2) were filled into each of the vials, which were closed and stored overnight at 25 °C [24]. Desorbed protein was quantified via size-

exclusion chromatography [24] (Agilent 1100 HPLC, Agilent 1200 fluorescence detector, Agilent Technologies GmbH, Boeblingen, Germany), using a TSKgel SW_{XL} guard column and a 3000SW_{XL} SEC-column (Tosoh Bioscience GmbH, Stuttgart, Germany). 400 μ l per sample were injected and eluted with desorption buffer as mobile phase at a flow rate of 0.75 ml/min. The intrinsic fluorescence signal of the protein was detected at $\lambda_{\text{ex}}/\lambda_{\text{em}}$ 280 nm/334 nm. A calibration line was included in each batch. All chromatograms were integrated manually using ChemStation Software Rev. B 02.01 (Agilent Technologies GmbH, Boeblingen, Germany).

For long-term adsorption study of IgG1, the vials were heat sterilized at 180 °C for 30 min after washing. After filling with 3.5 ml IgG1 solution, the vials were closed with Fluorotec[®] stoppers and sealed with Flip-Off[®] seals. The incubation time was set to 24 h, one or three months at temperatures of 2-8 °C, 25 °C or 40 °C, respectively. After incubation, the IgG1 solutions were removed from the vials and further used for analysis of the protein stability. Adsorbed protein was quantified according to the standard procedure described above.

For testing of different sterilization methods, the vials were washed and heat sterilized at 215 °C or 240 °C for 30 min or autoclaved at 121 °C, 2 bar for 15 min prior to filling with 3.5 ml IgG1 solution. Incubation, desorption and quantification followed the standard procedure.

2.6 Stability Testing of the HPG(OH)-Coating toward pH Change via QCM-D

The hydrolytic stability of HPG(OH) coatings at various pH was tested using a quartz crystal microbalance (QCM-D) (Q-Sense E1, Q-Sense AB, Gothenburg, Sweden) by measuring the adsorption of fibrinogen subsequent to treatment of the chip with the respective alkaline or acidic aqueous solution. QCM-D allows monitoring the changes in resonance frequency (f) and dissipation (D) of a piezoelectric quartz crystal as a function of time. f and D were recorded at the fundamental frequency (4.95 MHz) and its 3rd, 5th, 7th, 9th, 11th, and 13th overtone. Adsorption layer thickness and adsorbed mass were calculated using the Sauerbrey and Voigt model. The Sauerbrey equation is only valid for rigid adsorbed layers and does not take into account the dissipation change. Thus, it underestimates the adsorbed mass by up to 40%. In contrast, the adsorption of a well hydrated protein layer results in a highly viscoelastic film which does not fully follow the oscillation of the quartz crystal. Therefore, energy is dissipated which causes an increase in D . Since the Sauerbrey model underestimates the amount of the deposited mass, the thickness and the mass of the adsorbed protein layer was additionally calculated by combining the obtained data of three different overtones

($n = 3, 5, 7$) based on the Voigt model using the software package Qtools (version 3.0.15.553, Q-Sense AB, Gothenburg, Sweden). For intact coatings, where almost no protein adsorption occurred, the Voigt model does not fit well the measured data as it overestimates the thickness and mass by a factor of 10. Therefore, in these cases only the data calculated by the Sauerbrey model is shown.

Phosphate buffered saline (PBS, 10 x concentrated) (Lonza, Köln, Germany), was diluted to a 1 x concentration by Milli-Q, passed through a 0.22 μm filter, and degassed prior to use. Fibrinogen solutions were prepared at concentrations of 1 mg/ml in PBS (pH 7.4). Alkaline and acidic aqueous solutions were prepared by adjusting the pH by adding NaOH (1 M) and HCl (1 M) respectively.

All measurements were performed twice under dynamic conditions at flow rates of 0.1 ml/min according to the following protocol on HPG(OH) coated and bare quartz crystal sensors: injection of (i) Milli-Q water (0.2 mL), (ii) NaOH_{aq} and HCl_{aq} of pH 4, 8.5, 10, 11.5 or 12.5, respectively (3 ml), (iii) Milli-Q water (2 ml), (iv) PBS (1 ml), (v) fibrinogen (2.5 ml, 1 mg/ml), (vi) PBS (1 ml). The density of the adsorbed fibrinogen layer was assumed to be 1200 $\text{kg}\cdot\text{m}^{-3}$, the fluid density 1000 $\text{kg}\cdot\text{m}^{-3}$, and the fluid viscosity 0.001 $\text{kg}\cdot\text{ms}^{-1}$.

2.7 Protein Stability after Storage

The stability of the IgG1 formulation (10 mM PBS, 145 mM NaCl, pH 7.2) after 3 months storage was investigated in regard to changes in tertiary structure via extrinsic fluorescence and for particle formation. Spectra of 0.05 mg/ml IgG1 solutions with 5 μM bis-ANS were recorded with a Varian Cary Eclipse fluorescence spectrophotometer (Varian Deutschland GmbH, Darmstadt, Germany) at λ_{ex} 385 nm and λ_{em} 420 – 700 nm in 10 x 10 mm fluorescence quartz cuvettes at 25 °C. A solution of IgG1 heat stressed at 75 °C for 15 min was used as control for unfolded protein.

Particle formation in the protein solution was investigated by HP-SEC, turbidity measurements as well as visible and subvisible particle analysis. Protein aggregates and fragments in the protein solutions were quantified via HP-SEC (equipment see 2.5) using a YMC-Pack Diol-300 SEC-column (YMC Europe GmbH, Dinslaken, Germany) and a TSKgel SW_{XL} guard column (Tosoh Bioscience GmbH, Stuttgart, Germany) with UV-detection at λ_{ex} 280 nm. 100 μl of each sample with a concentration of 2 mg/ml was eluted with 10 mM PBS containing 145 mM NaCl, pH 7.2. The content of aggregates, monomer and fragments in the sample solutions was calculated in percent of the total protein content of the reference. Turbidity of the solutions was measured using a Nephla laboratory turbidimeter (Hach Lange

GmbH, Düsseldorf, Germany). Light scattering was detected at an angle of 90 ° in glass cuvettes, applying a filling volume of 1.7 ml. Visible particle inspection was performed by visual control of the solution in front of a dark background and a light source. Subvisible particle analysis was performed via light obscuration with a PAMAS SVSS-35 (PAMAS GmbH, Rutesheim, Germany). Three fractions of 0.3 ml of each sample with 0.3 ml pre-run volume were analyzed [25]. The system was rinsed with ultrapure water before each measurement until no particles larger than 10 µm and less than 100 particles per ml in total were measured. Amount and diameter of particles were determined by the PAMAS PMA software and are presented in cumulative particles per ml protein solution.

2.8 Tests of Significance

The means of two populations were tested for equality by a two-tailed *T*-test for independent samples. Statistical significance is given on the levels $p < 0.05$, $p < 0.01$ and $p < 0.001$. Statistics are depicted in the figures only for differences discussed in the text.

3 RESULTS

3.1 Effect of Different Polyglycerol Coatings on IgG1 and hGH Adsorption

To investigate the effect of LPG(OMe), HPG(OH) and HPG(OMe) coatings on protein adsorption, the adsorption of IgG1 at different formulation pH and ionic strength conditions was quantified and compared to the adsorption to non-coated type I glass vials. The pH values of 4 and 7.2 were selected to evaluate the influence of protein charge on IgG1 adsorption. At these pH values, the antibody exhibits a very strong or strong positive charge (pI of the protein ~8.5). The influence of ionic strength on both intermolecular protein interactions as well as protein surface interactions was taken into account by investigating adsorption at low (22 mM) and high (170 mM) ionic strength. At pH 4/170 mM, a high IgG1 adsorption of 4.2 mg/m² to type I glass vials was found, compared to less than 2 mg/m² at pH 7.2 (Figure III-2). At pH 4/22 mM, adsorption was lower than at 170 mM ionic strength. This corresponds to the pH and ionic strength dependent protein adsorption behavior described in the literature [24]. At all three conditions, IgG1 adsorption was significantly suppressed ($p < 0.01$) by all tested polyglycerol coatings (Figure III-2). The pH and ionic strength effect on the protein adsorption as seen for non-coated glass vials were of marginal relevance for the PG-coated vials. Adsorption to HPG(OH)-coated vials tended to be lower than to methoxylated HPG-coated vials, but the effect was not always significant.

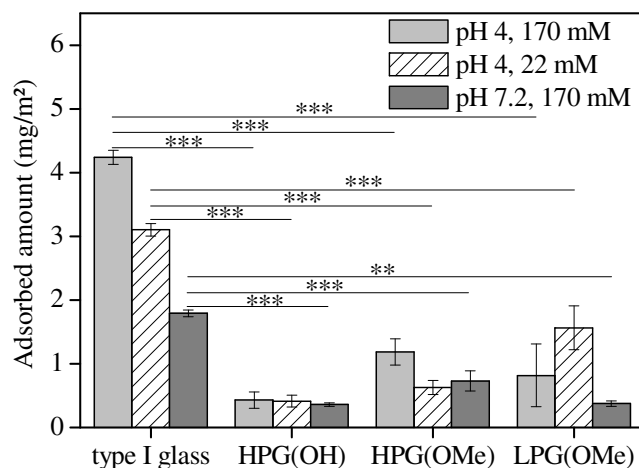


Figure III-2: IgG1 adsorption to type I borosilicate glass vials, HPG(OH)-, HPG(OMe)- and LPG(OMe)-coated glass vials at different pH values and ionic strength (* $p < 0.05$, ** $p < 0.01$, * $p < 0.001$). $n=3$.**

We also tested the adsorption of the therapeutic protein human Growth Hormone (hGH) to HPG(OH)-coated vials (Figure III-3) because this coating was superior compared to other PG-coatings at some conditions. The tests were based on the composition of the commercially available formulation of Genotropin® MiniQuick 0.6 I.E. aiming for highly relevant conditions. Again, the amount of hGH adsorbed was significantly lower on the HPG(OH)-coated vials compared to non-coated glass vials (Figure III-3). At 25 °C, hGH adsorption of 2.62 mg/m² to type I glass vials was reduced to 0.72 mg/m² by the HPG(OH)-coating. The higher adsorption to glass vials observed after storage at 25 °C compared to 2-8 °C was not observed with the HPG(OH)-coated vials.

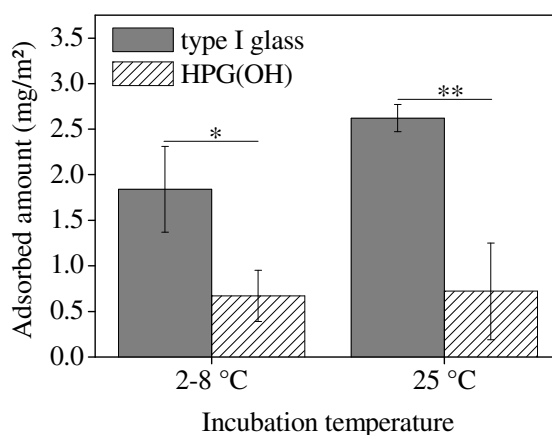


Figure III-3: Adsorption of hGH to type I glass vials and HPG(OH)-coated vials after 24 h incubation time at 2-8 °C and 25 °C (* $p < 0.05$, ** $p < 0.01$), $n=3$.

3.2 Influence of Sterilisation on Polyglycerol Coatings

For parenteral pharmaceutical products and for various other applications, sterilized vials are mandatory. Consequently, the protein repellent properties of the HPG(OH)-, HPG(OMe)-, and LPG(OMe)-coatings were tested after 30 min heat sterilization at 215 °C and 240 °C. Additionally, the effect of autoclaving (121 °C, 2 bar, 15 min) on the coating stability was investigated. mPEG served as reference.

Sterilization with dry heat for 30 min at 215 °C resulted in only slight changes of IgG1 adsorption for the HPG-coated vials. In contrast, adsorption to LPG(OMe) and mPEG-coated vials clearly increased (Figure III-4), indicating thermal damage, presumably decomposition of the coating. Sterilization at 240 °C led to increased adsorption to all coatings, due to the expected thermal instability of all PG-coatings. The results indicated higher resistance of HPG(OH)- and HPG(OMe)-coating at temperatures above 195 °C compared to mPEG and LPG(OMe). Again, protein adsorption was most efficiently suppressed on HPG(OH)-coated vials. Autoclaving of the vials did not cause an essential increase in IgG1 adsorption to HPG(OH)-, HPG(OMe)- and LPG(OMe)-coated vials compared to the non-sterilized vials (Figure III-4). Adsorption values for autoclaved mPEG-coated vials were below the range of the calibration line (data not shown).

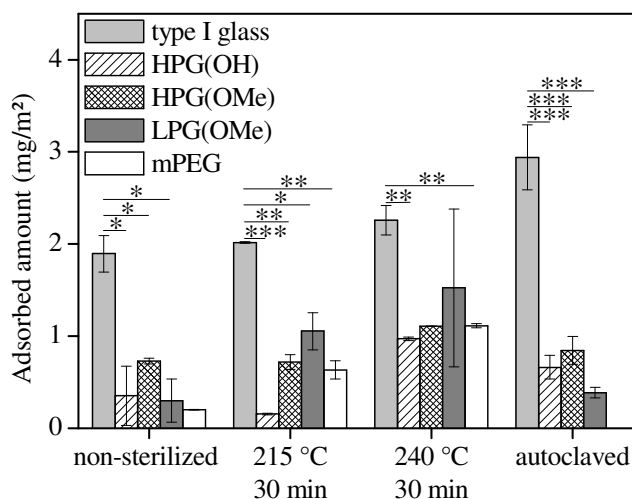


Figure III-4: Adsorption of IgG1 to type I borosilicate glass vials, HPG(OH)-, HPG(OMe)-, LPG(OMe)- and mPEG-coated glass vials after heat sterilization and autoclaving (*p < 0.05, **p < 0.01, *p < 0.001), n ≥ 2.**

3.3 Long-Term Effect of Polyglycerol Coating on Protein Adsorption

To test the stability of the protein repellent effects of the PG coating, IgG1 adsorption to HPG(OH)-coated vials up to 3 months was investigated. Again, we opted for the HPG(OH)

coated vials as they showed the best protein repellent effects and stability in the previous tests. IgG1 adsorption to type I borosilicate glass vials did not change significantly for 1 month (Figure III-5). After 3 months, the amount adsorbed at 2-8 °C and 40 °C was slightly higher than at 25 °C, but without statistical significance. IgG1 adsorption to HPG(OH)-coated vials was significantly lower than on type I glass vials at all temperatures and time points. IgG1 adsorption remained constant for 1 month. After 3 months, adsorption at 40 °C was significantly increased. A tendency to higher protein adsorption levels at 2-8 °C after 3 months might be speculated but the difference to the 24 h and 1 month data was not significant ($p < 0.05$).

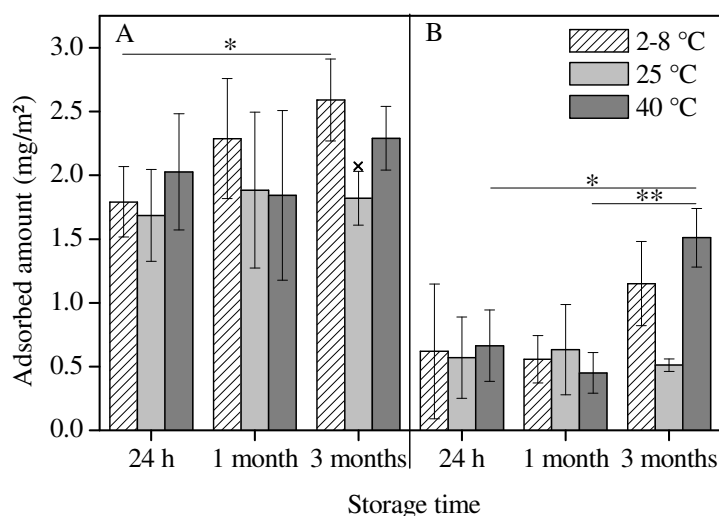


Figure III-5: Adsorption of IgG1 to type I glass vials (A) and HPG(OH)-coated vials (B) after storage for up to 3 months at different temperatures (* $p < 0.05$, ** $p < 0.01$, * $p < 0.001$), $n=3$, samples marked with \times : $n=2$.**

3.4 Effect of HPG(OH)-Coating on IgG1 Stability in Solution

To ensure protein stability upon prolonged exposure to HPG(OH)-coated vials, we analyzed protein solutions after 3 months storage for visual appearance, subvisible particles, the occurrence of aggregates and fragments as well as changes in protein structure by extrinsic fluorescence spectroscopy. All solutions were visually unchanged. Turbidity measurements revealed only marginal changes compared to a fresh IgG1 solution. The counts of particles $\geq 10 \mu\text{m}$ and $\geq 25 \mu\text{m}$ were found to be slightly increased compared to the IgG1 starting solution, but were still significantly below the pharmacopoeial acceptance level of less than 6000 particles $\geq 10 \mu\text{m}$ and 600 particles $\geq 25 \mu\text{m}$ per container [26] which equals 3.5 ml for the applied 2R vials and did not differ significantly between the vial species at the same storage temperatures (Figure III-6). The monomer content analyzed by HP-SEC remained

constant at about 94-96% (Figure III-7) and only samples stored at 40 °C showed a slightly enhanced fragmentation for both vial species.

The tertiary structure of IgG1 was analyzed by extrinsic fluorescence spectroscopy using bis-ANS as dye. The almost non-fluorescent dye exhibits a strong fluorescence in contact with a nonpolar environment such as hydrophobic domains in proteins [27]. Samples stored in type I glass vials and HPG(OH)-coated vials showed an equally pronounced, slight shift of the

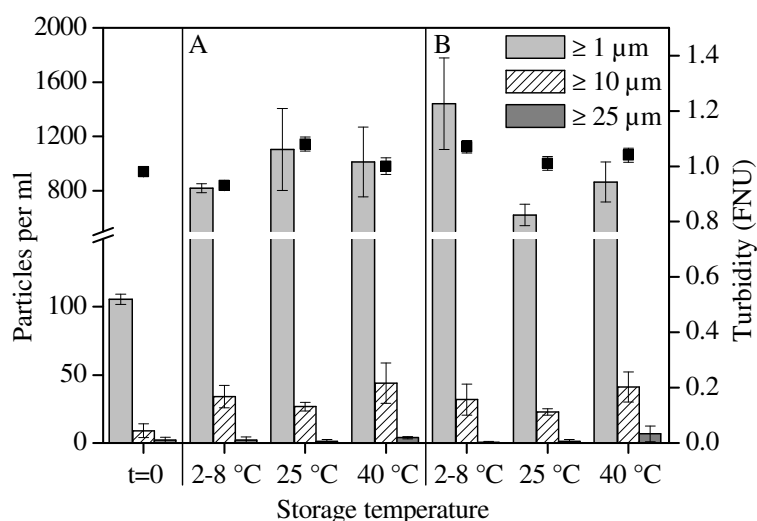


Figure III-6: Turbidity and number of particles determined in IgG1 solutions stored in type I glass vials (A) and HPG(OH)-coated vials (B) for 3 months at different temperatures, n=3.

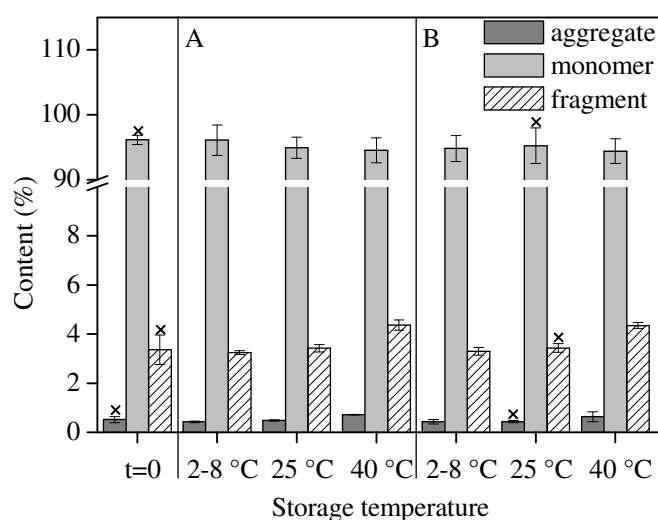


Figure III-7: Content of monomer, aggregates and fragments in IgG1 solutions stored in type I glass vials (A) and HPG(OH)-coated vials (B) for 3 months at different temperatures. Values given in percent of the total protein content of the reference. n=3, samples marked with x: n=2.

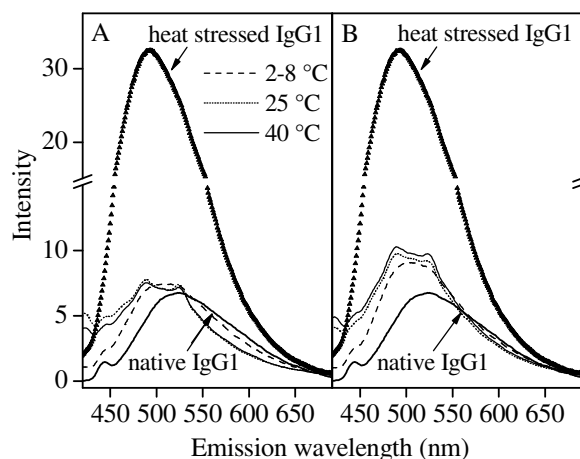


Figure III-8: Fluorescence spectra of IgG1 solutions after 3 months storage in type I glass vials (A) and HPG(OH)-coated vials (B) in presence of 5 μ M bis-ANS; storage temperature 2-8 $^{\circ}$ C (----), 25 $^{\circ}$ C (.....), 40 $^{\circ}$ C (—). Samples $n=3$, heat stressed and native reference $n=1$.

fluorescence maximum and slightly increased fluorescence intensity compared to the native antibody (Figure III-8). Storage at different temperatures did not change the extrinsic fluorescence. A heat stressed reference was included as a control to illustrate increased bis-ANS fluorescence due to protein unfolding with a distinct blue shift of the maximum from about 525 nm to about 494 nm.

3.5 Stability Testing of the HPG(OH)-Coating toward pH Change via QCM-D

The stability of HPG(OH) modified glass surfaces toward hydrolysis was tested by measuring the protein repellent effect of coated quartz crystals after treatment with aqueous solutions in the pH range from 4 to 12.5 by QCM-D. Hydrolytic cleavage of the siloxane bonds which link the polymer to the glass surface causes a loss of the tethered polymer, resulting in an increased protein adsorption. Values from QCM-D measurements as well as calculated values using the Sauerbrey and Voigt model are summarized in Table III-1. Typical plots of Δf and ΔD are shown in Figure III-9 a and b. Fibrinogen served as model protein for these experiments due to its high adsorption tendency to various surfaces [28, 29]. Thus, a high sensitivity of the measurements toward changes in the surface properties was ensured. Furthermore, fibrinogen had been previously used to investigate adsorption to PG-coated surfaces [20, 30] allowing good comparability of the results.

The total mass measured by QCM-D includes both the mass of the adsorbed fibrinogen and of the associated water, i.e., water trapped in cavities, the hydration layer, and hydrodynamically

Table III-1: QCM-D results for testing hydrolytic stability of HPG(OH)-silyl (3) coatings on quartz crystal sensors after injection of 2.5 mL fibrinogen (1 mg·ml⁻¹). Normalized data for the 3rd overtone are shown ($\Delta f_3/3$). Thickness and mass of the adsorbed fibrinogen layer were calculated according to the Voigt and the Sauerbrey model, respectively.

pH	$\Delta f_3/3$ [Hz]	ΔD_3 [10 ⁻⁶]	Average thickness of adsorbed fibrinogen layer [nm]		Mass of adsorbed fibrinogen layer ^a [mg/m ²]	
			Sauerbrey	Voigt	Sauerbrey	Voigt
4.0	-1.38±0.08	0.81±0.02	0.21±0.01	-	0.24±0.01	-
8.5	-1.34±0.12	0.69±0.05	0.20±0.01	-	0.24±0.02	-
10	-25.76±0.73	5.36±1.50	3.84±0.11	5.98±0.30	4.61±0.13	7.24±0.27
11.5	-68.31±0.90	14.74±0.41	10.01±17	15.50±0.79	12.23±0.18	18.60±0.93
12.5	-117.30±1.40	16.32±0.28	17.49±0.21	24.38±1.22	20.99±0.25	27.80±1.46
7.4	-1.56±0.17	0.89±0.11	0.23±0.03	-	0.27±0.03	-
bare SiO ₂	-108.30±2.08	11.29±1.37	16.15±0.31	27.15±6.96	21.67±1.93	32.57±8.35

^aThe total mass of the adsorbed fibrinogen layer includes the mass of the associated water, i.e. water trapped in cavities, the hydration layer, and hydrodynamically coupled water [29, 31].

coupled water [31]. Since the associated water content of an adsorbed fibrinogen layer can account for up to 70% of the detected mass, the values given in Table III-1 are considerably higher than adsorbed masses determined with optical techniques [29]. Taking into account this high water percentage of the adsorbed layer the results obtained by QCM-D are in good agreement with our previous protein adsorption studies on glass slides using fluorescence microscopy [20].

At pH 7.4, no protein adsorption occurred. After treatment with aqueous solution at pH 4 and 8.5 the amount of adsorbed fibrinogen was almost identical to the amount adsorbed onto untreated HPG(OH) modified glass surfaces (Figure III-9a and b). These results suggest that HPG(OH) modified glass surfaces are not susceptible toward hydrolysis under typically used protein formulation conditions. In contrast, at pH 10, the siloxane bond is more susceptible to hydrolysis, which becomes evident from the increased fibrinogen adsorption. By gradually increasing the pH leading to a loss of the HPG(OH) functionalization, the amount of adsorbed fibrinogen further increased. At pH 12.5 it reached the same level as fibrinogen adsorption to bare SiO₂ (Figure III-9a and b).

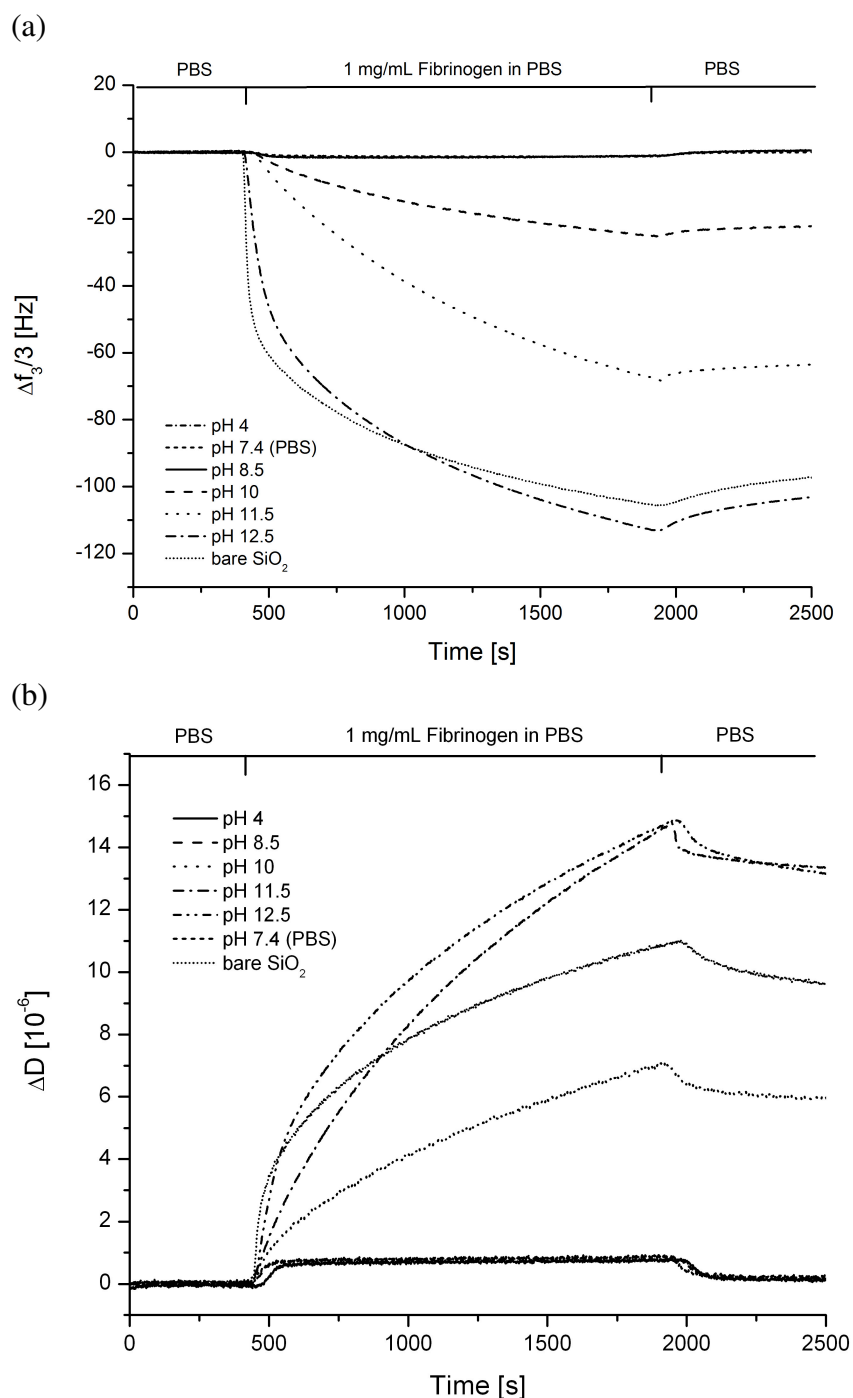


Figure III-9: QCM-D frequency changes $\Delta f_3/3$ (a) and dissipation changes ΔD_3 (b) of fibrinogen adsorption to HPG(OH)-silyl (3) coated and unmodified glass surfaces after 30 min. treatment with alkaline or acidic aqueous solutions.

4 DISCUSSION

Linear and hyperbranched (methoxylated) polyglycerols were synthesized and characterized previously [20] showing excellent protein repellent effects. However, to date only gold and flat glass slides have been coated with these polymers and to our best knowledge no studies

on relevant packaging material such as glass vials have been conducted. Therefore, we tested the protein adsorption to industrial relevant type I borosilicate glass vials coated with linear methoxylated (LPG(OMe)), hyperbranched (HPG(OH)) and hyperbranched methoxylated (HPG(OMe)) polyglycerol, and the coating stability to elucidate its feasibility for the application in the pharmaceutical industry.

Exemplary QCM-D measurements performed on HPG(OH)-coated quartz crystals revealed a very good coating stability (Table III-1, Figure III-9). At pH values above 10, fibrinogen adsorption increased significantly due to hydrolytic cleavage of the siloxane bond and a loss of the coating. Nevertheless, these alkaline pH values are not relevant for typical pharmaceutical protein formulations. Therefore, further protein adsorption experiments were performed at formulation relevant pH values between 4 and 7.2.

Protein adsorption was reduced significantly using the PG-coated vials compared to conventional glass vials. Furthermore, these coatings reduced the impact of the pH and of the ionic strength on the protein adsorption (Figure III-2). In contrast, using bare glass (vials) the unspecific protein adsorption strongly depends on these parameters (Figure III-2). Mathes et al. investigated the adsorption of IgG1 to borosilicate glass vials and found similar adsorption trends in regard to pH and ionic strength [24]. The author ascribed these trends to the interplay of attractive electrostatic protein-sorbent interactions and intermolecular repulsion on the surface which are both influenced by the ionic strength. Borosilicate glass was found to be negatively charged at pH values above pH 2.3 [24], whereas our antibody exhibited a very strong or strong positive charge at pH 4 and 7.2 respectively (pI~8.5). This stronger positive charge of the antibody at pH 4 thus supposedly led to increased electrostatic attraction and higher adsorbed amounts compared to pH 7.2. On the other hand, electrostatic repulsion between the molecules at pH 4 was increased due to the high positive charge of the protein. Decreasing the ionic strength at pH 4 from 170 mM to 22 mM resulted in a decreased shielding of this repulsion by ions in solution and thus to reduced adsorbed amounts, a trend which was described previously [24]. On PG-coated vials, the coating screened the charge of the surface and thus electrostatic attraction between the protein and sorbent. Similarly, Pasche et al. suggested that PEG layers of sufficient thickness facilitate the shielding of charges in the interface and thus contribute to adsorption prevention [32]. Hence, the marginal influence of pH and ionic strength on IgG1 adsorption to PG-coated vials may be related to the effective suppression of electrostatic interactions between the surface and the protein.

Besides protein repellent effects also good thermal stability of the coating material is important as basic industrial sterilization processes such as heat sterilization are normally

performed at temperatures ≥ 200 °C. Effective suppression of the protein adsorption can only be expected when the protein repelling coating is still intact and stable after the sterilization. Those preconditions cannot be met by PEG as its decomposition onset is at 195 °C. In contrast, polyglycerol is thermally stable up to 226 °C [13]. Our data clearly showed consistent protein resistance of the HPG-coatings after sterilization at 215 °C but increased adsorption to LPG(OMe)- and mPEG-coated vials compared to the non-sterilized vials (Figure III-4). The reduced repellent effects after sterilization at 240 °C may be ascribed to the onset of thermal decomposition that was observed above 226 °C for PG [13] although the protein resistance was still superior to the uncoated glass vials. Nevertheless, more detailed studies on the thermal stability of our coatings are needed.

In previous studies, LPG(OMe) exhibited a better protein resistance than HPG(OH) [20]. In comparison, our adsorption studies showed a superiority of HPG(OH) at low ionic strength (Figure III-2). This trend was confirmed after sterilization of the vials at 215 °C (Figure III-4). In contrast to our experiments, Weinhart et al. studied the protein adsorption on flat glass slides at one ionic strength and without considering industrially mandatory sterilization processes and storage stability [20]. Hence, the deviation of the obtained results supposedly resulted from the different protein formulations but also from the processing of the coated vials before adsorption. This underlines the importance of industrial relevant conditions during the testing of new coating materials. For all adsorption experiments with IgG1, saturation conditions and thus an unchanged adsorption mechanism should be provided. Adsorption isotherms of IgG showed adsorption plateau values at equilibrium concentrations of about 1 to 2 mg/ml [7, 33]. Therefore, we chose a concentration of 2 mg/ml IgG1 for the adsorption experiments. In comparison, hGH adsorption plateaus were possibly not reached at a concentration of 0.8 mg/ml in the original formulation.

Stability of the coating material in vials filled with formulation is another prerequisite for a primary packaging material of sensitive drugs. QCM measurements and adsorption experiments showed excellent protein repellent effects for the range pH 4-8.5. Nevertheless, the incubation times during these experiments were only 30 min and 24 h. Partial hydrolysis of the coating can occur over weeks and months which is even more relevant for pharmaceutical packaging material. Therefore, IgG1 adsorption onto HPG(OH)-coated vials was investigated for a longer period. Even after 3 month storage of IgG1 we did not see significant changes in the protein repellent effects of our coating material HPG(OH) for storage at 2-8 °C and 25 °C, a trend to a slight increase could be speculated (Figure III-5). In terms of protein stability, the focus lay on protein aggregates as they may cause severe

immunological reactions or affect the efficacy of the drug [34]. In our study, we did not detect considerable differences in soluble aggregates, subvisible and visible particles and extrinsic fluorescence between formulations stored in coated and non-coated vials (Figure III-6, Figure III-7 and Figure III-8), indicating that the HPG(OH)-coating material did not impair protein stability.

5 CONCLUSION

In conclusion, we describe the successful coating of type I borosilicate glass vials, which are the main primary packaging material for many biomacromolecular drugs including proteins, with polyglycerols. Especially the hyperbranched, hydroxy-terminated polyglycerol coatings exhibit excellent protein resistant effects also after sterilization and long-time storage. Therefore, it is a highly promising candidate for the improvement of biomedical packaging materials.

Due to the high protein concentrations used in this study, the relative protein loss was rather low. Nevertheless, the evaluation of protein repellent materials is of high importance as the protein loss can be substantial in low concentrated protein formulations. Finally, the potential for the formation of aggregates and thus an increased risk of immune responses [4] due to adsorption is presumably independent of the relative protein loss from solution.

6 REFERENCES

- [1] W. Wang, S. Singh, D.L. Zeng, K. King, S. Nema, Antibody structure, instability, and formulation, *J. Pharm. Sci.*, 96 (2007) 1-26.
- [2] McLeod, Walker, Zheng, Hayward, Loss of factor VIII activity during storage in PVC containers due to adsorption, *Haemophilia*, 6 (2000) 89-92.
- [3] E.Y. Chi, J. Weickmann, J.F. Carpenter, M.C. Manning, T.W. Randolph, Heterogeneous nucleation-controlled particulate formation of recombinant human platelet-activating factor acetylhydrolase in pharmaceutical formulation, *J. Pharm. Sci.*, 94 (2005) 256-274.
- [4] A.S. Rosenberg, Effects of protein aggregates: an immunologic perspective, *AAPS J.*, 8 (2006) E501-507.
- [5] H. Otsuka, Nanofabrication of Nonfouling Surfaces for Micropatterning of Cell and Microtissue, *Molecules*, 15 (2010) 5525-5546.
- [6] W. Norde, Proteins at solid surfaces, in: A. Baszkin, W. Norde (Eds.), *Physical Chemistry of Biological Interfaces*, Marcel Dekker Inc., Basel 2000, pp. 115-135.
- [7] J. Mathes, 2010, Protein Adsorption to Vial Surfaces: Quantification, Structural and Mechanistic Studies, Thesis, Ludwig-Maximilians Universität München.
- [8] R.A. Frazier, G. Matthijs, M.C. Davies, C.J. Roberts, E. Schacht, S.J.B. Tandler, Characterization of protein-resistant dextran monolayers, *Biomaterials*, 21 (2000) 957-966.
- [9] H. Urakami, Z. Guan, Living Ring-Opening Polymerization of a Carbohydrate-Derived Lactone for the Synthesis of Protein-Resistant Biomaterials, *Biomacromolecules*, 9 (2008) 592-597.
- [10] Y. Chang, S.-C. Liao, A. Higuchi, R.-C. Ruaan, C.-W. Chu, W.-Y. Chen, A Highly Stable Nonbiofouling Surface with Well-Packed Grafted Zwitterionic Polysulfobetaine for Plasma Protein Repulsion, *Langmuir*, 24 (2008) 5453-5458.
- [11] S. Chen, J. Zheng, L. Li, S. Jiang, Strong Resistance of Phosphorylcholine Self-Assembled Monolayers to Protein Adsorption: Insights into Nonfouling Properties of Zwitterionic Materials, *J. Am. Chem. Soc.*, 127 (2005) 14473-14478.
- [12] R.G. Chapman, E. Ostuni, S. Takayama, R.E. Holmlin, L. Yan, G.M. Whitesides, Surveying for Surfaces that Resist the Adsorption of Proteins, *J. Am. Chem. Soc.*, 122 (2000) 8303-8304.
- [13] C. Siegers, M. Biesalski, R. Haag, Self-Assembled Monolayers of Dendritic Polyglycerol Derivatives on Gold That Resist the Adsorption of Proteins, *Chem. Eur. J.*, 10 (2004) 2831-2838.
- [14] P. Harder, M. Grunze, R. Dahint, G.M. Whitesides, P.E. Laibinis, Molecular Conformation in Oligo(ethylene glycol)-Terminated Self-Assembled Monolayers on

- Gold and Silver Surfaces Determines Their Ability To Resist Protein Adsorption, *J. Phys. Chem. B*, 102 (1998) 426-436.
- [15] K.L. Prime, G.M. Whitesides, Self-assembled organic monolayers: model systems for studying adsorption of proteins at surfaces, *Science*, 252 (1991) 1164-1167.
- [16] Z. Yang, J.A. Galloway, H. Yu, Protein Interactions with Poly(ethylene glycol) Self-Assembled Monolayers on Glass Substrates: Diffusion and Adsorption, *Langmuir*, 15 (1999) 8405-8411.
- [17] J.D. Andrade, V. Hlady, Protein adsorption and materials biocompatibility: A tutorial review and suggested hypotheses, in: *Biopolymers/Non-Exclusion HPLC*, Springer Berlin Heidelberg, 1986, pp. 1-63.
- [18] E. Ostuni, R.G. Chapman, R.E. Holmlin, S. Takayama, G.M. Whitesides, A Survey of Structure–Property Relationships of Surfaces that Resist the Adsorption of Protein, *Langmuir*, 17 (2001) 5605-5620.
- [19] D.A. Herold, K. Keil, D.E. Bruns, Oxidation of polyethylene glycols by alcohol dehydrogenase, *Biochem. Pharmacol.*, 38 (1989) 73-76.
- [20] M. Weinhart, T. Becherer, N. Schnurbusch, K. Schwibbert, H.-J. Kunte, R. Haag, Linear and Hyperbranched Polyglycerol Derivatives as Excellent Bioinert Glass Coating Materials, *Adv. Eng. Mater.*, 13 (2011) B501-B510.
- [21] A. Sunder, R. Hanselmann, H. Frey, R. Mülhaupt, Controlled Synthesis of Hyperbranched Polyglycerols by Ring-Opening Multibranching Polymerization, *Macromolecules*, 32 (1999) 4240-4246.
- [22] A. Sunder, R. Mülhaupt, R. Haag, H. Frey, Hyperbranched Polyether Polyols: A Modular Approach to Complex Polymer Architectures, *Adv. Mater.*, 12 (2000) 235-239.
- [23] S. Roller, H. Zhou, R. Haag, High-loading polyglycerol supported reagents for Mitsunobu- and acylation-reactions and other useful polyglycerol derivatives, *Mol. Diversity*, 9 (2005) 305-316.
- [24] J. Mathes, W. Friess, Influence of pH and ionic strength on IgG adsorption to vials, *Eur. J. Pharm. Biopharm.*, 78 (2011) 239-247.
- [25] J.C. Kasper, D. Schaffert, M. Ogris, E. Wagner, W. Friess, Development of a lyophilized plasmid/LPEI polyplex formulation with long-term stability-A step closer from promising technology to application, *J. Controlled Release*, 151 (2011) 246-255.
- [26] 2.9.19 Particulate contamination: sub-visible particles, in: *European Pharmacopoeia*, 2011
- [27] A.O. Grillo, K.L. Edwards, R.S. Kashi, K.M. Shipley, L. Hu, M.J. Besman, C.R. Middaugh, Conformational origin of the aggregation of recombinant human factor VIII, *Biochemistry*, 40 (2001) 586-595.

-
- [28] E. Ostuni, R.G. Chapman, R.E. Holmlin, S. Takayama, G. Whitesides, A Survey of Structure-Property Relationships of Surfaces that Resist the Adsorption of Protein, *Langmuir*, 17 (2001) 5605-5620.
- [29] G. Anand, F. Zhang, R.J. Linhardt, G. Belfort, Protein-Associated Water and Secondary Structure Effect Removal of Blood Proteins from Metallic Substrates, *Langmuir*, 27 (2010) 1830-1836.
- [30] M. Wyszogrodzka, R. Haag, Study of Single Protein Adsorption onto Monoamino Oligoglycerol Derivatives: A Structure-Activity Relationship, *Langmuir*, 25 (2009) 5703-5712.
- [31] F. Höök, J. Vörös, M. Rodahl, R. Kurrat, P. Böni, J.J. Ramsden, M. Textor, N.D. Spencer, P. Tengvall, J. Gold, B. Kasemo, A comparative study of protein adsorption on titanium oxide surfaces using in situ ellipsometry, optical waveguide lightmode spectroscopy, and quartz crystal microbalance/dissipation, *Colloids Surf., B*, 24 (2002) 155-170.
- [32] S. Pasche, J. Vörös, H.J. Griesser, N.D. Spencer, M. Textor, Effects of Ionic Strength and Surface Charge on Protein Adsorption at PEGylated Surfaces, *J. Phys. Chem. B*, 109 (2005) 17545-17552.
- [33] A.W.P. Vermeer, C.E. Giacomelli, W. Norde, Adsorption of IgG onto hydrophobic teflon. Differences between the Fab and Fc domains, *Biochim. Biophys. Acta, Gen. Subj.*, 1526 (2001) 61-69.
- [34] H.-C. Mahler, W. Friess, U. Grauschopf, S. Kiese, Protein aggregation: Pathways, induction factors and analysis, *J. Pharm. Sci.*, 98 (2009) 2909-2934.

Chapter IV

Adsorption of IgG1 and its F(ab')₂ and Fc Fragment to Type I Borosilicate Glass Vials and Siliconized Vials – Influence of pH and Ionic Strength

The following chapter is intended for publication:

Kerstin Höger, Wolfgang Frieß

Adsorption of IgG1 and its F(ab')₂ and Fc Fragment to Type I Borosilicate Glass Vials and Siliconized Vials – Influence of pH and Ionic Strength

Abstract

The unspecific adsorption of therapeutic proteins to process materials or the primary packaging may lead to major concerns such as reduced drug concentration, protein aggregation or denaturation. Therefore, it is crucial to understand the mechanisms underlying the adsorption process. This study focuses on the adsorption of the F(ab')₂ and the Fc fragment of a monoclonal IgG1 antibody to borosilicate glass vials and siliconized glass vials as relevant containers for liquid pharmaceutical formulations. The adsorption behavior of the fragments and IgG1 was investigated at different pH and ionic strength conditions to evaluate the contribution of electrostatic interactions to the adsorption process. On borosilicate glass vials, the adsorption of IgG1 and the fragments was found to be strongly dependent on pH and ionic strength, a trend that was especially pronounced for F(ab')₂. The largely higher adsorbed amounts and the lower ionic strength dependence at basic pH values on siliconized vials showed the importance of hydrophobic interactions for adsorption of IgG1 and the fragments on this hydrophobic surface. In a competitive adsorption of Fc and F(ab')₂, the total adsorbed amount protein on borosilicate glass vials was lower than the corresponding IgG1 adsorption.

On siliconized vials, Fc / F(ab')₂ adsorption was found comparably high at some formulation conditions. The found adsorbed amounts of IgG1 and the fragments were correlated with calculated adsorption values for different molecular surface orientations. It was postulated, that IgG1, F(ab')₂ and Fc in a weakly charged state attach preferentially with the hinge region of the antibody to the hydrophobic siliconized glass surface. For highly charged IgG1, adsorption in an end-on conformation was suggested due to the high surface coverage found on borosilicate glass vials and siliconized glass vials.

1 INTRODUCTION

The adsorption of proteins to a variety of surfaces is a common phenomenon in nature which plays an important role in many biological processes. For pharmaceutical protein formulations, major problems may arise from the nonspecific binding of proteins to e.g. filters and tubings during processing, but also from the adsorption to the primary packaging material. Besides syringes that comprise about 25-30% of the containers for small volume injectables, more than 50% of these formulations are packed in vials [1]. As the transfer of plastic vials in an aseptic environment is a challenging task [1], the majority of the formulations is stored in glass vials or also siliconized vials. A thorough understanding of the mechanism of protein adsorption to these packaging materials is crucial to prevent adverse effects, which may lead to instabilities of the formulation. In the last decades, the influence of different formulation parameters such as pH, ionic strength and surfactants on protein adsorption was investigated in detail [2-5]. In particular, there has been a constant growth in research on the adsorption of antibodies to various surfaces [6-8], as monoclonal antibodies comprise a growing group of biopharmaceuticals on the market [9].

It is well known that protein adsorption to surfaces is governed e.g. by electrostatic or hydrophobic interactions [6, 10, 11]. However, there are many different opinions about the orientation of antibodies on hydrophilic and hydrophobic surfaces. Three main conformations have been postulated, which include the preferential binding of the antibody via the Fc fragment, the F(ab')₂ fragment or involving the hinge region of the antibody. One argument for Fc-mediated adsorption was the binding of anti-F(ab')₂ to adsorbed IgG [12]. Buijs et al. investigated the adsorption of IgG, F(ab')₂ and Fc and concluded that IgG adsorbed preferentially with the Fc fragment since the Gibbs energy barrier for adsorption was much higher for F(ab')₂ than for IgG in some cases [13]. He further suggested adsorption of IgG1 by its Fc part at some conditions due to the low structural stability of this fragment [14]. In

contrast, Vermeer suggested a binding of IgG to hydrophobic Teflon by its more hydrophobic Fab' fragment [15]. Finally, in some recent studies it was suggested, that IgG adsorbs neither with Fab' nor Fc to hydrophobic surfaces, but attaches primarily with the hinge region and parts of the Fc fragment [7, 16].

In most of these investigations, model surfaces or hydrophobic membranes were used to study the adsorption of IgG and its fragments. The present study examines the adsorption behavior of IgG1, the F(ab')₂ and the Fc fragment to borosilicate glass vials and siliconized glass vials as relevant pharmaceutical packaging materials. The adsorption of the proteins was investigated at different pH values and ionic strengths to evaluate the influence of electrostatic and hydrophobic interactions on the adsorption process. Moreover, the total adsorbed amount of protein in a competitive adsorption of the Fc and F(ab')₂ fragment was investigated. Finally, the calculated theoretical surface concentration for different orientations of the molecules on the surface was correlated with the found adsorbed amounts of IgG1. This allowed us to evaluate the possible orientations of IgG1 on siliconized glass vials and borosilicate glass vials at different pH and ionic strength.

2 MATERIALS AND METHODS

2.1 Chemicals

Trometamol was obtained from Merck KGaA (Darmstadt, Germany) and NaH₂PO₄ was from Merck Chemicals (Darmstadt, Germany). Na₂HPO₄, sodium dodecyl sulfate (SDS), cysteine, ethylene diamine tetraacetate (EDTA), iodoacetamide as well as the papain suspension from papaya latex and pepsin from porcine gastric mucosa were purchased from Sigma-Aldrich Chemie GmbH (Munich, Germany). NaCl, NaOH and HCl were purchased from VWR International (Darmstadt, Germany).

2.2 IgG1 Antibody

The 2 mg/ml IgG1 antibody formulated in 10 mM phosphate buffer and 145 mM NaCl (pH 7.2) was kindly donated by Merck Serono (Darmstadt, Germany). For an adjustment of the ionic strength, the formulation was dialyzed in 10 mM phosphate buffer pH 7.2, using a Vivaflow[®] 50 tangential flow cartridge (Sartorius-Stedim Biotech, Goettingen, Germany) with a 30 kD MWCO polyethersulfone membrane. The concentration of the protein solution was determined by UV-spectroscopy. For adsorption experiments at different pH values, the

pH was adjusted by addition of 1 M NaOH or HCl and a consistent ionic strength of 170 mM was adjusted by adding adequate amounts of NaCl to the dialyzed solution.

2.3 Fc Fragments

Fc fragments were generated by digestion of the antibody with papain. Prior to digestion, the IgG1 antibody was dialyzed into a digestion buffer containing 100 mM trometamol, 10 mM cysteine and 40 mM EDTA, pH 7.4, using Vivaflow[®] cartridges with a 30 kDa MWCO polyethersulfone membrane (Sartorius AG, Goettingen, Germany). The IgG1 concentration was measured by UV-spectroscopy and adjusted to 2 mg/ml. Just before use, the papain suspension was diluted with 5 mM cysteine buffer to a final concentration of 1 mg/ml, and 10 µg papain per mg IgG1 were added to the antibody solution. The mixture was incubated for 5-7 h at 37 °C until at least 95% of the protein molecules were digested. Then the reaction was stopped by addition of iodoacetamide to a final concentration of 30 mM. In-process controls were performed by HP-SEC. Fc fragments were separated from the digestion mixture on an ÄKTApurifier 10 (GE Healthcare Europe GmbH, Freiburg, Germany) with a Pierce[®] Protein A Chromatography Cartridge (Thermo Fisher Scientific Inc., IL, USA). The column was equilibrated with binding buffer consisting of 100 mM phosphate and 3 M NaCl, pH 9, at a flow rate of 1 ml/min. After injection of the digestion mixture, Fab' fragments were immediately eluted from the column. Fc fragments and non-digested IgG1 antibody were eluted from the column by applying a gradient toward 100% elution buffer containing 100 mM phosphate, pH 3, and were collected by an automated fraction collector (Frac-920, GE Healthcare Europe GmbH, Freiburg, Germany). UV-absorption at 280 nm was used to detect eluted protein. Subsequently, the Fc fragments were dialyzed extensively against 10 mM phosphate buffer pH 7.2 using Vivaspin[®] centrifuge tubes with a 10 kDa MWCO polyethersulfone membrane (Sartorius AG, Goettingen, Germany). A purity of about 95% Fc with small quantities of residual larger fragments was found in non-denaturing HP-SEC and was visualized by SDS-PAGE (Figure IV-1a). The isoelectric point of the Fc fragment was determined by IEF in a pH range of 6.5-7.6 (Figure IV-1b). pH and ionic strength adjustments were performed as described for the IgG1 antibody solution.

2.4 F(ab')₂ Fragments

For the preparation of F(ab')₂ fragments, the IgG1 antibody was dialyzed into a digestion buffer containing 100 mM Na-acetate, pH 3.5, using Vivaflow[®] cartridges with a 30 kDa MWCO polyethersulfone membrane (Sartorius AG, Goettingen, Germany). The protein

concentration was measured by UV-spectroscopy and adjusted to 2 mg/ml. 10 µg pepsin dissolved in digestion buffer were added per mg IgG1. For digestion, the reaction solution was incubated at 37 °C for 1 h and subsequently stopped by addition of 3 M tris buffer to a final pH of 8.8. For adsorption experiments, the solution was dialyzed extensively against 10 mM phosphate buffer pH 7.2 to remove smaller fragments and pepsin from the solution. The purity of the F(ab')₂ fraction was found to be about 96% in non-denaturing HP-SEC with some smaller fragments remaining from digestion which was also shown by SDS-PAGE (Figure IV-1a). The isoelectric point was determined to be in a pH range of 7.6-8.3 (Figure IV-1b). Both pH and ionic strength adjustments were performed as described for the IgG1 antibody solution.

2.5 Vials and Closure Systems

Adsorption experiments were performed in pre-siliconized (Dow Corning 365) and baked 2R glass vials and bare Fiolax[®] glass vials which were kindly provided by SCHOTT AG (Mainz, Germany). All vials were washed with ultrapure water of 80 °C in a vial washing machine FAW 500 (Bausch&Stroebel GmbH & Co. KG, Ilshofen, Germany). Subsequently, siliconized vials were autoclaved at 121 °C, 2 bar for 15 minutes whereas Fiolax[®] glass vials were heat sterilized at 250 °C for 1 h. After filling, the vials were closed with Fluorotec[®] stoppers and sealed with Flip-Off[®] seals (West Pharmaceutical Services, Eschweiler, Germany). The inner surface area of a vial covered with protein formulation was calculated as 5.06 cm² for a filling volume of 1 ml.

2.6 Adsorption Process

The adsorption process followed the procedure described by Mathes & Friess [6]. For adsorption testing of the individual fragments or IgG1, 1 ml protein solution containing IgG1, F(ab')₂ or Fc fragment in equal molar concentration, corresponding to 1 mg/ml IgG1, 0.66 mg/ml F(ab')₂ fragment or 0.33 mg/ml Fc fragment, was filled into the pre-processed vials (n=2). The simultaneous adsorption of F(ab')₂ and Fc fragment was investigated with solutions containing 0.66 mg/ml F(ab')₂ fragment and 0.33 mg/ml Fc fragment (n=2). After filling, the vials were closed, sealed and incubated at 25 °C for 24 h. The vials were emptied using a syringe with an injection needle. Each vial was rinsed four times with corresponding formulation buffer. For desorption of bound protein, 1 ml of 10 mM PBS containing 145 mM NaCl and 0.05% sodium dodecyl sulfate, pH 7.2, was filled into each vial. The vials were closed and stored overnight at 25 °C.

2.7 UV-Spectroscopy

UV-spectroscopy to determine the concentration of the protein solutions was performed on an Agilent 8453 UV/VIS spectrophotometer (Agilent Technologies GmbH, Boeblingen, Germany) in 10 x 10 mm quartz cuvettes at $\lambda = 280 \text{ nm} / 25 \text{ }^\circ\text{C}$. For IgG1 an extinction coefficient of $1.4 \text{ cm}^2/\text{mg}$ for antibodies was applied. For concentration determination of the $\text{F(ab}')_2$ or Fc fragment, the experimentally determined extinction coefficients of $1.45 \text{ cm}^2/\text{mg}$ or $1.51 \text{ cm}^2/\text{mg}$, respectively, were applied.

2.8 HP-SEC

In-process controls of IgG1 digestion with papain or pepsin as well as purity analysis of the fragments were performed by HP-SEC on an Agilent 1100 HPLC device with an Agilent UV-detector (Agilent Technologies GmbH, Boeblingen, Germany) using a YMC-Pack Diol-300 SEC-column (YMC Europe GmbH, Dinslaken, Germany) for sample separation. 10 mM phosphate buffer containing 145 mM NaCl, pH 7.2, was used as eluent. A flow rate 0.5 ml/min was applied with UV-detection at 280 nm. Agilent ChemStation Software Rev. B 02.01 was used for manual integration of the chromatograms. The purity of the Fc and $\text{F(ab}')_2$ fractions was determined by calculating the percentage of the AUC of each fragment from the total AUC of the digestion mixture ($n \geq 1$).

Quantitative analysis of the desorbed protein was performed using a YMC-Pack Diol-300 SEC-column (YMC Europe GmbH, Dinslaken, Germany) for sample separation. Intrinsic protein fluorescence was detected at $\lambda_{\text{ex}}/\lambda_{\text{em}}$ 280 nm/334 nm. Desorption buffer was used as mobile phase. For the quantification of IgG1 or the separated fragments, a calibration line of each of the proteins was included in an HPLC batch. For protein quantification in samples containing Fc and $\text{F(ab}')_2$, a calibration line with different ratios of Fc and $\text{F(ab}')_2$ as well as pure Fc and pure $\text{F(ab}')_2$ was included in each HPLC batch. The chromatograms were integrated manually using the Agilent ChemStation Software Rev. B 02.01.

2.9 Determination of the Molar Extinction Coefficient of Fc and $\text{F(ab}')_2$ Fragments

The molar extinction coefficient ε of Fc and $\text{F(ab}')_2$ fragments was calculated from experimentally obtained values according to the following equation:

$$\varepsilon = \frac{A_{280}}{c \cdot d} \quad (1)$$

c constitutes the molar concentration of the analyte obtained by micro BCA-assay, A_{280} is the corresponding UV-absorption of the solution at 280 nm ($n=3$) and d equals the pathlength of the cuvette. The experimentally obtained values were confirmed by calculation of the theoretical molar extinction coefficients from the protein sequence applying equation (2). This equation is based on experimentally determined intrinsic extinction coefficients of tryptophan, tyrosine and cystine residues and their number n in the protein sequence [17, 18]:

$$\epsilon_{280} = 5540n_{\text{Trp}} + 1480n_{\text{Tyr}} + 134n_{\text{S-S}} \quad (2)$$

The sequence of the fragments was obtained from the amino acid sequence of the full antibody under consideration of the cleavage sites of papain between histidine-threonine in the upper hinge region for the Fc fragment [19, 20] or pepsin between leucine-leucine for the F(ab')₂ fragment in the lower hinge region [20], respectively. The theoretical extinction coefficients were calculated as 1.45, 1.44 and 1.46 cm²/mg for IgG1, Fc and F(ab')₂ and an assumed molecular weight of 150, 50 and 100 kDa, respectively.

2.10 Micro BCA-Assay

The protein concentration of Fc and F(ab')₂ in 10 mM phosphate buffer pH 7.2 was determined with a micro BCA protein assay kit (Thermo Fisher Scientific Inc., IL, USA). From each fragment solution, two dilutions were prepared in triplet each and analyzed in a 96-well plate with UV-detection at 562 nm. A 6-point calibration line of non-fragmented IgG1 in a concentration range of 2.5-40 µg/ml was used as reference for quantification.

2.11 SDS-PAGE

The digestion products were analyzed by SDS-PAGE using NuPAGE[®] 7% tris-acetate gels (Life Technologies GmbH, Darmstadt, Germany). Samples were diluted with formulation buffer to 0.0125 mg/ml and heat denatured at 95 °C for 20 min. A Mark12™ Unstained Standard (Life Technologies GmbH, Darmstadt, Germany) was applied for band identification. Electrophoresis was performed at a consistent current of 0.04 A for approx. 1.5 h, followed by silver staining with a SilverQuest™ Silver Staining Kit (Life Technologies GmbH, Darmstadt, Germany).

2.12 Isoelectric Focusing

The isoelectric point of IgG1, Fc and F(ab')₂ fragments was determined by isoelectric focusing (IEF) using precast SERVALYT PRECOTES[®] 6-9 IEF plates with a thickness of 300 µm. 10 µl per sample with a concentration of 0.5 mg/ml adjusted by dilution with ultrapure water and SERVA Liquid Mix IEF marker 3-10 (SERVA Electrophoresis GmbH, Heidelberg, Germany) were applied to the gel. Electrophoresis was performed at 2000 V and 6 mA at 5 °C. The gels were stained with SERVA Blue W (SERVA Electrophoresis GmbH, Heidelberg, Germany).

3 RESULTS AND DISCUSSION

3.1 Adsorption of IgG1, F(ab')₂ and Fc Fragment

The adsorption behavior of IgG1 and the individual Fc and F(ab')₂ fragments to borosilicate glass vials and siliconized glass vials was investigated using solutions of equimolar concentration. Adsorption was tested at the pH values 4.0, 7.2 and 8.6, so that the impact of different charge states of the molecules on the adsorption process could be examined. To investigate the influence of electrostatic interactions in between the protein molecules as well as between the protein and the sorbent, the adsorption was additionally determined at two different ionic strength levels of 40 mM and 170 mM.

3.1.1 Adsorption to Borosilicate Glass Vials

At first, the adsorption behavior of IgG1, the F(ab')₂ and the Fc fragment on borosilicate glass vials is presented. All proteins showed the same pH- and ionic strength-dependent adsorption behavior at the tested conditions (Figure IV-2a). Maximum adsorption was found at pH 4.0, decreasing via pH 7.2 toward pH 8.6. Increasing the ionic strength from 40 mM to 170 mM led to enhanced adsorption at pH 4.0, whereas adsorption was reduced at pH 7.2 and 8.6. Compared to IgG1 and Fc, these changes were more pronounced for F(ab')₂. At most of the conditions, the adsorbed amount of the fragments was lower than of the full IgG1. The mass of adsorbed Fc was remarkably high and exceeded the F(ab')₂ adsorption at pH 7.2 and 8.6. At pH 8.6 and 170 mM ionic strength, F(ab')₂ adsorption could not be quantified anymore. Adsorption maxima at pH values below the pI were reported for several proteins [6, 21]. Isoelectric focussing showed 6 to 7 characteristic isoforms in the pH range from about 7.6 to 8.2 for IgG1 (Figure IV-1b). The F(ab')₂ fragment exhibited 4 to 5 distinct bands in a similar

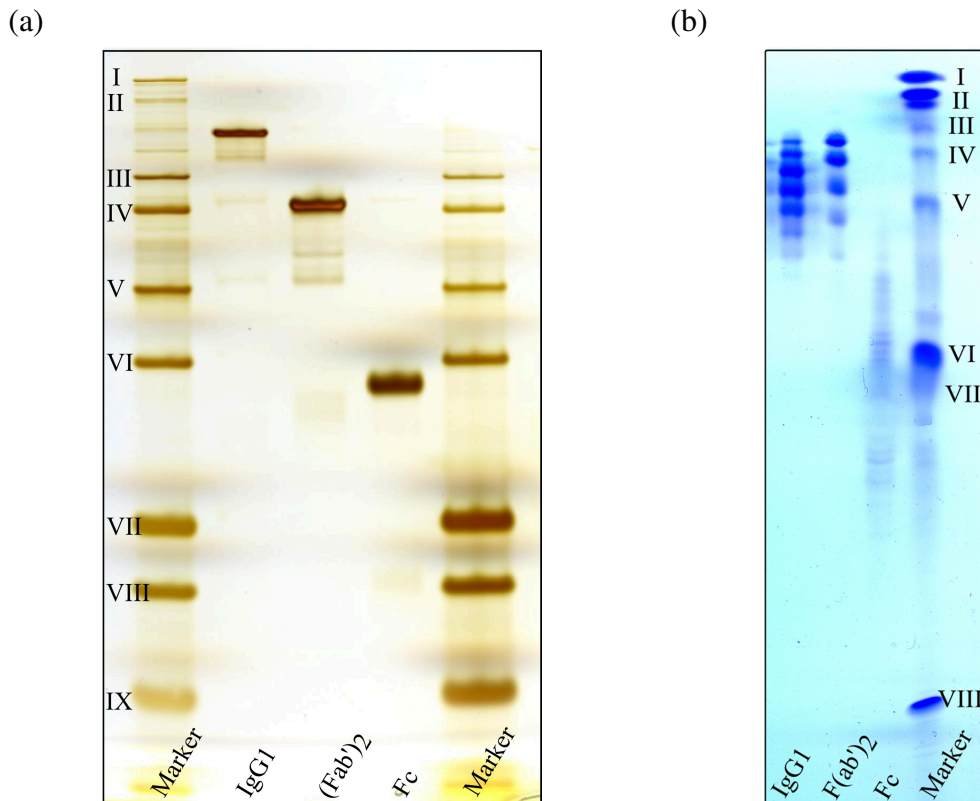


Figure IV-1: (a) SDS-PAGE of IgG1, Fc and F(ab')₂ fragment separated on a 7% tris-acetate gel. Marker bands: (I) 400 kDa, (II) 200 kDa, (III) 116 kDa, (IV) 97 kDa, (V) 66 kDa, (VI) 55 kDa, (VII) 36 kDa, (VIII) 31 kDa, (IX) 21 kDa. (b) Isoelectric focusing gel in the pH range of 6-9 for the determination of the isoelectric point (IEP) of IgG1, F(ab')₂ and Fc fragment. Marker bands can be assigned to the pH values of (I) 10.7, (II) 9.5, (III) 8.3, (IV) 8.0, (V) 7.8, (VI) 7.4, (VII) 6.9 and (VIII) 6.0.

pH range of about 7.6 to 8.3, whereas for the Fc fragment, a rather broad distribution with several less defined bands between about pH 6.5 and 7.6 was detected (Figure IV-1b). IgG1 and F(ab')₂ were thus positively charged at pH 4.0 and 7.2 and exhibited a negative net charge at pH 8.6 whereas a fraction of the Fc fragments exhibited a negative net charge already at pH 7.2. Charge heterogeneity may originate from differences in glycosylation, glutamine and asparagine deamidation [22], the presence or absence of C-terminal lysins [23] or the formation of pyroglutamate from N-terminal heavy chain glutamine [24]. Similar to our finding, a comparable pI of the F(ab')₂ fragment and IgG1 and a more acidic pI of the Fc fragment was reported for IgG1B [13]. If Fc and F(ab')₂ fragment exhibit a lower and higher pI than the full antibody, respectively, the full antibody carries a dipole moment at its pI [25]. A dipole moment of our antibody can thus be expected at pH values between the pI of the Fc and the F(ab')₂ fragment. Borosilicate glass exhibits a pI of about pH 2.3 [6] so that the hydrophilic glass surface was negatively charged in the whole investigated pH range.

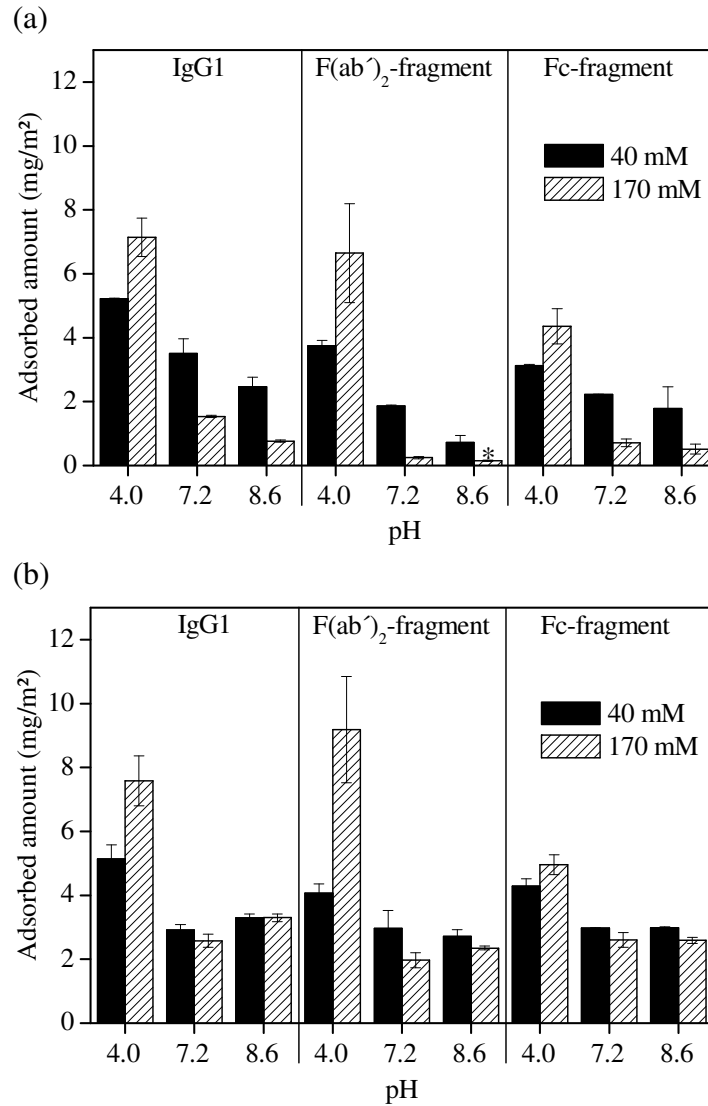


Figure IV-2: Adsorption of IgG1, Fc and F(ab')₂ fragment to type I borosilicate glass vials (a) and siliconized glass vials (b) at different pH and ionic strength; incubation time 24 h at 25 °C; solutions contained equimolar protein concentration in 10 mM phosphate buffer at 40 mM (grey bars) or 170 mM (striped bars) ionic strength (n=2). Adsorbed amounts of samples labeled with star (*) could not be quantified any more.

At pH 4, IgG1 and both fragments exhibited a strong positive net charge and were electrostatically attracted toward the negatively charged glass surface. At the same time, the strong intermolecular repulsion opposed adsorption. This repulsion, but also the electrostatic attraction toward the sorbent surface may be reduced at higher salt concentrations [26]. Higher adsorbed amounts at an ionic strength of 170 mM compared to 40 mM reflected a prevalent reduction of intermolecular repulsive forces by ions in our experiment (Figure IV-2a).

Table IV-1: Average pKa of side chains of amino acids in folded proteins according to [29] and percentage of acidic form at pH 4.0, 7.2 and 8.6.

Amino acid	pKa [29]	Percentage of acidic form		
		pH 4.0	pH 7.2	pH 8.6
Lysine	10.5 ± 1.1	100.0	99.9	98.7
Tyrosine	10.3 ± 1.2	100.0	99.9	98.0
Cysteine	6.8 ± 2.7	99.8	28.4	1.5
Histidine	6.6 ± 1.0	99.7	20.0	1.0
Glutamate	4.2 ± 0.9	61.3	0.1	0.0
Aspartate	3.5 ± 1.2	24.0	0.0	0.0

With increasing pH toward 7.2 and 8.6, the positive net charge of the proteins decreased. At pH 7.2, the pI range of the Fc fragment was reached so that a fraction of the Fc molecules already exhibited no net charge or a negative net charge. Despite the expected electrostatic repulsion between the negatively charged fragments and the negatively charged sorbent surface, considerable adsorption was found at low ionic strength. In this regard, the net charge as the sum of positive and negative charges of a molecule and thus the amino acid composition of the fragment has to be considered. About 95% of the amino acid sequence in human IgG1 antibodies are conserved [24]. The human IgG1 CH2 and CH3 regions, which are part of the Fc fragment, contain together 15 glutamate, 10 aspartate and 5 cysteine residues per heavy chain, but also 6 arginine, 6 histidine and 19 lysine residues. 99.9% of the lysine side chains and about 20% of the histidine side chains are still positively charged at pH 7.2 (Table IV-1) so that the Fc fragment is expected to carry a considerable number of positive charges at this pH. It was further emphasized, that the distribution of charges rather than the average net charge of a protein influences adsorption [27] and intermolecular interactions [28]. We therefore ascribe the adsorption of the Fc fragment to the electrostatic attraction toward the sorbent surface via positively charged protein patches. This assumption was underlined by the reduced adsorbed amounts at a higher ionic strength of 170 mM, which indicated a screening of electrostatic attractive forces by ions. Furthermore, weak hydrophobic interactions between the protein molecules and the sorbent supposedly contributed to adsorption. IgG1 and F(ab')₂ both exhibited a positive net charge at pH 7.2 and were thus electrostatically attracted toward the borosilicate glass.

Slightly above the pI range of IgG1 and F(ab')₂ at pH 8.6, the full antibody and both fragments exhibited a slightly negative net charge. Due to the intermolecular repulsion and

the electrostatic repulsion between the negatively charged protein and the sorbent surface, reduced adsorbed amounts could be expected. However, Fc adsorption was only marginally lower than at pH 7.2. This may be ascribed to the almost unchanged protonation degree of lysine compared to pH 7.2 (Table IV-1), enabling electrostatic attraction of the molecules toward the sorbent via positively charged protein patches. Furthermore, a contribution of hydrophobic interactions to adsorption of the molecules can be assumed. Compared to IgG1 and Fc, the adsorbed amount of F(ab')₂ was very low at pH 8.6 which indicated a very weak electrostatic and hydrophobic attraction of this fragment toward the surface. Due to the variable part of the F(ab')₂ fragment, larger differences in sequence between different IgG1 antibodies may occur. Several lysine residues in the CH1 region of human IgG1 imply also for this fragment the possibility to adsorb via positively charged protein patches to the negatively charged glass surface. However, these positive charges may be buried in the interior of the molecule or outweighed by negative charges in the variable part.

Our IgG1 and F(ab')₂ exhibited a comparable pI and adsorption trend which has been similarly described in literature for other antibodies and their fragments on different surfaces [30]. In our experiment, also the Fc fragment showed basically the same adsorption behavior. In contrast, Buijs et al. found a marginal pH- and ionic strength-dependence of Fc adsorption to silica and methylated silica and ascribed it to the low influence of protein-sorbent interactions on Fc adsorption [13]. Lower pH-effects on the adsorption of Fc than of F(ab') in a competitive adsorption were further ascribed to the dominance of hydrophobic forces for Fc adsorption [31].

On borosilicate glass vials, Fc adsorption was by trend slightly higher at pH 7.2 and 8.6 and slightly less dependent on ionic strength than adsorption of F(ab')₂. Therefore it may be hypothesized that IgG1 adsorption is driven rather by the Fc fragment, especially at slightly basic pH values. Adsorption of IgG with the Fc fragment was also proposed by Nagaoka for a hydrophobic surface [12]. In addition, Buijs determined a much higher Gibbs energy barrier for the adsorption of F(ab')₂ than for IgG on silica at some conditions and suggested that the IgG molecule attaches preferentially with the Fc fragment onto the surface [13]. Furthermore it was shown that membrane-bound IgG was able to bind antigen from solution [32, 33]. In contrast, Vermeer et al. suggested a preferential adsorption of IgG2b to hydrophobic Teflon particles with the F(ab') fragments which exhibited a higher hydrophobicity [15]. We considered this orientation rather unlikely for the very hydrophilic glass, because lower adsorbed amounts were found for the F(ab')₂ fragment than for the Fc fragment at pH 7.2 and 8.6.

3.1.2 Adsorption to Siliconized Glass Vials

Similar to borosilicate glass vials, almost no difference between the fragments and IgG1 in the pH- and ionic strength-dependent adsorption behavior was observed on siliconized glass vials. Again, maximum adsorption was found at pH 4.0 with lower, rather similar adsorbed amounts at pH 7.2 and pH 8.6 (Figure IV-2b). Increasing the ionic strength from 40 mM to 170 mM led to increased adsorption at pH 4.0 for all protein molecules, but was most pronounced for F(ab')₂. This effect was marginal at pH 7.2 and 8.6.

Siliconized glass shows a pI of about pH 3.4 (Chapter II3.1.1) and thus exhibits a negative net charge over the tested pH range of 4.0 to 8.6. In contrast to the hydrophilic glass surface, the siliconized glass surface allows strong hydrophobic interactions with the proteins in addition to electrostatic interactions. This was demonstrated by the largely higher adsorbed amounts of IgG1 and the fragments on the siliconized surface compared to borosilicate glass, especially at pH 7.2 and 8.6. The minor importance of electrostatic interactions for adsorption at these higher pH values was underlined by the low effect of changing ionic strength on the adsorbed amount. Similarly, Buijs et al. stated that the adsorption of IgG and its F(ab')₂ fragment to hydrophobic lattices is mainly governed by hydrophobic interactions but is still influenced by electrostatic forces [30]. At pH 7.2 and 8.6, the adsorbed amount of Fc and F(ab')₂ did not differ noticeably, so that no conclusion about the preferential orientation of adsorbed IgG1 on this basis could be drawn. In contrast, the strong increase in IgG1 adsorption at pH 4.0 with higher ionic strength was also observed for the F(ab')₂ fragment but was only marginal for the Fc part. In the following section, the possible steric reasons for the similarity in adsorbed amounts of Fc, F(ab')₂ and IgG1 on siliconized vials will be discussed.

3.2 Simultaneous Adsorption of F(ab')₂/ Fc Fragments and Orientation Considerations

Besides the separate adsorption of the fragments, the total protein adsorption from solutions containing Fc and F(ab')₂ fragments in equimolar concentration was investigated. Overall, the adsorption of the Fc / F(ab')₂ mixtures to siliconized and bare borosilicate glass vials showed a similar dependency on pH and ionic strength as the full antibody and the individual fragments (Figure IV-3a, b). However, on borosilicate glass vials, the adsorbed protein mass from the Fc / F(ab')₂ mixture was consistently lower than that of the full IgG1 (Figure IV-3a), whereas on siliconized glass vials the adsorption of the mixture was in some cases almost the same or even higher (Figure IV-3b).

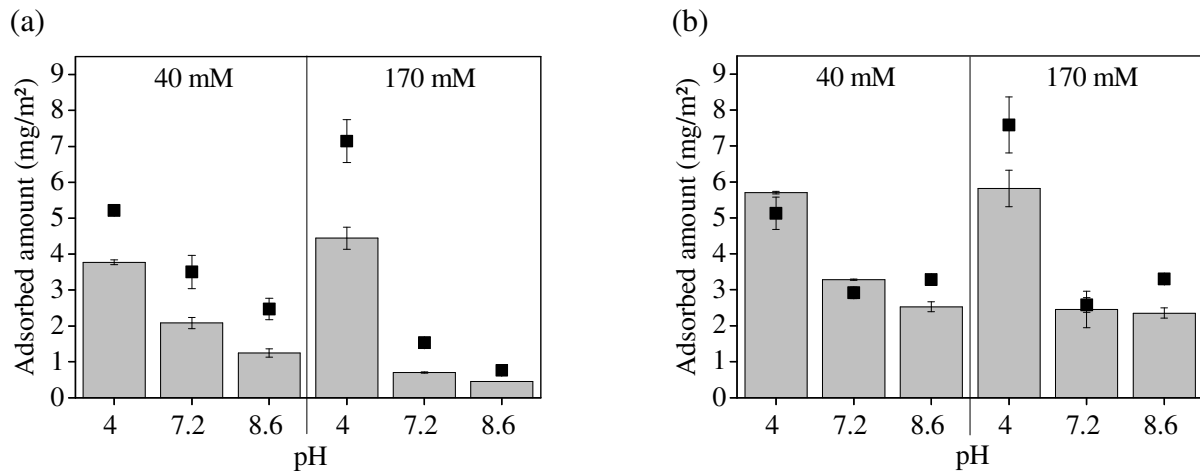


Figure IV-3: Total adsorbed protein amount from mixtures of F(ab')₂ and Fc fragment to type I borosilicate glass vials (a) and siliconized glass vials (b) at different pH and ionic strength (grey bars). Adsorbed amounts of IgG1 are depicted as reference (■); incubation time 24 h at 25 °C; solutions contained equal molar concentration of Fc and (Fab')₂ in 10 mM phosphate buffer with 40 mM or 170 mM ionic strength (n=2).

Besides the interplay of attractive and repulsive forces between protein and sorbent and in between the protein molecules, the adsorbed amount of protein on a surface is also related to the orientation of the molecules on the surface. As shown in Figure IV-4, the maximum surface coverage of IgG1 and its fragments at different surface conformations can be calculated in approximation from the dimensions of crystallized F(ab') and Fc [30], assuming a 100% coverage of the sorbent surface area with protein.

According to the calculated values in Figure IV-4, adsorbed amounts of IgG1 higher than approximately 2.9 mg/m² require an end-on orientation of the molecules (orientation A, B) or multilayer coverage. On borosilicate glass vials this applies at pH 4.0 as well as at pH 7.2 / 40 mM ionic strength, whereas at the other formulation conditions, also a side-on orientation (Figure IV-4, orientation D, E) of the molecules was possible. This means that at conditions of high electrostatic attraction between IgG1 and the surface but also high intermolecular repulsion, a small contact area between proteins and sorbent, as obtained in an end-on orientation, was sufficient for adsorption. At less attractive conditions, a side-on orientation of the molecules may be required to increase the interaction with the surface.

For adsorption of isolated F(ab')₂, at pH 7.2 and 8.6 all surface orientations were possible based on the adsorbed amount. At pH 4.0 / 40 mM ionic strength and under the precondition of monolayer coverage, the measured adsorbed amount required F(ab')₂ adsorption in a rather collapsed conformation (orientation F) if adsorption in a comparable conformation as in the full antibody is assumed. Due to the strong inter- and intramolecular repulsion at this

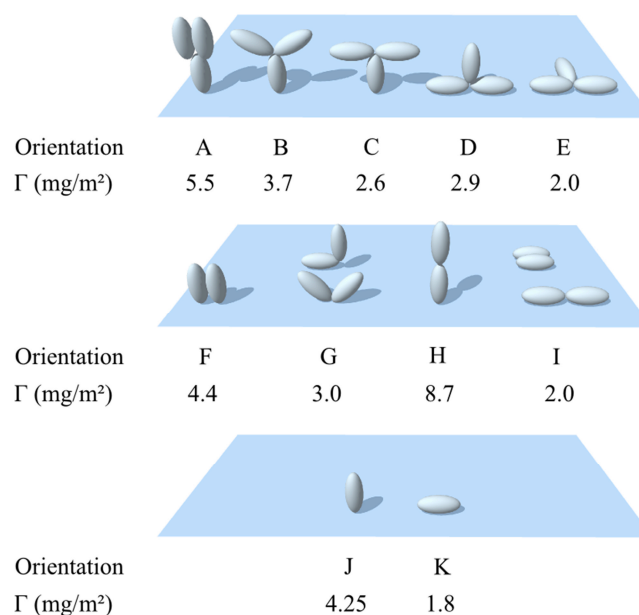


Figure IV-4: Surface conformations and calculated adsorbed amount Γ in mg/m² for adsorbed IgG1 (A-E), F(ab')₂ fragment (F-I) and Fc fragment (J, K). Calculated adsorbed amounts and schematic drawing of orientations A-C and E-I are reproduced and adapted from [30]. Side-on orientation D with one F(ab') fragment directed toward the solution was adapted from Wiseman & Frank [34]. Calculations of adsorbed amounts of orientations D, J and K are based on the dimensions of crystallized F(ab') (8.2 x 5.0 x 3.8 nm³) and Fc (7.0 x 6.3 x 3.1 nm³) as used by Buijs et al. [30], applying a molecular weight of 50, 100 and 150 kDa for Fc, F(ab')₂ and IgG1. Calculations are based on the assumption of a 100% possible surface coverage with protein.

formulation condition, however, (partial) adsorption of the molecules in a stretched orientation (orientation H) or in multilayers seems more likely. This stretched conformation H was suggested by Buijs et al. for F(ab')₂ at increased protein charge density when the F(ab') units electrostatically repel each other [30]. At 170 mM ionic strength, the molecules supposedly adsorbed in a stretched orientation (H) or formed multilayers. For the Fc fragment, adsorption in all theoretical orientations was considered possible based on the adsorbed amount.

Assuming an exclusively flat-on adsorption of the antibody (orientation E) and a comparable orientation of the isolated fragments (orientations I and K), adsorbed amounts of < 1.8-2 mg/m² for all proteins were required which applied at pH 7.2 and 8.6 at 170 mM ionic strength. In general, the total protein adsorption from Fc / F(ab')₂ mixtures did not reach the IgG1 adsorption level (Figure IV-3a) which might be ascribed to different possible packing densities or different molecular orientations of the proteins. The orientation of Fc and F(ab')₂

in the simultaneous adsorption will not be considered further as this will depend on the fragment ratio on the surface which cannot be hypothesized.

On siliconized glass vials, at pH 4.0 the antibody molecules can be assumed to adsorb in an end-on orientation as well. The rather high IgG1 adsorption of 2.6-3.3 mg/m² (Figure IV-2b) at pH 7.2 and 8.6 allowed an end-on adsorption but also a side-on adsorption of IgG1 with one F(ab') pointing toward the solution (orientation D as suggested by [34]) for the majority of the molecules. Considering the similar adsorbed amounts of IgG1, Fc and F(ab')₂ at pH 7.2 and 8.6, adsorption in a certain conformation which is favored on the hydrophobic siliconized glass surface may be speculated. Recent publications proposed the adsorption of IgG to hydrophobic membranes with the hinge region and a part of the Fc fragment [7, 16]. Sun et al. concluded this from the ability of membrane-bound IgG to bind Protein A and antigen, and from the antigen binding by separated, adsorbed F(ab')₂ fragment [16]. An adsorption of Fc, F(ab')₂ and the antibody with the hinge region, as proposed in literature, may actually explain the similar adsorbed amounts of the proteins as observed on siliconized vials. At pH 7.2 and 8.6, the adsorbed amounts of Fc and F(ab')₂ between 2.0 and 3.0 mg/m² theoretically allow (at least largely) adsorption of both fragments with the hinge region. Although adsorption of IgG1 at these pH values exclusively via the hinge region was not possible, a mix of initially adsorbed IgG1 molecules preferentially with their middle region and further end-on adsorption may be considered. An initial flat-on adsorption of IgG1 to a hydrophobic membrane and further adsorption in various vertical surface orientations with increasing surface coverage was also suggested by Wiseman & Frank [34]. Thus it may be concluded, that on siliconized vials a preferential adsorption with the hinge region of the antibody is an option for the orientation of weakly charged IgG1 on the surface.

4 CONCLUSION

In this study the adsorption behavior of IgG1, the F(ab')₂ and the Fc fragment on borosilicate glass vials and siliconized glass vials was investigated in dependence of pH and ionic strength. On both vial qualities, the adsorption maxima of the different proteins were found at an acidic pH value due to strong attractive electrostatic interactions between the protein and the negatively charged sorbent. On borosilicate glass, a strong dependence of adsorption on pH and ionic strength was observed. In contrast, the contribution of hydrophobic interactions to the adsorption process on siliconized vials led to quite high adsorbed amounts even when the proteins exhibited only a weak or neutral net charge. On both surfaces, adsorption of the

Fc fragment could be observed even at electrostatic repulsive conditions between protein and sorbent surface. Different molecular orientations of IgG1 were considered in dependence of the adsorbed amounts measured on borosilicate glass and siliconized glass. Protein net charge and surface charge distribution are specific properties of each individual antibody. The obvious importance of these parameters for adsorption in our experiments thus implies that found adsorption trends cannot be simply transferred to other antibodies or are easily predictable just from pI determination.

5 REFERENCES

- [1] G.A. Sacha, W. Saffell-Clemmer, K. Abram, M.J. Akers, Practical fundamentals of glass, rubber, and plastic sterile packaging systems, *Pharm. Dev. Technol.*, 15 (2010) 6-34.
- [2] F.Y. Oliva, L.B. Avalle, O.R. Cámara, C.P. De Pauli, Adsorption of human serum albumin (HSA) onto colloidal TiO₂ particles, Part I, *J. Colloid Interface Sci.*, 261 (2003) 299-311.
- [3] O. Joshi, J. McGuire, Adsorption behavior of lysozyme and Tween 80 at hydrophilic and hydrophobic silica-water interfaces, *Appl. Biochem. Biotechnol.*, 152 (2009) 235-248.
- [4] M. van der Veen, W. Norde, M.C. Stuart, Electrostatic interactions in protein adsorption probed by comparing lysozyme and succinylated lysozyme, *Colloids Surf., B*, 35 (2004) 33-40.
- [5] M.R. Duncan, J.M. Lee, M.P. Warchol, Influence of surfactants upon protein/peptide adsorption to glass and polypropylene, *Int. J. Pharm.*, 120 (1995) 179-188.
- [6] J. Mathes, W. Friess, Influence of pH and ionic strength on IgG adsorption to vials, *Eur. J. Pharm. Biopharm.*, 78 (2011) 239-247.
- [7] D. Yu, R. Ghosh, Method for Studying Immunoglobulin G Binding on Hydrophobic Surfaces, *Langmuir*, 26 (2009) 924-929.
- [8] H. Xu, X. Zhao, J.R. Lu, D.E. Williams, Relationship between the Structural Conformation of Monoclonal Antibody Layers and Antigen Binding Capacity, *Biomacromolecules*, 8 (2007) 2422-2428.
- [9] G. Walsh, Biopharmaceuticals: recent approvals and likely directions, *Trends Biotechnol.*, 23 (2005) 553-558.
- [10] M. Malmsten, Ellipsometry studies of the effects of surface hydrophobicity on protein adsorption, *Colloids Surf., B*, 3 (1995) 297-308.
- [11] M.G.E.G. Bremer, J. Duval, W. Norde, J. Lyklema, Electrostatic interactions between immunoglobulin (IgG) molecules and a charged sorbent, *Colloids Surf., A*, 250 (2004) 29-42.
- [12] S. Nagaoka, K. Ashiba, H. Kawakami, Interaction between biocomponents and surface modified fluorinated polyimide, *Mater. Sci. Eng., C*, 20 (2002) 181-185.
- [13] J. Buijs, P.A.W. van den Berg, J.W.T. Lichtenbelt, W. Norde, J. Lyklema, Adsorption Dynamics of IgG and Its F(ab')₂ and Fc Fragments Studied by Reflectometry, *J. Colloid Interface Sci.*, 178 (1996) 594-605.
- [14] J. Buijs, D.D. White, W. Norde, The effect of adsorption on the antigen binding by IgG and its F(ab')₂ fragments, *Colloids Surf., B*, 8 (1997) 239-249.

-
- [15] A.W.P. Vermeer, C.E. Giacomelli, W. Norde, Adsorption of IgG onto hydrophobic teflon. Differences between the Fab and Fc domains, *Biochim. Biophys. Acta, Gen. Subj.*, 1526 (2001) 61-69.
- [16] X. Sun, D. Yu, R. Ghosh, Study of hydrophobic interaction based binding of immunoglobulin G on synthetic membranes, *J. Membr. Sci.*, 344 (2009) 165-171.
- [17] H. Mach, C.R. Middaugh, R.V. Lewis, Statistical determination of the average values of the extinction coefficients of tryptophan and tyrosine in native proteins, *Anal. Biochem.*, 200 (1992) 74-80.
- [18] L.A. Kueltzo, C.R. Middaugh, Ultraviolet Absorption Spectroscopy, in: W. Jiskoot, D. Crommelin (Eds.), *Methods for structural analysis of protein pharmaceuticals*, American Association of pharmaceutical scientists, 2005.
- [19] A.C. Wang, I.Y. Wang, Cleavage sites of human IgG1 immunoglobulin by papain, *Immunochemistry*, 14 (1977) 197-200.
- [20] R.J. Brezski, R.E. Jordan, Cleavage of IgGs by proteases associated with invasive diseases: an evasion tactic against host immunity?, *mAbs*, 2 (2010) 212-220.
- [21] S. Salgin, S. Takaç, T.H. Özdamar, Adsorption of bovine serum albumin on polyether sulfone ultrafiltration membranes: Determination of interfacial interaction energy and effective diffusion coefficient, *J. Membr. Sci.*, 278 (2006) 251-260.
- [22] W. Jiskoot, E.C. Beuvery, A.M. de Koning, J. Herron, D.A. Crommelin, Analytical Approaches to the Study of Monoclonal Antibody Stability, *Pharm. Res.*, 7 (1990) 1234-1241.
- [23] K. Ahrer, A. Jungbauer, Chromatographic and electrophoretic characterization of protein variants, *J. Chromatogr., B*, 841 (2006) 110-122.
- [24] R.J. Harris, S.J. Shire, C. Winter, Commercial manufacturing scale formulation and analytical characterization of therapeutic recombinant antibodies, *Drug Dev. Res.*, 61 (2004) 137-154.
- [25] J. Zhou, H.-K. Tsao, Y.-J. Sheng, S. Jiang, Monte Carlo simulations of antibody adsorption and orientation on charged surfaces, *J. Chem. Phys.*, 121 (2004) 1050-1057.
- [26] K.L. Jones, C.R. O'Melia, Protein and humic acid adsorption onto hydrophilic membrane surfaces: effects of pH and ionic strength, *J. Membr. Sci.*, 165 (2000) 31-46.
- [27] Y. Kamiyama, J. Israelachvili, Effect of pH and salt on the adsorption and interactions of an amphoteric polyelectrolyte, *Macromolecules*, 25 (1992) 5081-5088.
- [28] S. Yadav, T.M. Laue, D.S. Kalonia, S.N. Singh, S.J. Shire, The Influence of Charge Distribution on Self-Association and Viscosity Behavior of Monoclonal Antibody Solutions, *Mol. Pharm.*, 9 (2012) 791-802.
- [29] A. Kessel, N. Ben-Tal, *Introduction to Proteins: Structure, Function, and Motion*, CRC Press, Taylor & Francis Group, 2011.

-
- [30] J. Buijs, J.W.T. Lichtenbelt, W. Norde, J. Lyklema, Adsorption of monoclonal IgGs and their F(ab')₂ fragments onto polymeric surfaces, *Colloids Surf., B*, 5 (1995) 11-23.
- [31] H. Kawaguchi, K. Sakamoto, Y. Ohtsuka, T. Ohtake, H. Sekiguchi, H. Iri, Fundamental study on latex reagents for agglutination tests, *Biomaterials*, 10 (1989) 225-229.
- [32] R. Ghosh, Membrane chromatographic immunoassay method for rapid quantitative analysis of specific serum antibodies, *Biotechnol. Bioeng.*, 93 (2006) 280-285.
- [33] W.L. Hoffman, A.A. Jump, P.J. Kelly, A.O. Ruggles, Binding of antibodies and other proteins to nitrocellulose in acidic, basic, and chaotropic buffers, *Anal. Biochem.*, 198 (1991) 112-118.
- [34] M.E. Wiseman, C.W. Frank, Antibody Adsorption and Orientation on Hydrophobic Surfaces, *Langmuir*, 28 (2011) 1765-1774.

Chapter V

Summary of the Thesis

Adsorption of therapeutic proteins to pharmaceutical packaging materials leads to several problems such as a loss in protein concentration and potential protein aggregation. These and the arising consequences, e. g. increased costs and immunogenic risks, were presented in detail in the general introduction. The two major possibilities to avoid protein adsorption are the adaption of the formulation and the selection of an appropriate packaging material, potentially with a suitable coating. This thesis focuses on the protein adsorption to coated glass vials, especially siliconized glass vials as a commercial, widely used container, but also to vials coated with protein repellent polyglycerol. Two IgG1 antibodies as therapeutically relevant proteins and lysozyme as a model protein were used for the adsorption studies and their adsorption behavior to the coated vials and bare glass vials was investigated.

In chapter II, the influence of various formulation parameters on the adsorption of a monoclonal IgG1 antibody to siliconized vials and glass vials was investigated. Maximum adsorption at an acidic pH value between the isoelectric points of the sorbent surface and the protein demonstrated the importance of attractive electrostatic conditions for the adsorbed amount. Calculation of the charge transfer between the protein-sorbent interface and the surrounding solution showed a correlation between the minimum ion uptake into the interface and the pH of maximum adsorption. A second adsorption maximum around the pI of IgG1 was ascribed to hydrophobic protein-sorbent interactions. In addition, adsorption in presence of common excipients such as nonionic surfactants, sugars and polyols, as well as at different ionic strength was investigated. Both tested surfactants polysorbate 80 and poloxamer 188 efficiently reduced IgG1 adsorption to siliconized vials. Long-term storage of IgG1 at different pH values and temperatures revealed a correlation between the stability of the protein formulation and the adsorbed amount. For lysozyme, maximum adsorption close to the pI of the protein demonstrated the prevalent importance of the intermolecular electrostatic repulsion for the adsorbed amount of this protein.

Protein adsorption to new, polyglycerol coated vials was investigated in chapter III. All coatings efficiently suppressed IgG1 adsorption to the vials at different pH values and ionic strength. Especially the hyperbranched, non-methoxylated polyglycerol (HPG(OH))-coated vials showed excellent protein resistant properties even after long-time storage with protein solution and after sterilization. Polyglycerol coated vials are thus a promising candidate for the packaging of biopharmaceuticals.

Antibodies are molecules with different subunits which may influence the adsorption behavior of the whole molecule. Therefore, the IgG1 antibody was cleaved and the adsorption behavior of the isolated Fc and F(ab')₂ fragments was investigated in siliconized and non-coated glass vials in chapter IV. The influence of electrostatic and hydrophobic interactions on adsorption was evaluated by quantifying the adsorbed amount at different pH and ionic strength. On glass vials, especially electrostatic interactions influenced the adsorption pattern of IgG1 and the fragments, whereas hydrophobic interactions dominated the adsorption behavior on siliconized vials when the molecules were weakly charged. Possible molecular orientations were aligned with the adsorbed amount and an end-on adsorption for highly charged IgG1 was suggested. For siliconized vials, adsorption with the middle region of the antibody at basic pH conditions was hypothesized.

In summary, the described investigations on protein adsorption to various coated glass surfaces demonstrated the influence of the formulation composition, the protein and sorbent charge and the protein stability on the adsorption behavior. Especially the pH value and the ionic strength were found to affect the adsorbed amount. The study shows that by choosing appropriate excipients or new coatings such as polyglycerols, the formulation scientist can effectively minimize the unspecific protein adsorption to packaging materials. Finally, this thesis may encourage further investigations on the understanding and prevention of protein adsorption phenomena and the development of new protein repellent packaging materials.